AN ABSTRACT OF THE THESIS OF

Shinya Ichikawa for the M. S. in Chemical Engineering
(Name) (Degree) (Major)

Date thesis is presented October 19, 1966

Title THE EFFECT OF CAPILLARY TUBE DIMENSIONS ON THE VISCOSITY OF LIQUID-LIQUID DISPERSIONS IN LAMINAR FLOW

Abstract approved Redacted for Privacy
(Major professor)

The purpose of this research was to study the effect of capillary tube dimensions on the apparent viscosity of an unstable dispersion of two immiscible liquids. The study was limited to laminar flow at a constant temperature.

The dispersions were composed of a commercial solvent, Shellsolv 360, manufactured by the Shell Oil Company, and water. The composition of the dispersions ranged from 5 volume % to 50 volume % solvent dispersed in water.

The laminar flow viscosities were determined by measurements made using a capillary tube viscometer. Capillary tubes of varying lengths and diameters were used to determine the apparent viscosity at different flow rates. Measured viscosities of the dispersions were found to be dependent on the tube dimensions as well as the flow rate.

Viscosities were calculated by means of Poisueille's equation corrected for entrance and exit effects,

$$\mu_a = \frac{\pi r^4 \Delta P_m \theta g_c}{8LV} - 0.149 \frac{\rho V}{\pi L \theta}$$

where μ_a is the measured apparent viscosity, r is the radius of the capillary tube, ΔP_m is the measured pressure drop across the tube, θ is the elapsed time of a run, g_c is the gravitational conversion factor, ρ is the density of the fluid and V is the volume collected in time θ.

The apparent viscosity of the dispersions increased with solvent concentration and tube diameter and decreased with tube length and flow rate. The diameter and length effects as well as the apparent pseudoplastic behavior may be explained by the presence of a film of the continuous phase adjacent to the wall, due either to radial migration of the solvent particles or phase separation and coalescence, or both.

The dispersions showed changing behavior as they flowed through the capillary tubes, the pressure drop over a given increment of tube decreasing along the tube length.

The relationship of relative fluidity versus volume fraction of the dispersed phase compared favorably with the result of a previous study.

THE EFFECT OF CAPILLARY TUBE DIMENSIONS ON THE VISCOSITY OF LIQUID-LIQUID DISPERSIONS IN LAMINAR FLOW

by

SHINYA ICHIKAWA

A THESIS

submitted to

OREGON STATE UNIVERSITY

in partial fulfillment of
the requirements for the
degree of

MASTER OF SCIENCE

June 1967

APPROVED:

Redacted for Privacy

Professor of Chemical Engineering
In Charge of Major

Redacted for Privacy

Head of Department of Chemical Engineering

Redacted for Privacy

Dean of Graduate School

Date thesis is presented October 19, 1966

Typed by Joanne Wenstrom

ACKNOWLEDGEMENTS

The author wishes to express his sincere appreciation to Dr. James G. Knudsen for suggesting the project, for his guidance and aid, and simply for his presence. A thank you is extended to Professor Jesse S. Walton for the use of departmental facilities and to Mr. William B. Johnson for his invaluable suggestions and assistance in constructing the equipment. The author is indebted to the Engineering Experiment Station for financial assistance.

TABLE OF CONTENTS

LIST OF FIGURES

LIST OF TABLES

THE EFFECT OF CAPILLARY TUBE DIMENSIONS ON THE VISCOSITY OF LIQUID-LIQUID DISPERSIONS IN LAMINAR FLOW

INTRODUCTION

In handling and transporting fluids, knowledge of the viscosity is necessary for the prediction of friction losses and power requirements. The flow of water and other single-phase liquids is a relatively simple problem compared to complex multiphase systems. These multiphase systems, which are frequently encountered in the process industries, present a fertile area for study in that they show different and sometimes contrasting behavior.

There has been considerable study of gas-liquid, gas-solid and liquid-solid systems as well as combinations of these systems such as liquid-liquid-solid dispersions. Relatively little has been accomplished in the region of liquid-liquid flow. A recent review article concerning chemical engineering flow topics listed only one paper dealing with liquid-liquid dispersions.

Greater knowledge of the physical properties, especially the viscosity, of liquid-liquid dispersions is necessary from a practical standpoint in the design of process equipment.

The research described in this report is a study of the flow of liquid-liquid dispersions in laminar flow in capillary tubes. The effects of tube length and diameter on the viscosity are determined for dispersions of various concentrations.

THEORY AND BACKGROUND

If portions of a mass of fluid are caused to move relative to one another, the motion gradually subsides unless sustained by external forces. This resistance to deformation or shear by a real fluid is called the coefficient of viscosity, or more simply, viscosity.

Viscosity is defined by the relationship,

$$\tau = \frac{F}{A} = \mu \frac{du}{dy} \tag{1}$$

where τ is the shear stress or the force F exerted tangentially on a plane of area A to produce a velocity gradient $\frac{du}{dy}$, or rate of shear, perpendicular to the plane at the point of application. The coefficient of viscosity μ is a property of the fluid. Its numerical value for any particular fluid is dependent upon the temperature, static pressure and rate of shear.

The viscous force may also be expressed as a rate of momentum transfer between fluid layers. The shear stress is equivalent to a rate of change of momentum flux.

Basically, experimental methods devised to determine fluid viscosities make use of Equation (1) in which a known shear stress is applied to the fluid and the resultant rate of shear determined. The viscosity is calculated from these two quantities.

In the capillary viscometer, a pressure difference maintained between the two ends of a capillary tube causes the fluid to flow through the tube. The force exerted by the pressure P on a fluid cylinder of radius r is

$$F_p = \pi r^2 P, \tag{2}$$

while the resistance offered by the surface of the cylinder, caused by the fluid viscosity is, according to Equation (1),

$$F_u = 2\pi r L \mu \frac{du}{dy}. \tag{3}$$

For steady flow, $F_p = -F_u$. Assuming that the fluid velocity at the wall of the tube is zero, an equation is derived by which viscosities may be calculated, knowing the pressure drop through the tube, the tube dimensions and the volumetric flow rate,

$$\mu = \frac{\pi r^4 \Delta P_m \theta}{8 LV} \tag{4}$$

where r is the radius of the capillary tube; ΔP_m, pressure drop measured across the tube; L, length of tube; V, volume of measured efflux from tube; and θ, time to collect efflux.

Newtonian and Non-Newtonian Fluids

The viscosity of a Newtonian fluid is independent of the rate of shear and depends only on temperature and pressure. Generally, all gases and liquids and solutions of low molecular weight exhibit Newtonian behavior.

The viscosity of a gas increases with increasing temperature; the viscosity of a liquid, which is much larger than that of the same substance in its vapor state at the same temperature, decreases with temperature. The viscosity of an ideal gas is independent of pressure, but the viscosities of real gases and liquids usually increase with pressure.

At constant temperature and pressure, the viscosity of a non-Newtonian fluid is a function also of the rate of shear. These fluids may be classified into several types: (1) Bingham plastics, (2) pseudoplastics, and (3) dilatant. Referring to Figure 1, for a Newtonian fluid, the shear stress is directly proportional to the rate of shear (curve I). A Bingham plastic (curve III) requires the application of a finite yield stress to initiate flow. At stresses below this finite stress, the material behaves like a solid; when this stress is exceeded, the system behaves as a Newtonian fluid. A pseudoplastic fluid (curve II) exhibits a continuous decrease of viscosity with an increase in shear rate, approaching Newtonian behavior at very high or very low rates of shear. The apparent viscosity of a dilatant fluid (curve IV) increases with increasing rate of shear.

Figure 2 shows how the viscosities of Newtonian, dilatant and pseudoplastic fluids are affected by rate of shear.

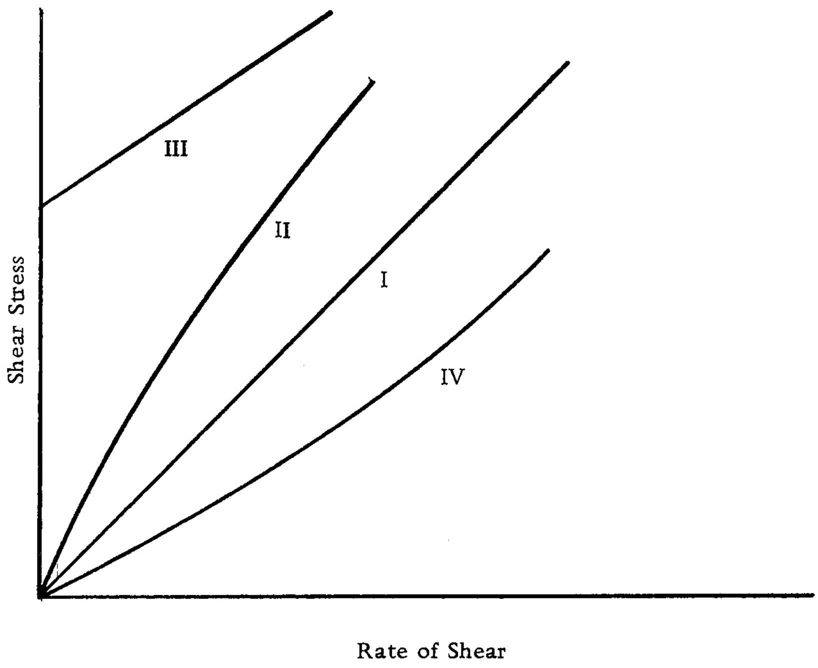

Figure 1. Viscous Characteristics of Fluids

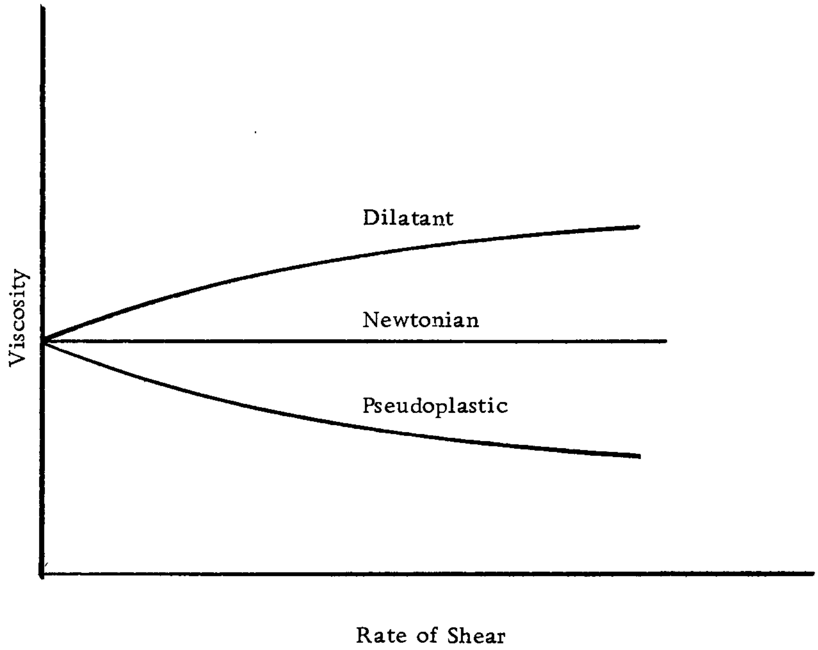

Figure 2. Effect of Rate of Shear on Viscosity

Dispersions

Dispersion is a general term which may be defined roughly as a quasi-homogeneous product resulting from a mixture of two or more immiscible fluids or one or more fluids with finely divided solids (39, p. 1196). The continuous phase in a dispersion is the external phase, while the discontinuous, or dispersed phase is the internal phase. If the internal phase is liquid, the dispersion is an emulsion; if it is a solid, the dispersion is a suspension; and if it is gas, it is a foam.

At low concentrations of a finely divided phase, a dispersion behaves as a Newtonian fluid. As the concentration of the dispersed phase increases to a certain critical concentration, the dispersion becomes non-Newtonian. However it is an over-simplification to classify non-Newtonian dispersions as Bingham plastic, pseudo-plastic or dilatant. It is known that the classification of a fluid, and even the numerical values assigned to its rheological properties, is dependent upon the experimental conditions under which the measurements are made. At different shear rates, a given dispersion may behave as a Bingham plastic, a pseudoplastic or, at very high rates of shear, even as a Newtonian fluid (31).

At constant temperature, the viscosity of dispersions depends upon several factors (3):

1. Volume concentration of dispersed phase
2. Rate of shear
3. Viscosities of continuous and dispersed phases
4. Size and shape of dispersed particles
5. Distribution of particles
6. Interfacial tension

In general, as the concentration of the dispersed phase increases, viscosity increases to a maximum value. For a liquid-liquid dispersion, inversion occurs when the maximum value is reached due to interchange of the phases.

Einstein (15) considering the problem of two phases, formulated the equation,

$$\mu_m = \mu_c (1 + k\phi) \tag{5}$$

where μ_m is the apparent viscosity of the dispersion; μ_c, viscosity of continuous phase; ϕ, volume fraction of dispersed phase; and k, Einstein constant, 2.5. Equation (5) is derived for dispersions of uniform, rigid spheres which are separated by distances much larger than the sphere diameter, and are non-agglomerating and low in concentration. The equation is limited to volume fractions less than 0.02 for the dispersed phase.

Many subsequent workers, attempting to correlate data, expanded Equation (5) into polynomial form,

$$\mu_m = \mu_c\,(1+k\phi+a\phi^2+b\phi^3+\ldots) \tag{6}$$

where k is Einstein's constant and a and b are constants for a particular dispersion. One example is that of Vand (57),

$$\mu_m = \mu_c\,(1+2.5\phi+7.349\phi^2+16.2\phi^3). \tag{7}$$

Taylor (54) proposed a modification of Einstein's equation which includes the viscosity of the dispersed phase and which was reported to be applicable to liquid-liquid systems,

$$\mu_m = \mu_c\left[1+2.5\phi\left(\frac{\mu_d+0.4\mu_c}{\mu_d+\mu_c}\right)\right] \tag{8}$$

where μ_d is the viscosity of the dispersed phase.

As an example of a logarithmic relationship, Leviton and Leighton (25) obtained an empirical equation from data on oil-in-water emulsions,

$$\ln\frac{\mu_m}{\mu_c}\left(\frac{\mu_d+0.4\mu_c}{\mu_d+\mu_c}\right)(\phi+\phi^{5/3}+\phi^{11/3}). \tag{9}$$

Richardson (42) proposed an exponential relationship applicable to oil-in-water emulsions,

$$\mu_m = \mu_c\,(e^{a\phi}) \tag{10}$$

where a is a constant depending upon the system.

Finnigan (17, p. 109) reported a correlation for petroleum solvent in water,

$$\mu_m = \mu_c\ (1+2.5\phi+5.6\phi^2). \tag{11}$$

Cengal (4, p. 76), working with the same system, reported

$$\mu_m = \mu_c\ (1+2.5\phi-11.01\phi^2+52.62\phi^3). \tag{12}$$

Higgenbotham, Oliver and Ward (21), working with spherical particles of polymer, proposed the relationship,

$$\mu_m = \frac{\mu_c}{(1-k\phi)} \tag{13}$$

where k varied from 2.33 to 2.46 for ϕ less than 0.28.

Siebert (52) included the effects of interaction between the liquid and particles,

$$\mu_m = \mu_c \left(\frac{1}{1-a\phi}\right)^k \tag{14}$$

where k is the Einstein constant defined as $5\ b/a$, a and b are parameters indicating behavior due to interaction of liquid and particles.

Nishimura (33) derived a relationship applicable for extremely concentrated solutions of polymer by allowing for volume shrinkage,

$$\frac{d \log \mu_m}{d\phi} = \frac{a}{\phi^b(1-\phi)} \tag{15}$$

where a and b are empirically determined constants.

Saunders (46), working with a series of monodisperse polystyrene latexes, obtained experimental results with a capillary viscometer which appeared to fit the equation,

$$\mu_m = \mu_c \exp \frac{k\phi}{1-\alpha\phi} \tag{16}$$

with a value of 2.504 for k in good agreement with Einstein's value of 2.5. The interaction coefficient α varied from 1.118 to 1.357 increasing with increasing particle diameter.

Thomas (55) showed that an expression containing three terms of a power series and an exponential term with two adjustable constants fit experimental data as well as a power series with six terms,

$$\mu_m = \mu_c \left[1+2.5\phi+10.05\phi^2+a \exp (b\phi)\right] \tag{17}$$

where coefficients a and b were 0.00273 and 16.6 respectively.

Rutgers (45) reviewed 280 references on the effect of concentration on viscosity and concluded that only five relationships (16, 27, 32, 53, 57) can be used for spheres over the entire concentration range.

Sherman (51) claimed that the emulsion viscosity is directly related to the viscosity of the continuous phase but no other generalization could be made regarding formulation variables.

Viscosity Measurement of Dispersions by Capillary Tubes

The capillary viscometer provides a means of studying the rheological properties of dispersions. Workers have found that the apparent viscosity measured in this manner depended on the rate of shear as well as the tube dimensions, diameter and length.

It has been shown that the measured viscosity of a dispersion increases with increasing diameter (16, 28, 57). Various explanations have been given for this anomalous effect. Vand (57) assumed slip to take place between the tube wall and dispersion, the dispersion acting as though there is a layer of pure fluid adjacent to the wall. He theoretically determined this thickness to be 1.301 a, where a is the radius of a spherical particle. DeBruijn (11) states that mechanical interaction of the particles causes their movement perpendicular to the plane of shear. Near the tube wall, perpendicular movement can be in one direction only and therefore causes shift of particles away from the wall.

Higgenbotham, Oliver and Ward (21) also reported a form of wall effect present which causes the apparent viscosity of a dispersion to increase with increasing diameter.

Whitmore (58) suggested that particles entering the capillaries along a streamline which passes closer to the wall than the particle radius are displaced radially toward the more rapidly moving stream in the center of the tube. Photographs showed a longitudinal gradient of concentration in the advancing front of dilute suspensions of spheres.

Young (60), studying the flow of aqueous suspensions of fine spherical glass particles in a vertical glass tube, noted a collection of particles near the tube center in upward flow, while in downward flow, they collected near the wall.

Segré and Siberberg (47) have correlated the radial particle displacement, which they refer to as the tubular pinch effect, in a system of reduced coordinates. These same investigators (48) were the first to observe that particles migrated away both from the tube axis and wall, reaching equilibrium at some intermediate radial position.

Oliver (35) observed that rotating particles moved outward while in the absence of rotation, the particles normally drifted toward the tube center. He suggested that these radial movements may not be marked at high concentrations when particle collisions become frequent.

Karnis, Goldsmith and Mason (22) explained why rigid spheres migrated to an equilibrium radial position, while deformable liquid droplets migrated to the tube axis. In a subsequent investigation (23), they also reported the effects of flow rate, particle size and radial displacement from an equilibrium position on the rate of migration. Explaining the radial equilibrium position, they concluded that when the sedimentation velocity is in the direction of flow, the particles reach equilibrium at a radial position at which the inward directed force arising from the proximity of the wall balances the outward directed lift force.

The consequence of radial migration is that there is a lubricating action of the layer of pure liquid near the tube wall which reduces the pressure drop for a given length of tube. Hence the observed viscosity is less than would be expected for the dispersion itself.

In addition to the radial migration phenomenon, a major portion of dispersions also exhibit a pseudoplastic behavior in which there is a continuous decrease of the viscosity as the rate of shear increases (13, p. 84, 42). Ostwald (37) and Philippoff (40) were the first to propose that the flow curve (shear stress versus rate of shear) of these dispersions consists of clear-cut sections: a Newtonian region at low and high rates of shear, a pseudoplastic region at medium rates of shear, and an increase in viscosity with the onset of turbulence.

Berkowitz (2), studying pipeline flow of coal-in-oil suspensions, reported pseudoplastic behavior at volume concentrations greater than 10%. Claesson and Lohmander (9) reported pseudoplastic behavior of long stiff molecules of cellulose nitrate in ethyl acetate. Shaver and Merrill (49) discussed pseudoplastic behavior of linear polymers in laminar, transition and turbulent flow.

Segré and Siberberg (47) noted the decrease in viscosity at higher throughput velocities. They reasoned that as the radial particle displacements, mentioned previously, depend on the velocity of flow, the viscosity due to the particles is velocity dependent.

Cengel and coworkers (5) observed a decrease in viscosity with Reynolds number for a liquid-liquid dispersion of a petroleum solvent in water for laminar flow. They however suggested that this behavior could be due to phase separation, although some observations were made on vertical capillary tubes in which phase separation may not have been significant.

An informative correlation (59, p. 28-33) in capillary viscometry is the plot of shear stress at the wall versus a volumetric flow rate term, as shown in Figure 3. Assuming that laminar flow exists, that there is no slip at the wall, and that the rate of shear at a point depends only on shearing stress at that point and is independent of time, all data should fall on one line regardless of the tube dimensions. If the possibility of non-laminar flow can be ruled out and the fluid is known to be time-independent, a separation of the curves for different tube diameters can be interpreted as evidence of anomalous flow behavior or slip at the tube wall. In this case, as shown in Figure 3, by increasing the diameter at a constant length or by increasing the length at constant diameter,

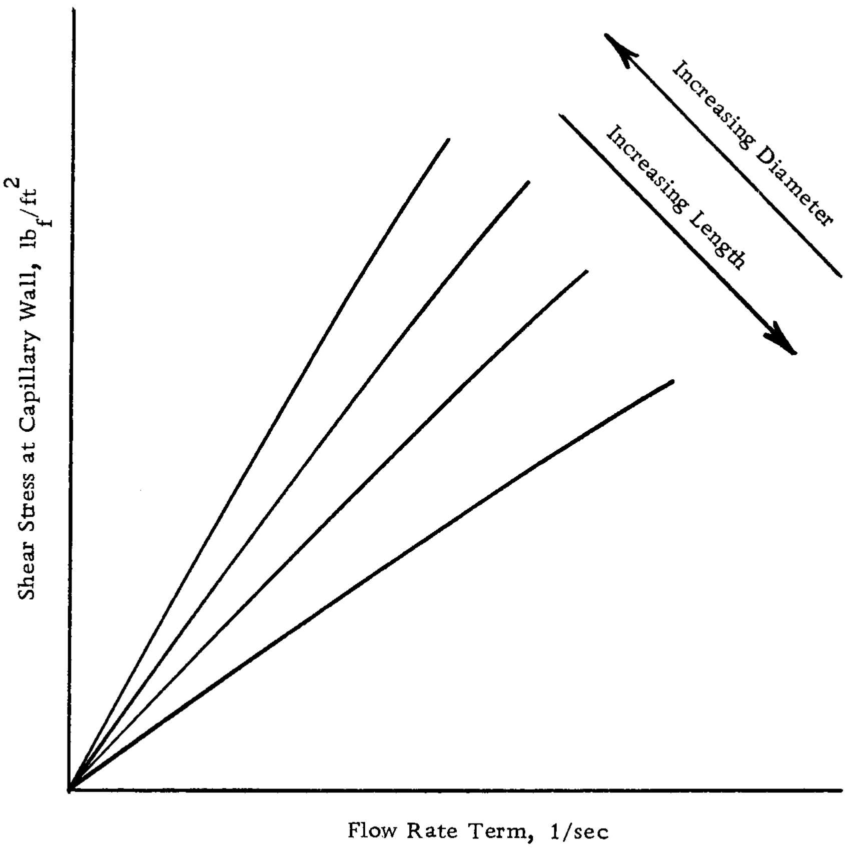

Figure 3. Shear Stress at Wall of Capillary versus Reciprocal Second

different values of shear stress at the wall are obtained for a given flow (13, p. 144). Since viscosity depends upon shear stress, the measured viscosities will depend on tube dimensions.

Corrections in Capillary Tube Viscometry

Van Wazer (56, p. 199-215) and Ram and Tamir (41) list and discuss the major sources of error for capillary viscometers. Of these, the most important is for pressure dissipated due to kinetic energy losses at the exit. When a fluid stream discharges with high speed from a capillary directly into air, the stream possesses an appreciable amount of kinetic energy which may represent an appreciable portion of the total pressure difference.

The correction is given by

$$\Delta P = \Delta P_m - m\rho\left(\frac{V}{\theta \pi r^2}\right)^2 \tag{18}$$

where ΔP_m is the measured pressure drop and ΔP the corrected value. Most investigators (24, 41) use a value of $m = 1.12$ which also accounts for the contraction correction effect from the large diameter of a vessel into the capillary.

Langhaar (24) recommends $m = 1.14$ in deriving the viscosity relationship for a capillary, thus combining Equations (4) and (18),

$$\mu = \frac{\pi r^4 \Delta P_m \theta g_c}{8 L V} - 0.149 \frac{\rho V}{\pi L \theta}. \tag{19}$$

Bagley (1) describes a method of determining the entrance effect correction by measuring pressure drops for various lengths of tube and extrapolating the data to zero length.

EXPERIMENTAL EQUIPMENT

The flow diagram in Figure 4 illustrates the apparatus used to determine laminar flow viscosities of liquid-liquid dispersions. The design was based in part on an apparatus previously constructed to study both heat transfer coefficients and laminar and turbulent viscosities of liquid-liquid dispersions (4, p. 22-31, 17, p. 27-34). Figure 5 shows details of the capillary viscometer and manometer lines.

Supply Tank and Pump

A stainless steel supply tank was used for preparing the liquid mixtures and for mixing. It was cylindrical in shape with a hemispherical bottom and had a total capacity of 7.5 gallons. A square, brass plate placed at the bottom of the tank, above the outlet opening, acted as a baffle to prevent vortex formation. The plate was of such a size and shape to allow sufficient flow between it and the hemispherical tank bottom.

A propeller-type agitator with a variable speed drive was mounted on the edge of the tank. Although most of the mixing action was provided by circulating the liquids through the system with the pump, at very low flow rates through the system (high pressure), the agitator provided all the mixing action.

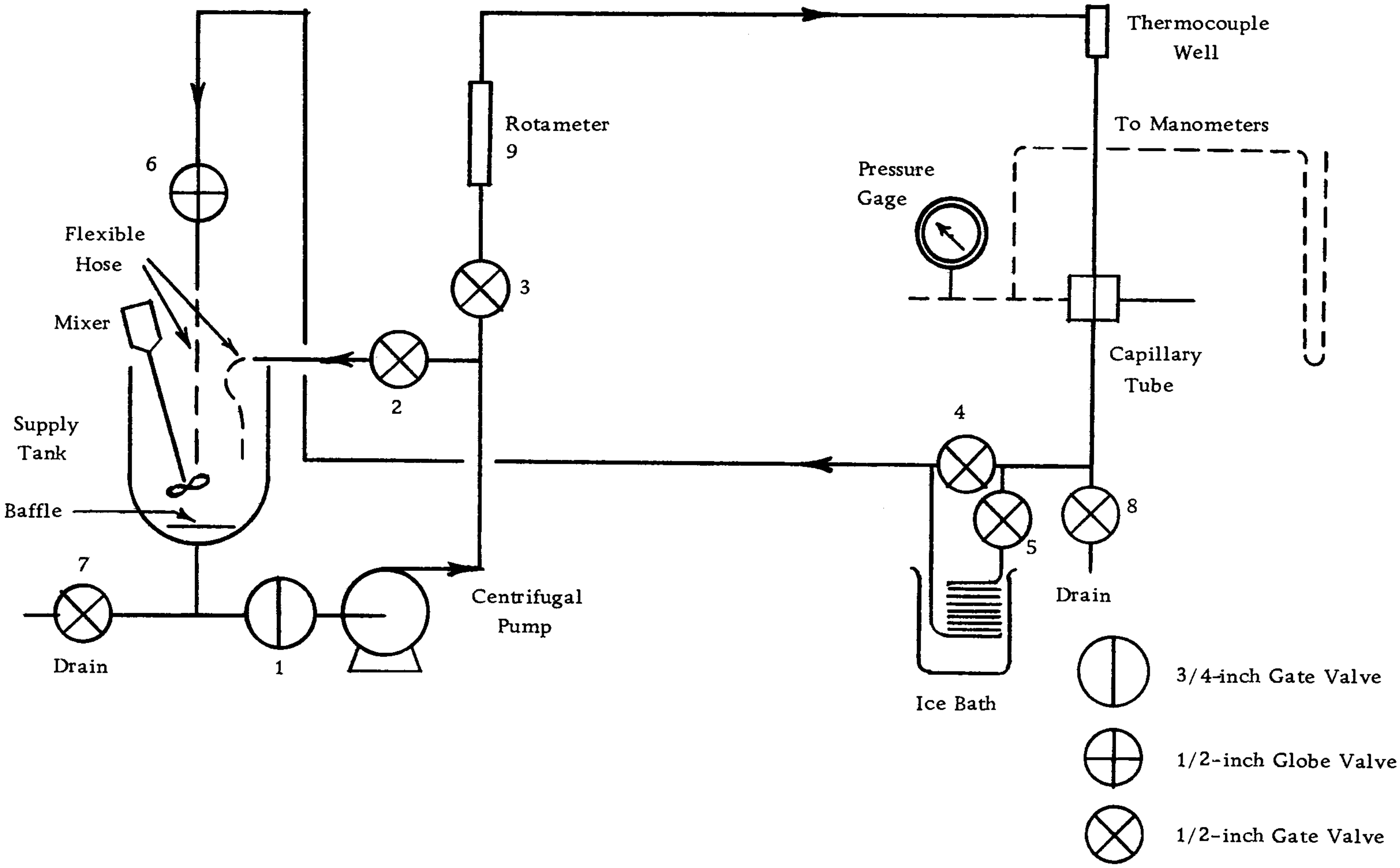

Figure 4. Schematic Flow Diagram

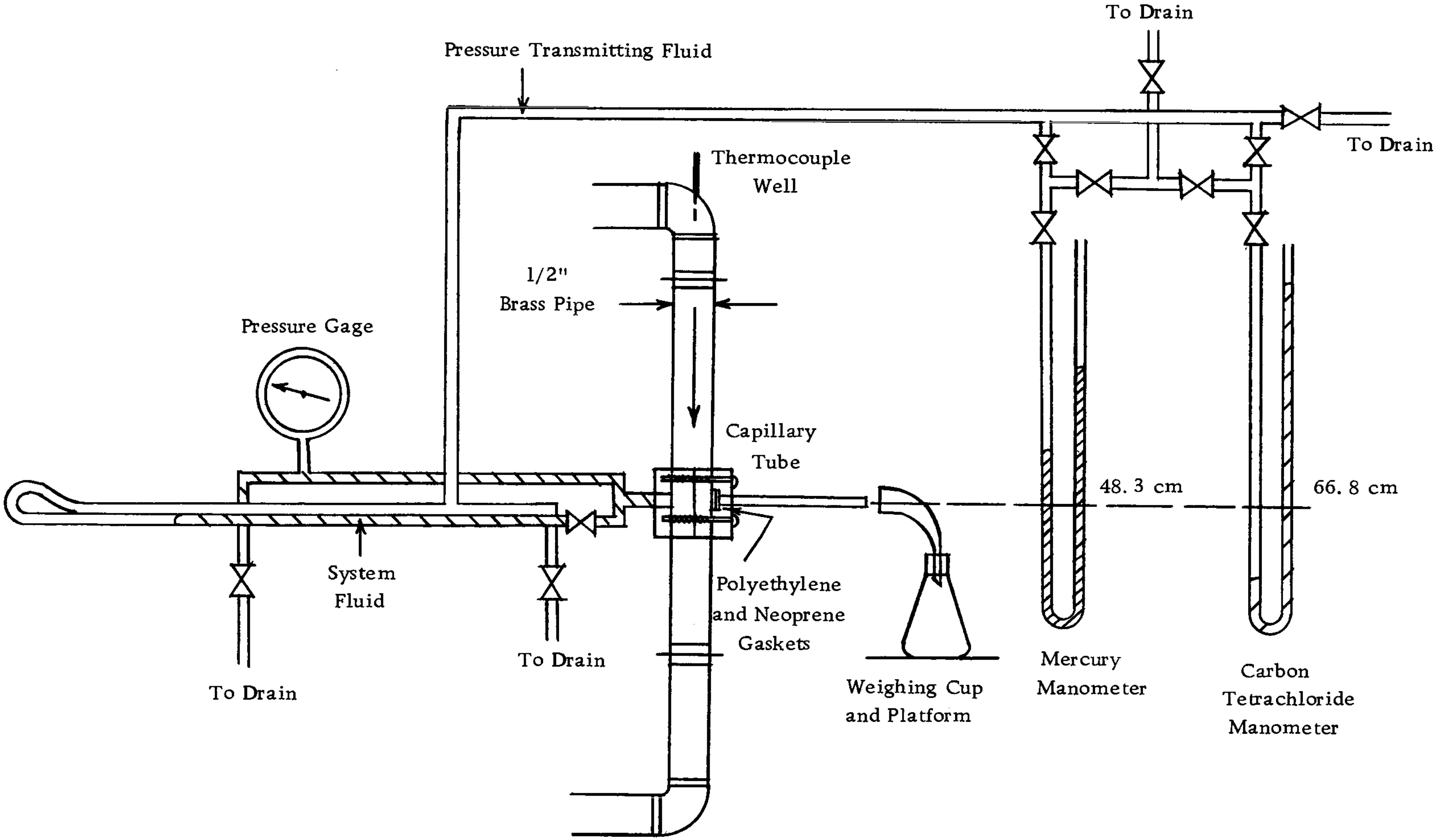

Figure 5. Test Section and Manometer Lines

The pump was an Eastern Industries centrifugal pump driven by a 1/2 horsepower electric motor.

Piping System

The piping system was constructed of nominal 1/2-inch brass pipe, nominal 3/4-inch brass pipe, 3/8-inch soft copper tubing, and sections of flexible polyethylene hose. The 3/4-inch pipe was located between the supply tank and the pump, and between the pump and the separation point of the by-pass and main streams. The copper tubing, serving as a cooling coil, was attached to the bottom, horizontal section of the system and immersed in an ice bath. The flexible hose was located at the two efflux points of the system. All other piping was 1/2-inch standard brass.

Referring to Figure 4, a 3/4-inch gate valve (number 1) was installed between the supply tank and pump so that the piping could be drained independently of the tank. A 1/2-inch gate valve was placed between the pump and by-pass line (number 2) and between the pump and main system (number 3). Both valves were used to aid in controlling the amount of flow through the test section. With the main system valve closed, changes could be made on the test section without disturbing the mixing. Two 1/2-inch gate valves, one located between the two points of attachment of the cooling coil loop onto the main stream (number 4) and the other located on the loop (number 5) aided in controlling the liquid temperature by regulating the flow through the loop. A 1/2-inch globe valve (number 6) was installed at the efflux point to regulate flow. Finally two 1/2-inch gate valves (numbers 7 and 8) were installed to facilitate drainage of the supply tank and piping system.

All threaded connections were made using teflon tape to prevent leakage. Unions were installed liberally throughout the system for quick disassembly and repair of equipment.

A Fisher and Porter Company rotameter (number 9), with a maximum capacity of 4.35 gpm water, was placed directly above the main stream valve. This served to indicate a steady flow through the system and also offered visual assurance that no air bubbles had entered the system. No attempt was made to measure flow rates through the main piping system.

Test Section

Figure 5 illustrates the test section used to determine laminar flow viscosities. The main flow was vertically downward through the 1/2-inch brass pipe. The static pressure tap was located directly opposite the inserted capillary by drilling a 1/32-inch diameter hole perpendicular to the pipe wall and soldering a short length of 1/4-inch copper tubing in place. The inside surface was smoothed and cleaned with emery cloth to insure an opening free of burrs and flush with the inside pipe wall. The tap was connected by tygon tubing to an 8-foot U-shaped, horizontal glass tube, followed by another length of tygon tubing extending vertically to the manometers. The horizontal section was installed to prevent transfer of the dispersion solvent from the flow system to the vertical portion of the line due to movement of the manometer columns. Transparent tygon tubing and glass tubing were used in the manometer line to enable visual assurance that no air was in the line and that only water filled the line from the vertical section to the manometers.

One manometer contained water over mercury as the measuring fluid and the other water over carbon tetrachloride, thus permitting a wide range of pressure measurements to be made. The mercury manometer was 3 feet in length and the carbon tetrachloride manometer 4 feet in length. Individual meter sticks fastened to the manometer board between manometer legs served as length scales.

The pressure gage, also connected to the pressure tap, was used only to indicate directly the static pressure reading in psi. These readings were not used in calculating the viscosities.

A glass capillary tube was inserted into the main stream and held in place by two cylindrical sections of plastic, secured together by four 2-inch, brass machine screws. This arrangement also served to hold polyethylene and neoprene gaskets in place. A hole drilled through the center of each section accommodated the copper tube of the pressure line and the glass capillary tube. The hole drilled through the main pipe and one plastic section for the capillary tube was sized for the largest capillary diameter. The capillary tube was leveled by adjusting the tightness of the four screws.

The capillary tubes were heavy-wall, soft pyrex tubing. After cutting to their proper lengths, the ends were smoothed by polishing with progressively finer-grain emery cloth. To insure a level end, the tube was held snugly upright in a hole drilled in a block of wood, and the end rubbed against the emery cloth, using a circular motion. This was found to be the best method after several futile attempts to obtain a smooth end.

The diameter of each capillary tube was determined by weighing the mercury required to fill the tube. The tube dimensions are listed in Table 1.

A 500 ml Erlenmeyer flask, fitted with an adaptor, served as a collecting and weighing cup. The cup was placed in a large pan supported on an adjustable platform. The liquid caught in the cup was weighed on a triple-beam balance having an accuracy of ± 0.5 grams. Time of efflux of the weighed volume of dispersion was measured by a stopwatch.

The temperature of the flowing dispersion was measured by means of an iron-constantan thermocouple situated directly upstream of the test section. The voltage was read from a Leeds and Northrup type K potentiometer. Temperatures were maintained at $70^{o}F \pm 0.4^{o}F$.

Table 1. Capillary Tube Dimensions

Tube Number	Length, inches	Inside Diameter, inches x 10^2	Length/Diameter Ratio
A- 6	6.02	1.886	319
A- 9	8.70	1.886	461
A-12	11.98	1.886	635
A-15	15.02	1.886	796
B- 6	5.91	2.661	222
B- 9	8.70	2.661	327
B-12	11.77	2.661	447
B-15	14.92	2.661	561
C- 6	5.94	4.181	142
C- 9	8.98	4.181	215
C-12	11.97	4.181	286
C-15	15.00	4.181	359
D- 6	5.94	7.559	77
D- 9	8.94	7.559	118
D-12	11.89	7.559	157
D-15	14.94	7.559	198

EXPERIMENTAL PROCEDURE

The unstable liquid-liquid dispersion studied was composed of a petroleum solvent, Shellsolv 360, dispersed in water. Physical properties of the solvent was measured by Finnigan (17, p. 129-141). The following pure liquids and dispersions (volume % solvent) were studied:

1. Pure water	4. 20% solvent
2. Pure solvent	5. 35% solvent
3. 5% solvent	6. 50% solvent

After construction of the system was complete, the piping was cleaned by flushing with sodium tripolyphosphate. The dispersions were prepared by adding measured volumes of solvent and water to the supply tank. A total volume of 5 gallons was mixed in the supply tank. This was found to be the proper amount to avoid entrance of air bubbles into the system as well as to avoid liquid splashing out of the tank.

Samples were analyzed periodically to insure that proper mixing was occurring and to check the composition. Table 2 shows the measured compositions.

At each concentration, measurements were made of the manometer liquid column, rate of efflux from the capillary tube and fluid temperature. A series of flow rates through each capillary was studied.

Table 2. Nominal and Measured Composition

Nominal Volume % Solvent	Measured Volume % Solvent
5	4.9
20	20.0
35	35.6
50	51.3

RESULTS AND DISCUSSION

Laminar Flow Viscosities

It was previously stated that the apparent viscosity of a non-Newtonian dispersion depends on the experimental conditions under which the measurements are made. In this study, the apparent viscosity is a function not only of the shear rate but also of the tube dimensions, diameter and length.

The viscosities were calculated by the modified Poiseuille's equation (Equation 19) and used to determine the Reynolds numbers in the capillary tubes. The Reynolds numbers were all in the laminar range (i. e. less than 2000). The different cases studied are summarized in Table 3.

Experimental viscosities of water, pure solvent and various dispersions are plotted in Figure 6 as a function of Reynolds numbers in the capillary tube. In Figure 6a, the viscosity of water agrees well with the literature value (Figure 12) while the viscosity of the pure solvent in Figure 6b agrees favorably with the value determined by Finnigan (Figure 12) using an Ostwald viscometer. This agreement indicated that the apparatus gave satisfactory results.

Figures 6c, 6d and 6e show results for the dispersions for tubes A, Figures 6f, 6g, 6h and 6i for tubes B, Figures 6j, 6k,

Table 3. Summary of Cases Studied

System	Capillary Tube	Number of Runs	System	Capillary Tube	Number of Runs
5% Dispersion	A- 6	10	50% Dispersion	A- 6	6
	A- 9	13		A- 9	4
	A-12	7		A-12	5
	A-15	5		B- 6	8
	B- 6	7		B- 9	5
	B- 9	7		B-12	9
	B-12	9		B-15	5
	B-15	7		C- 6	7
	C- 6	5		C- 9	8
	C- 9	5		C-12	8
	C-12	6		C-15	8
	C-15	5		D- 6	7
				D- 9	7
20% Dispersion	A- 6	7		D-12	7
	A- 9	7		D-15	10
	A-12	5			
	A-15	5	Solvent	A- 6	3
	B- 6	6		A- 9	6
	B- 9	6		A-12	12
	B-12	11		A-15	6
	B-15	9			
	C- 6	5	Water	A-12	10
	C- 9	14			
	C-12	7			
	C-15	6			
	D- 6	7			
	D- 9	7			
	D-12	7			
	D-15	7			
35% Dispersion	A- 6	5			
	A- 9	5			
	A-12	6			
	A-15	6			
	B- 6	7			
	B- 9	9			
	B-12	7			
	B-15	5			
	C- 6	10			
	C- 9	10			
	C-12	9			
	C-15	8			
	D- 6	9			
	D- 9	10			
	D-12	10			
	D-15	7			

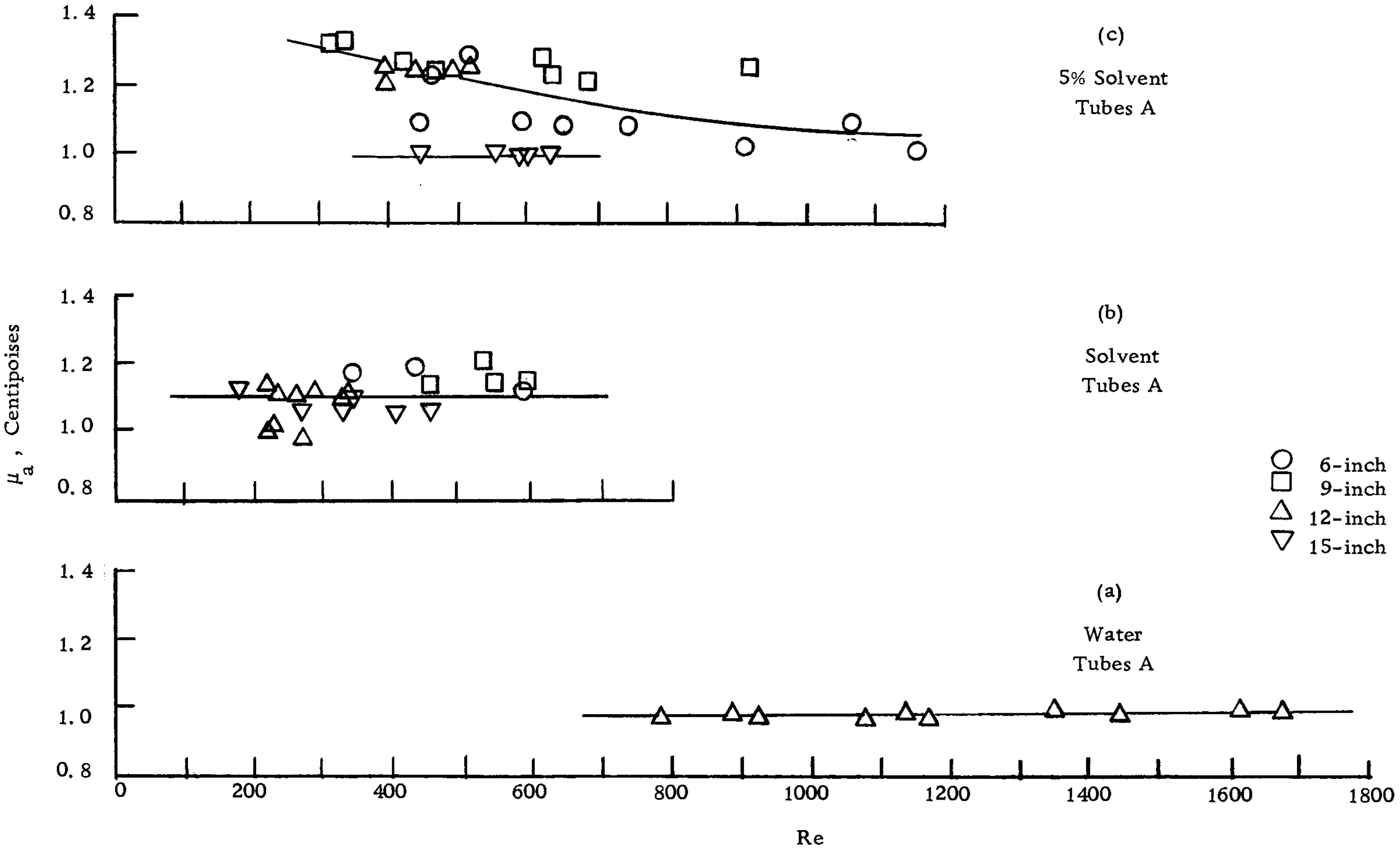

Figure 6 a, b, c. Laminar Flow Viscosities

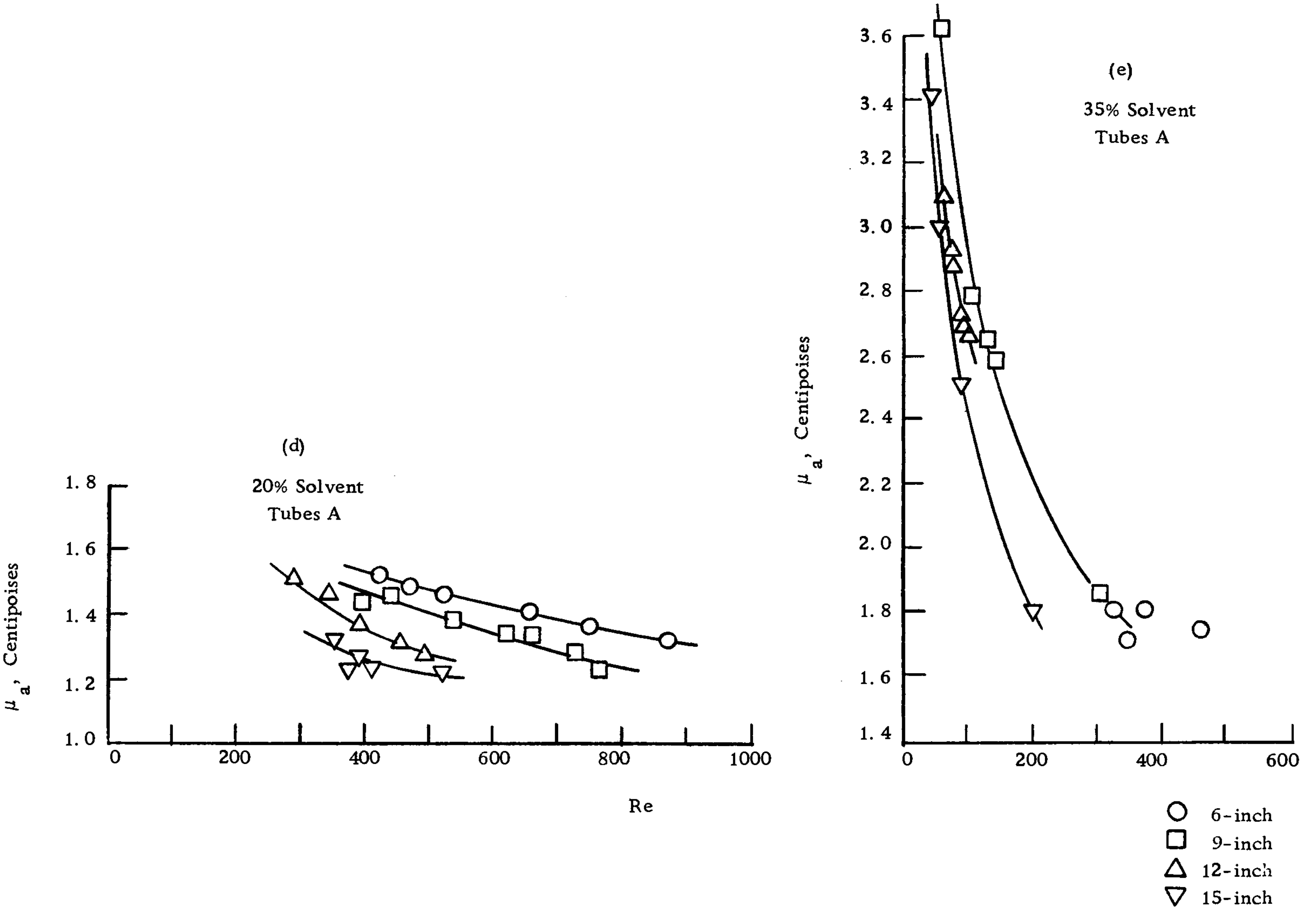

Figure 6 d, e. Laminar Flow Viscosities

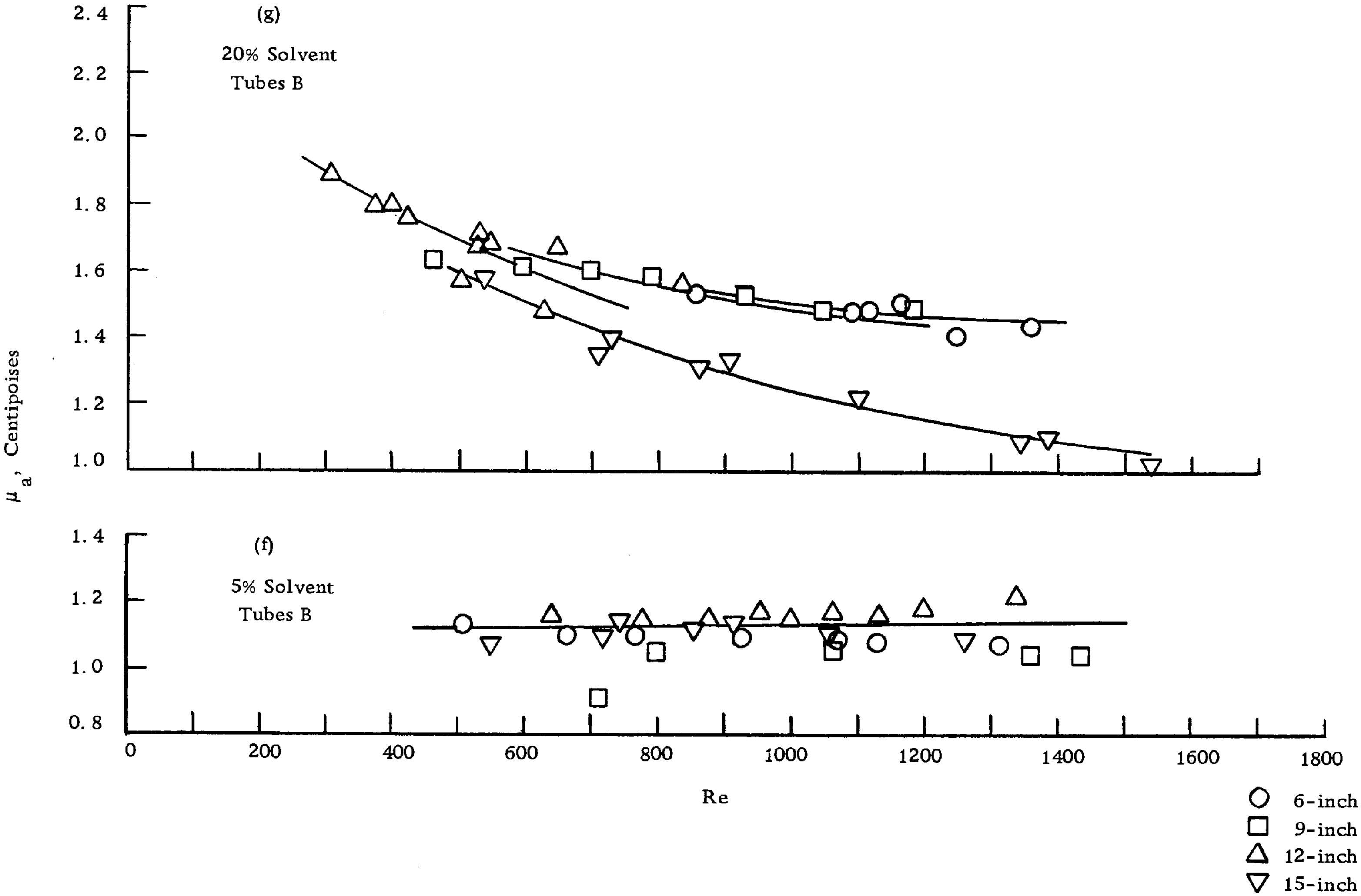

Figure 6 g, f. Laminar Flow Viscosities

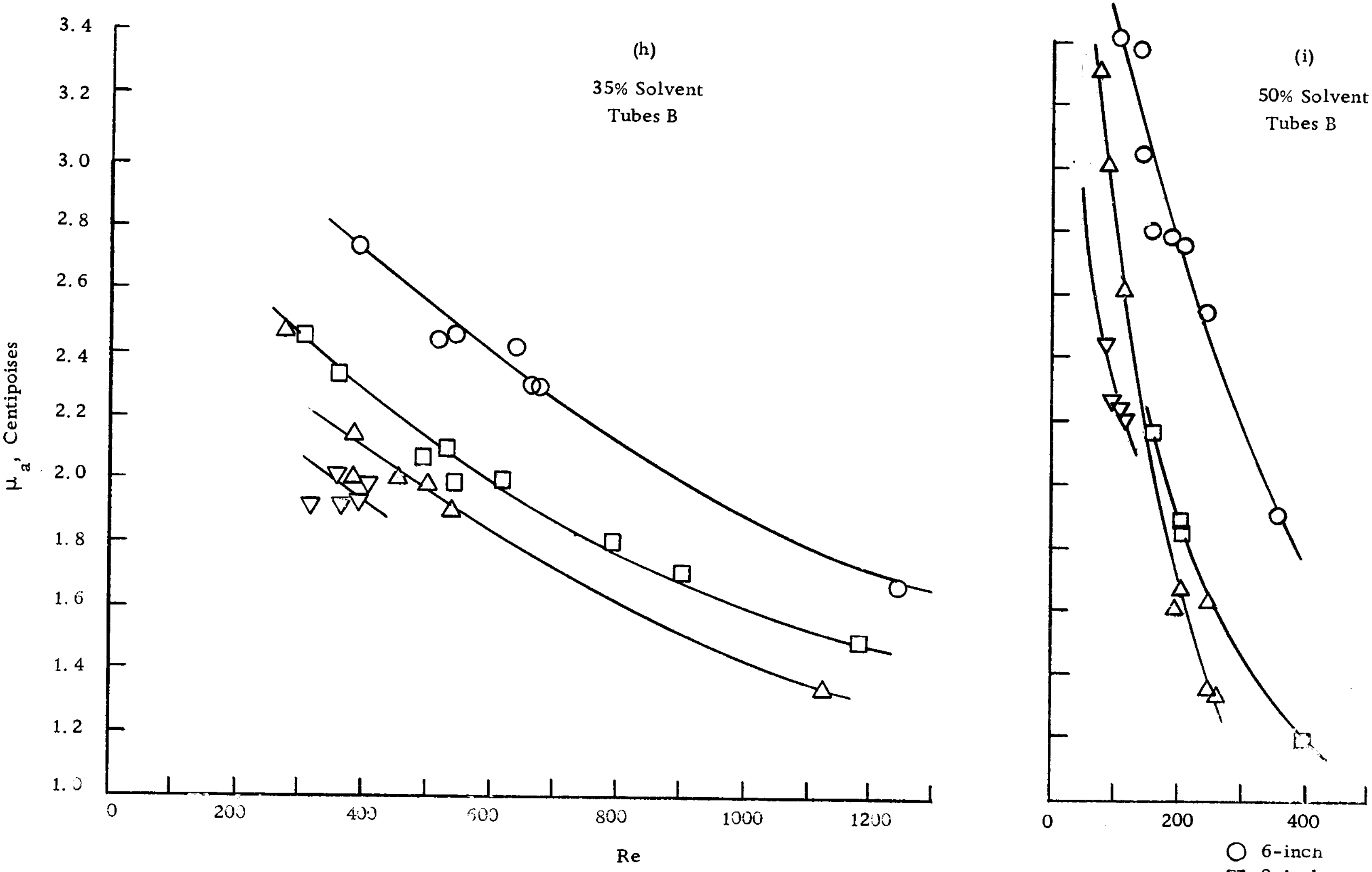

Figure 6 h, i. Laminar Flow Viscosities

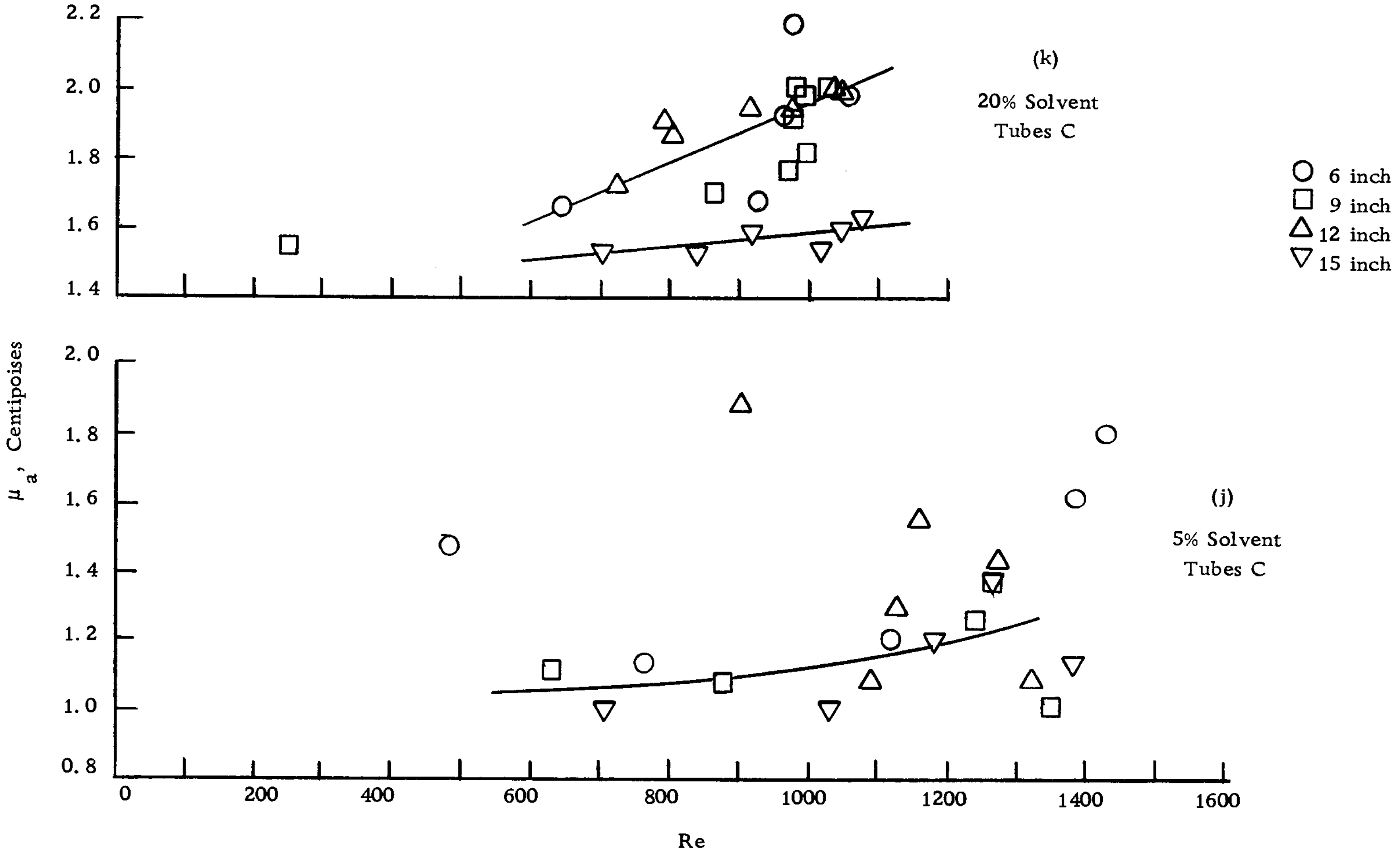

Figure 6 j, k. Laminar Flow Viscosities

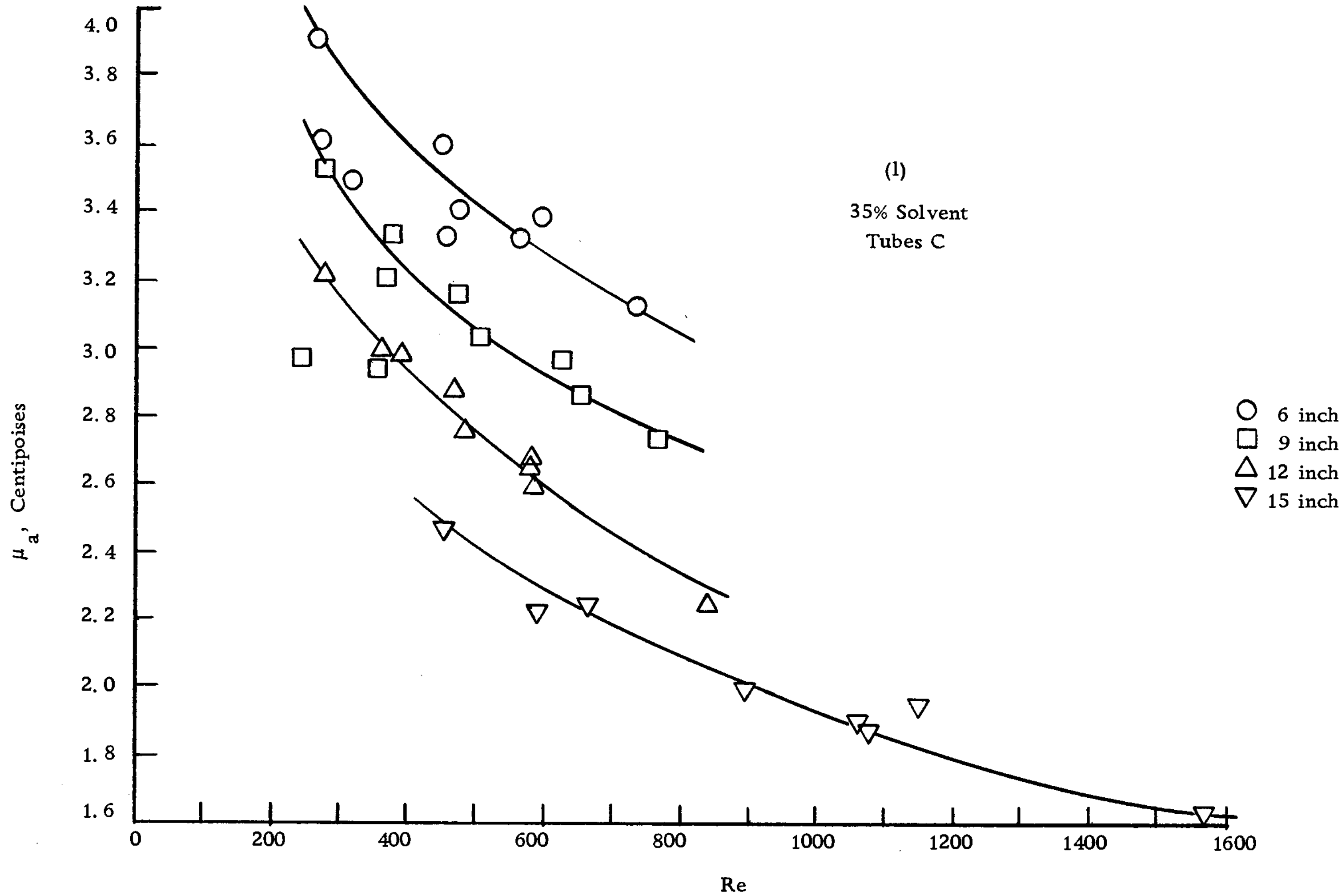

Figure 6 1. Laminar Flow Viscosities

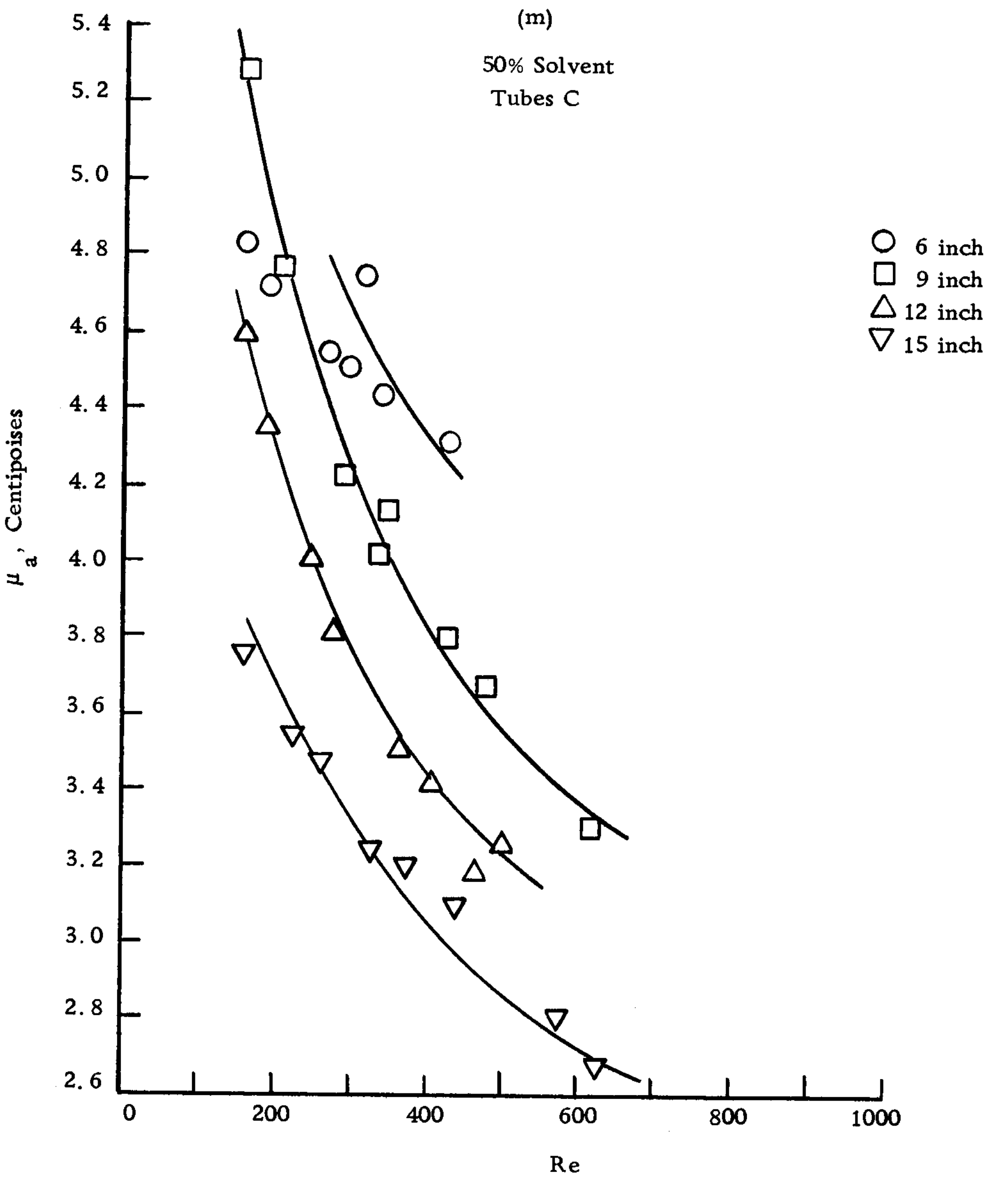

Figure 6 m. Laminar Flow Viscosities

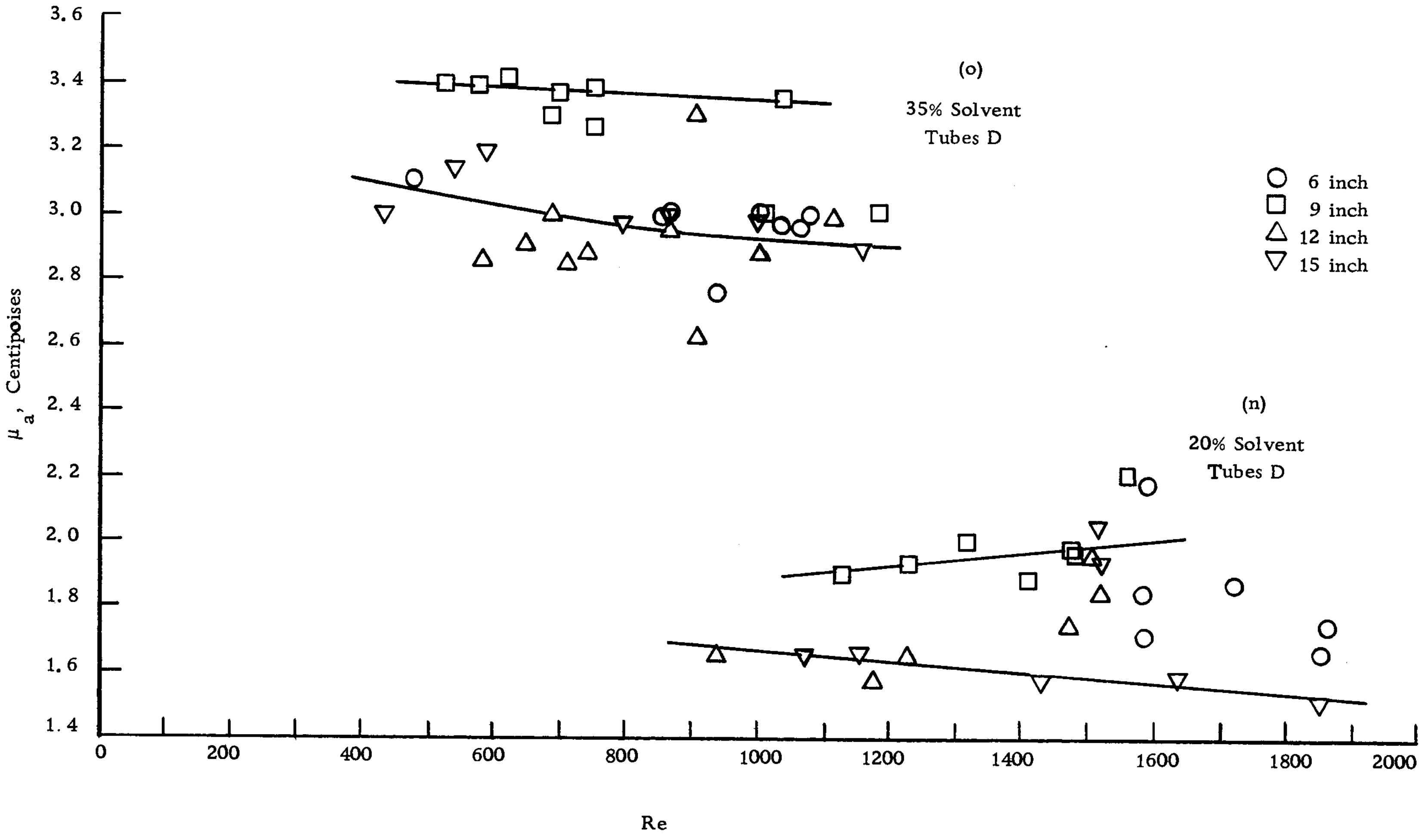

Figure 6 n, o. Laminar Flow Viscosities

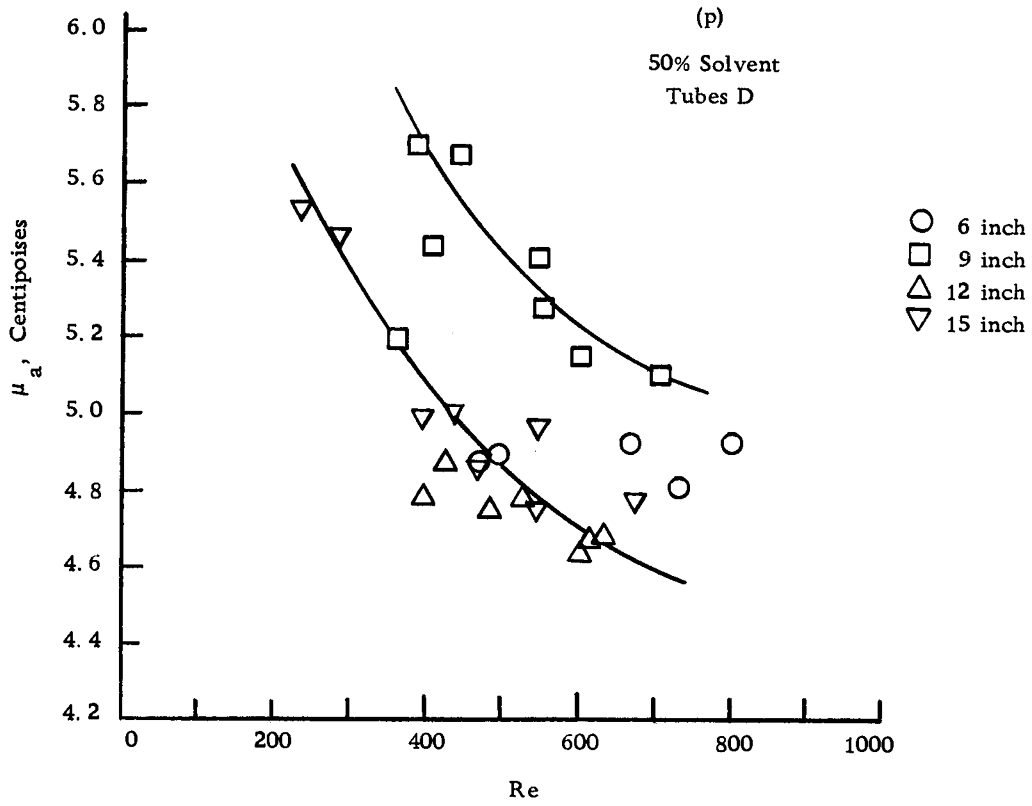

Figure 6 p. Laminar Flow Viscosities

6l and 6m for tubes C and Figures 6n, 6o, and 6p for tubes D. Several generalizations can be made concerning the behavior of the dispersions. The measured apparent viscosity increases with solvent concentration, it increases with tube diameter for a given length and composition, and it decreases with tube length for a given diameter and composition. The apparent viscosity decreases with an increase in Reynolds number. For dilute concentrations in the larger diameter tubes, Figures 6j, 6k and 6n, the viscosity appears to increase with increasing Reynolds numbers.

Figures 6c, 6f and 6j show comparable viscosities for the 5% dispersions. Comparison of Figures 6d, 6g, 6k and 6n however, show that, for the 20% dispersions, the viscosity increases with increasing diameter. This is more clearly evident with the 35% dispersions, Figures 6e, 6h, 6l and 6o, and the 50% dispersions, Figures 6i, 6m and 6p. For the 50% dispersions, at Re = 400, tube C-9 gave a viscosity 25% higher than tube B-9, while tube D-9 gave a value 30% higher than tube C-9.

Many previous workers (16, 28, 57) have noticed this diameter effect for solid suspensions. This has been called the Sigma effect (16). The phenomenon is explained on the basis of radial migration of particles toward the faster moving liquid at the tube axis, thus causing a reduction of the apparent viscosity because of the liquid layer adjacent to the wall. Such a migration has been observed experimentally (28) by differences between the inlet and exit concentrations of the capillary. There is also photographic evidence of this migration (23, 48, 58).

To explain the effect of radial migration on the apparent viscosity, Maude (28) postulated that the amount of displacement is a function of particle diameter and not the tube diameter. As the thickness of the liquid layer adjacent to the wall depends upon the particle diameter rather than the tube size, its importance increases as the diameter of the tube is reduced, explaining the observed effect that the measured viscosity decreases with decreasing tube diameter.

Cengal et al. (5), working with a liquid-liquid dispersion, reported a viscosity increase with tube diameter for solvent concentrations greater than 20%. He also attributed this to radial migration. Assuming that the thickness of the continuous phase liquid adjacent to the wall is the same regardless of the tube diameter, this liquid layer would have a greater effect for the smaller diameter tubes since it represents a larger portion of the total fluid in the tube. In this respect, it can be assumed that the larger diameter tubes give a more accurate value for the viscosity of the dispersion.

For the 5% dispersions, in Figure 6c, only the 15-inch tube data can be differentiated from the others, while for Figures 6f and

6j, no effect of tube length is observed. For the 20% dispersions, data fall on separate curves for all the A and B tubes, Figures 6d and 6g, while separate curves are apparent only for the 15-inch C and D tubes in Figures 6k and 6n. For the 35% and 50% dispersions, Figures 6e, 6h, 6i, 6l and 6m show separate curves for each tube length of tubes A, B and C, and for the 9-inch D tubes in Figures 6o and 6p. From these results, there appears to be a concentration-tube diameter effect related to the tube length, that is, tube lengths influence the apparent viscosity only above a certain concentration for a given tube diameter.

In practically all cases where the tube length has an effect, the viscosity decreases with increasing tube length. This again may be explained on the basis of radial migration of the dispersed solvent particles or on the basis of phase separation. For a constant diameter, as the tube length is increased, the residence time of the fluid in the tube increases for a given velocity. With a greater residence time the formation of a layer of the continuous phase near the wall may be enhanced. Also phase separation of the unstable dispersion could be of importance. Phase separation may occur in the form of a slug of solvent surrounded by a film of water adjacent to the wall. In either case, the measured pressure drop for a given length is reduced due to the lubricating action of the pure water adjacent to the wall.

For dispersions of 20% and higher concentrations, the apparent viscosity decreased with increasing Reynolds numbers. This behavior, which typifies a pseudoplastic fluid, has been observed by other workers studying various non-Newtonian systems (13, p. 84, 43), and in fact appears to hold for the majority of non-Newtonian systems. Ostwald (37) described three separate flow regimes: (I) low rates of shear where viscosity decreased with increasing rate of shear, (II) intermediate rates of shear where viscosity was relatively constant, and (III) high rates of shear where the viscosity increased due to the onset of turbulence. Region I is clearly indicated in the figures. A tendency towards a constant viscosity can also be seen.

The usual physical explanation (13, p. 85, 59, p. 4) of pseudoplastic behavior is that intermolecular or interparticle interactions smoothly decrease with increasing rates of shear. Particles or molecules, initially randomly oriented, align during shear so that their interactions are minimized. Each layer of aligned particles move parallel to the other with little interaction of the particles between adjacent layers. Since the aligning forces of shear increase with increasing flow rate, the particles become progressively more perfectly aligned at higher shear rates, causing the apparent viscosity to continually decrease until at extremely high shear rates, no further perfection of alignment is possible.

Cengal *et al.* (5) questioned the apparent pseudoplasticity of their liquid-liquid system, claiming that the decrease in viscosity with flow rate could be caused by phase separation and drop coalescence in the capillary. However, it appears that their reasoning is faulty since phase separation would be more probable at low flow rates resulting in a reduced viscosity at these flow rates

In Figures 6j, 6k and 6n, there is observed a definite increase in viscosity with Reynolds number, indicating dilatant behavior. The usual explanation for dilatant behavior (13, p. 86) assumes a high concentration, so the present case cannot be explained in these terms. It may however be explained by phase separation at low flow rates which would account for the lower viscosity. At higher flow rates, the effect of phase separation would not be so significant because of low residence time in the tube.

Lindgren (26) observed, but left unexplained, a rectilinear increase of apparent viscosity with Reynolds number for a dilute suspension as well as for the flow of distilled water.

Deviation from Newtonian Behavior

Metzner and Reed (31) defined a characteristic quantity n', sometimes referred to as the flow-behavior index, which is a measure of the deviation of a fluid from Newtonian characteristics.

The quantity n' is defined as

$$n' = \frac{d\,(\log \frac{D\,\Delta P}{4L})}{d\,(\log \frac{32V}{\pi D^3})} \quad . \tag{20}$$

For many fluids, a plot of log $(D\Delta P/4L)$ versus log $(32V/\pi D^3)$ is a straight line, thus n' is constant and the fluid obeys the power law,

$$\tau = K \; (\frac{du}{dy})^{n'} \tag{21}$$

When $n' = 1$, the fluid is Newtonian; when n' is less than 1, the fluid is pseudoplastic; when n' is greater than 1, the fluid is dilatant. K', called the consistency index, defines the consistency of the fluid. The larger the value of K' the "thicker" or "more viscous" the fluid. For a Newtonian fluid, $n' = 1$ and $K' = \mu$.

Figure 7 is a log-log plot of $(D\,\Delta P)/(4L)$ versus $(32V)/(\pi D^3)$ for water (7a), solvent (7b), and for dispersions for tubes A (7c, 7d, 7e), tubes B (7f, 7g, 7h, 7i), tubes C (7j, 7k, 7l, 7m) and tubes D (7n, 7o, 7p). The values of n' are indicated, as determined by a least squares analysis of the data. Where distinguishable, n' is indicated for each length of tube at each concentration. It should be emphasized that the values of n' indicate the overall fluid behavior within the entire tube length. The fluid may behave differently at different portions of the tube length.

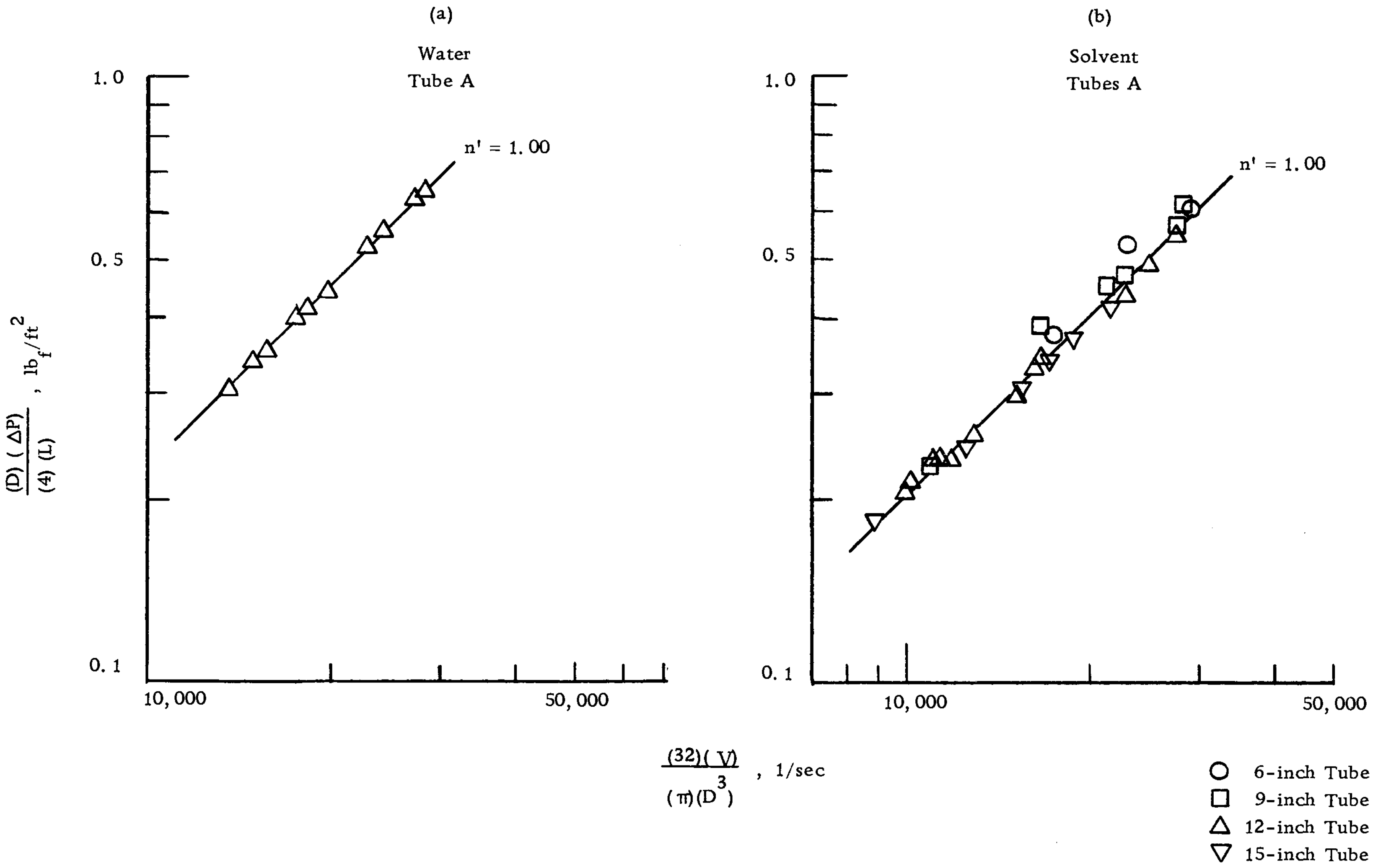

Figure 7 a, b. Shear Stress at Capillary Wall versus Reciprocal Second

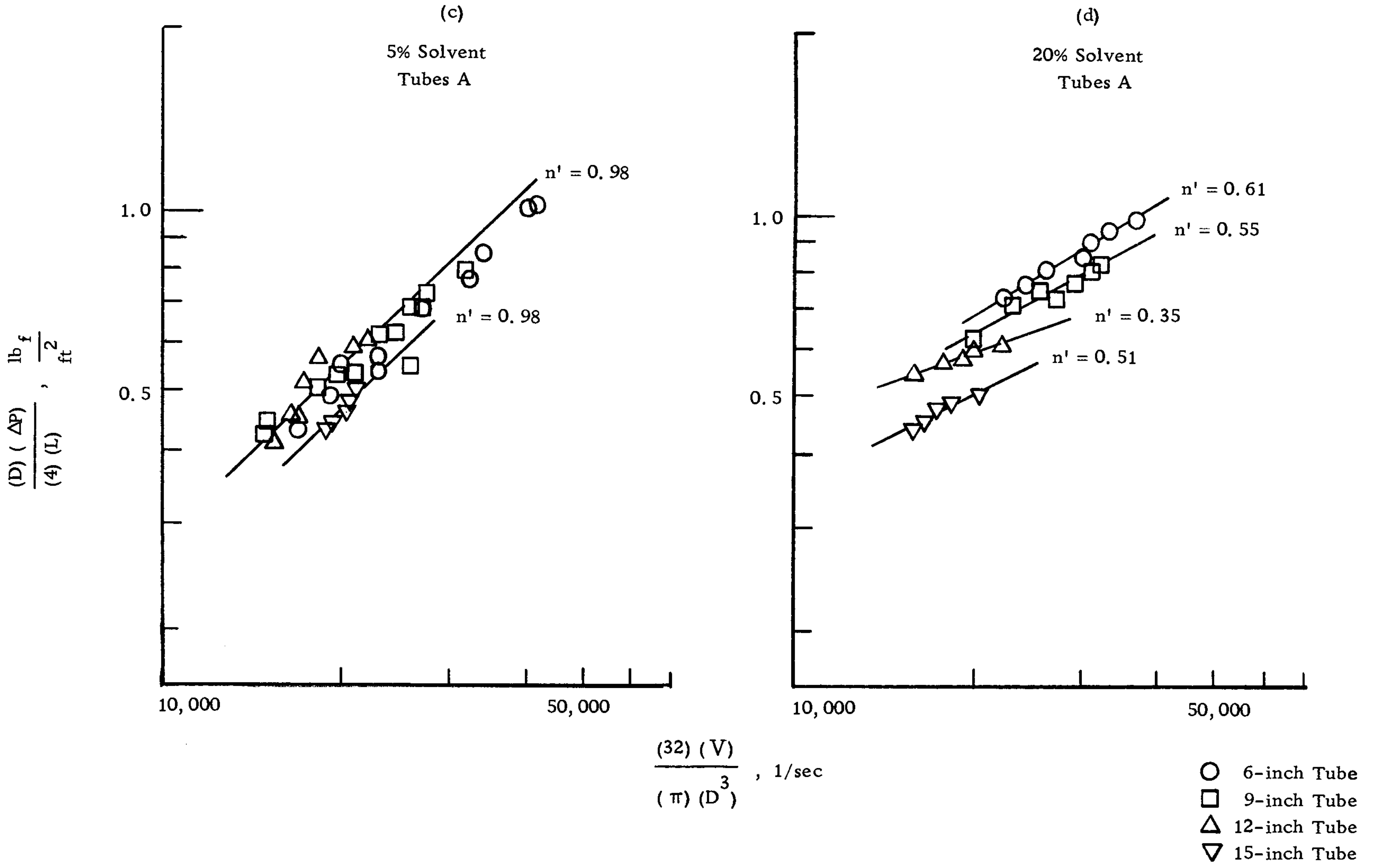

Figure 7 c, d. Shear Stress at Capillary Wall versus Reciprocal Second

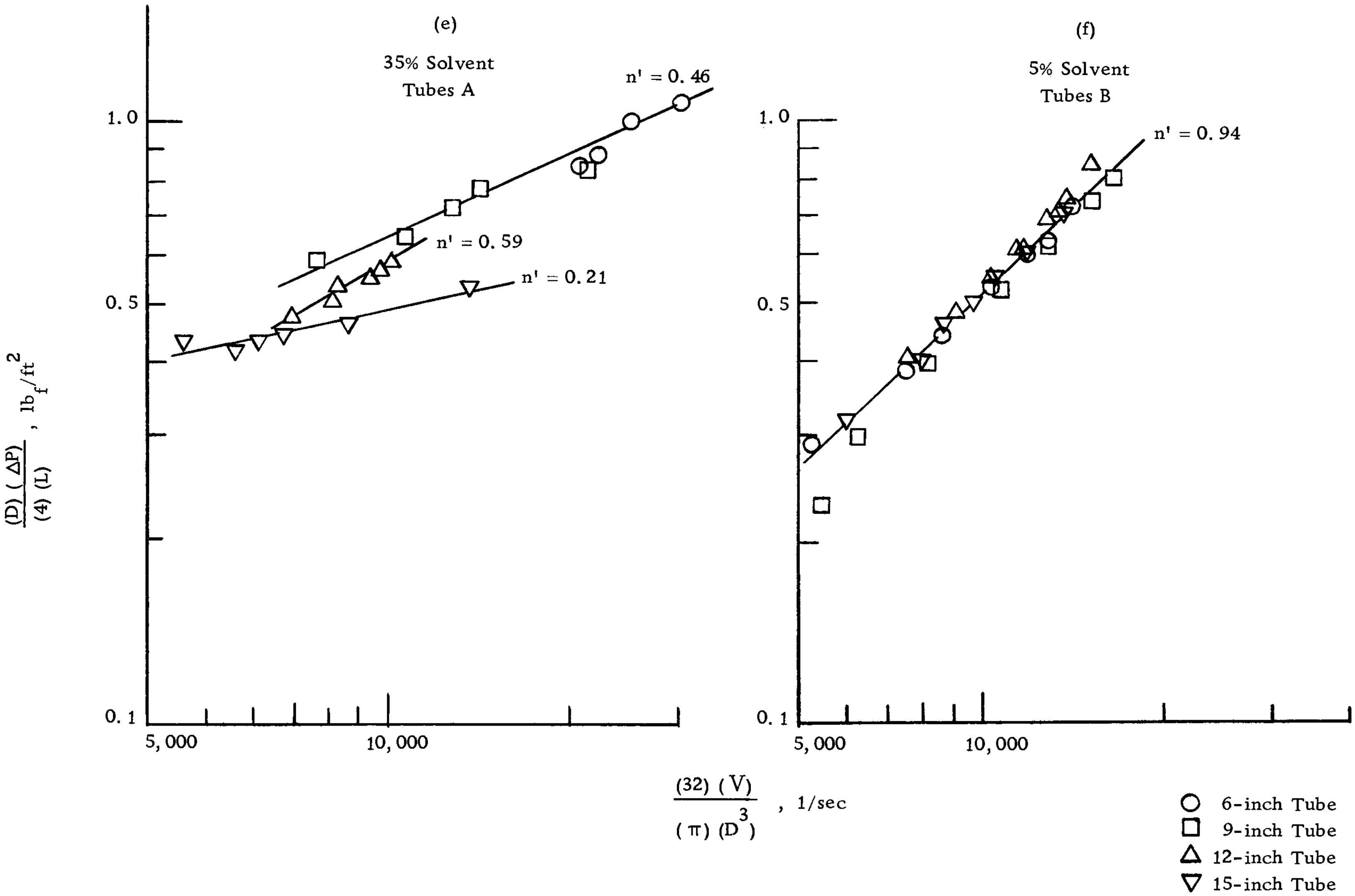

Figure 7 e, f. Shear Stress at Capillary Wall versus Reciprocal Second

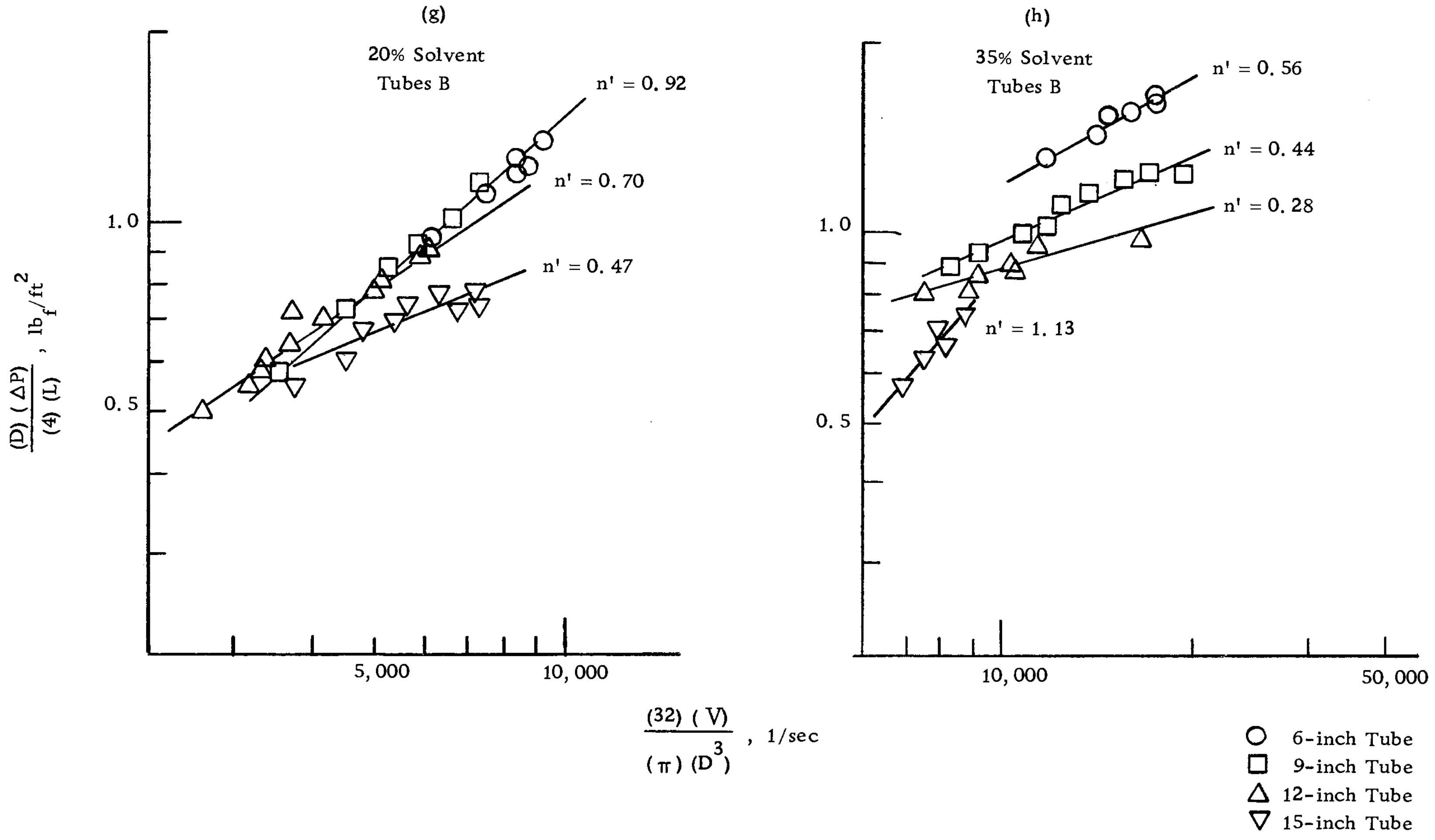

Figure 7 g, h. Shear Stress at Capillary Wall versus Reciprocal Second

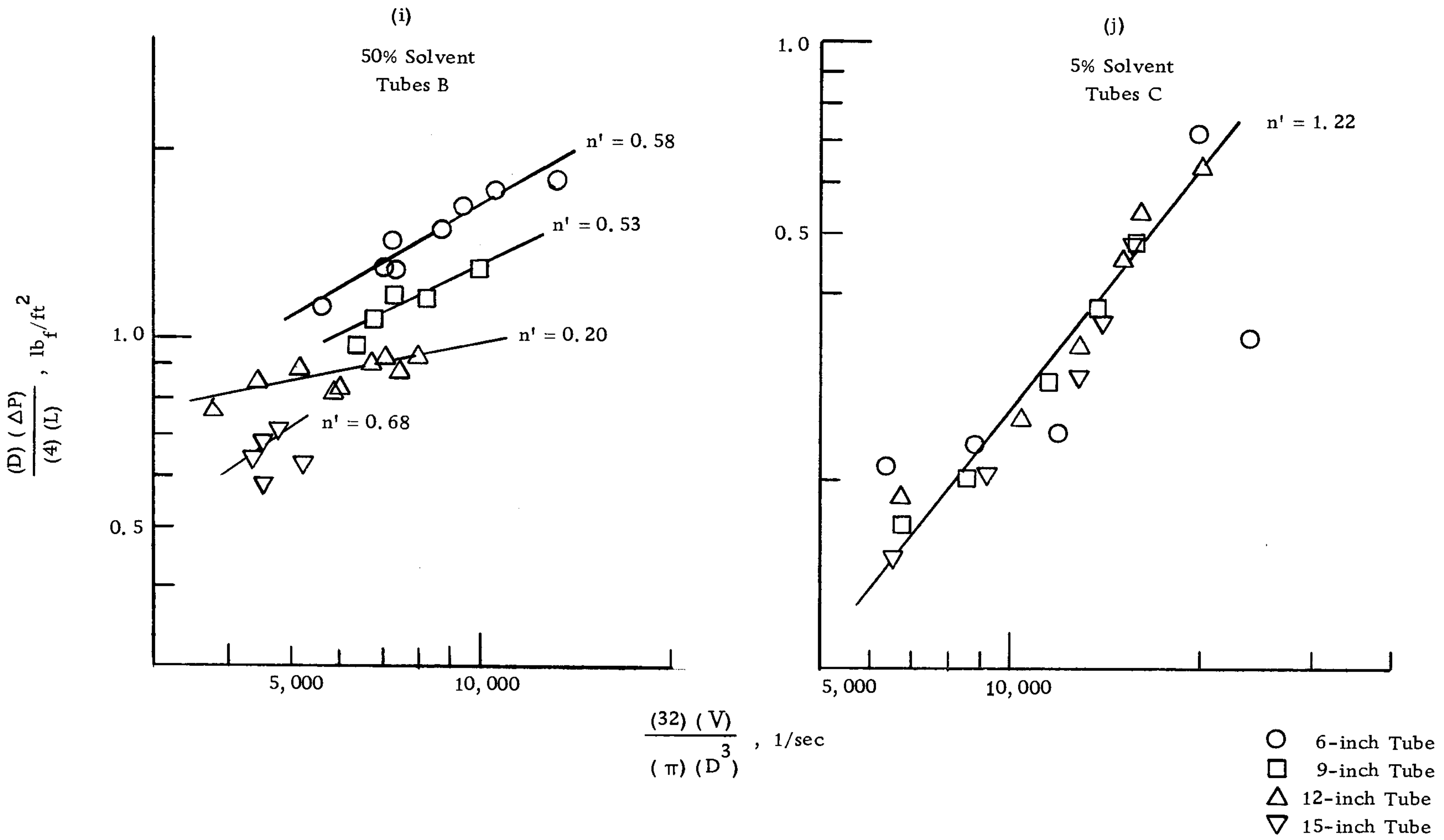

Figure 7 i, j. Shear Stress at Capillary Wall versus Reciprocal Second

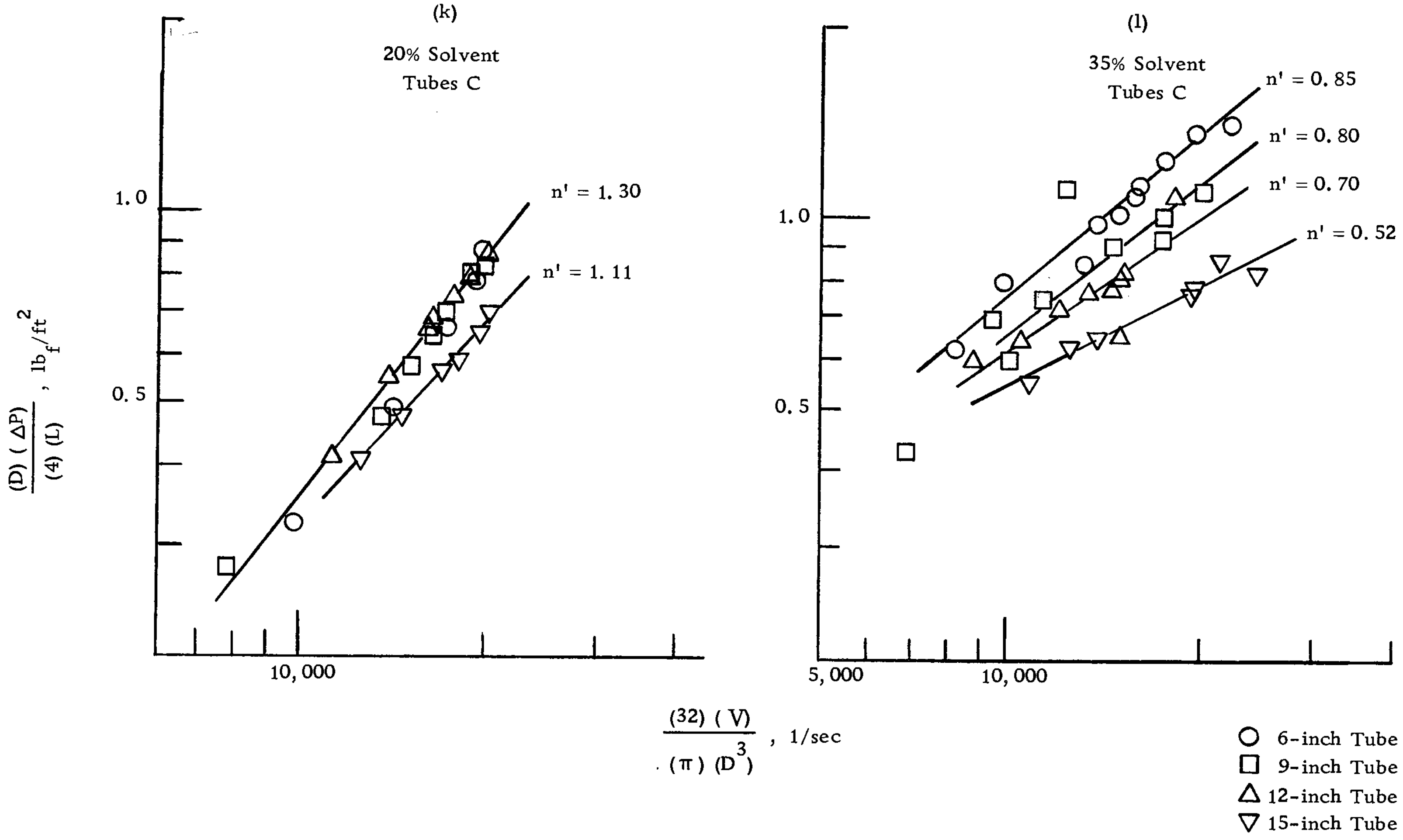

Figure 7 k, 1. Shear Stress at Capillary Wall versus Reciprocal Second

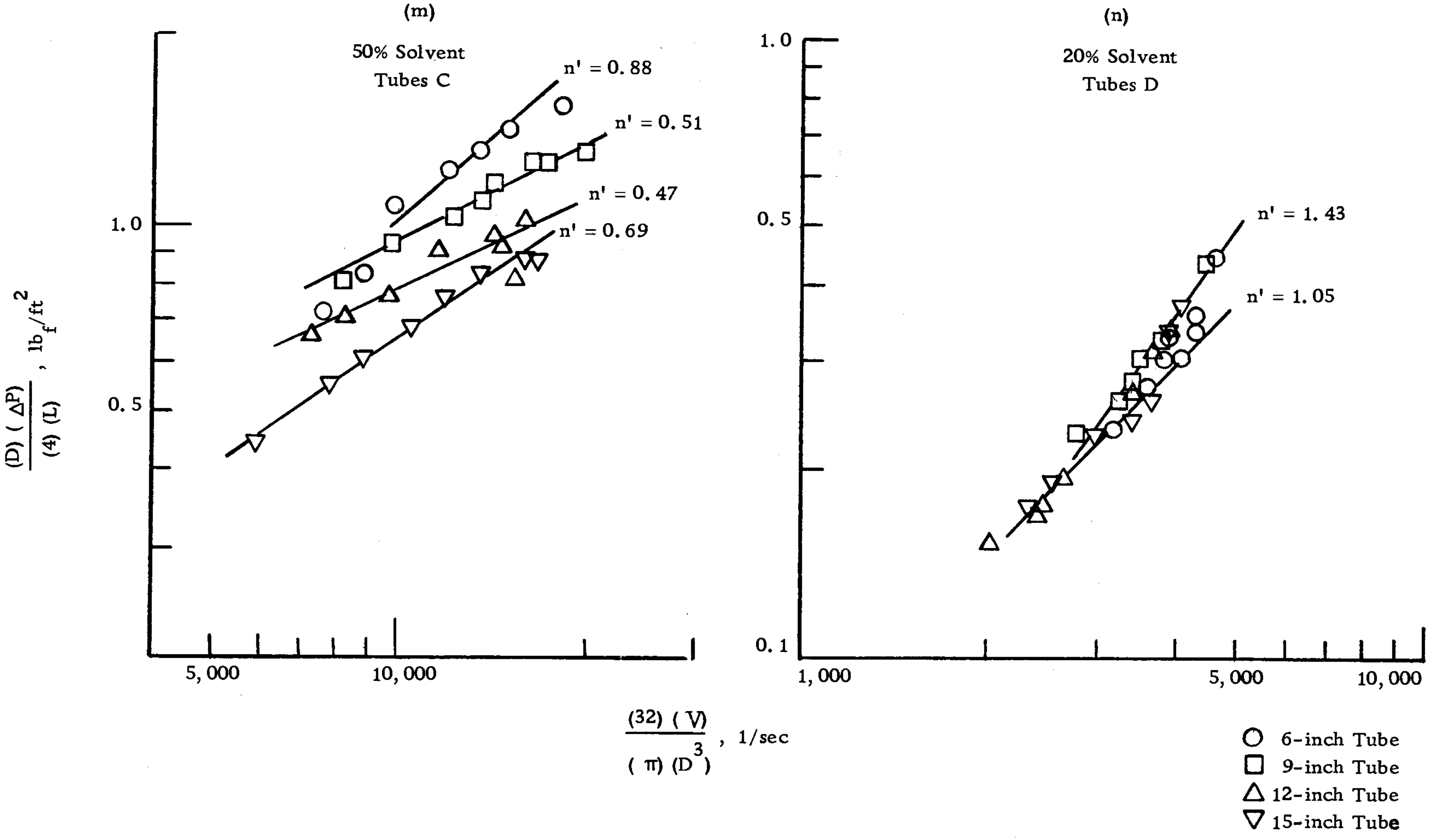

Figure 7 m, n. Shear Stress at Capillary Wall versus Reciprocal Second

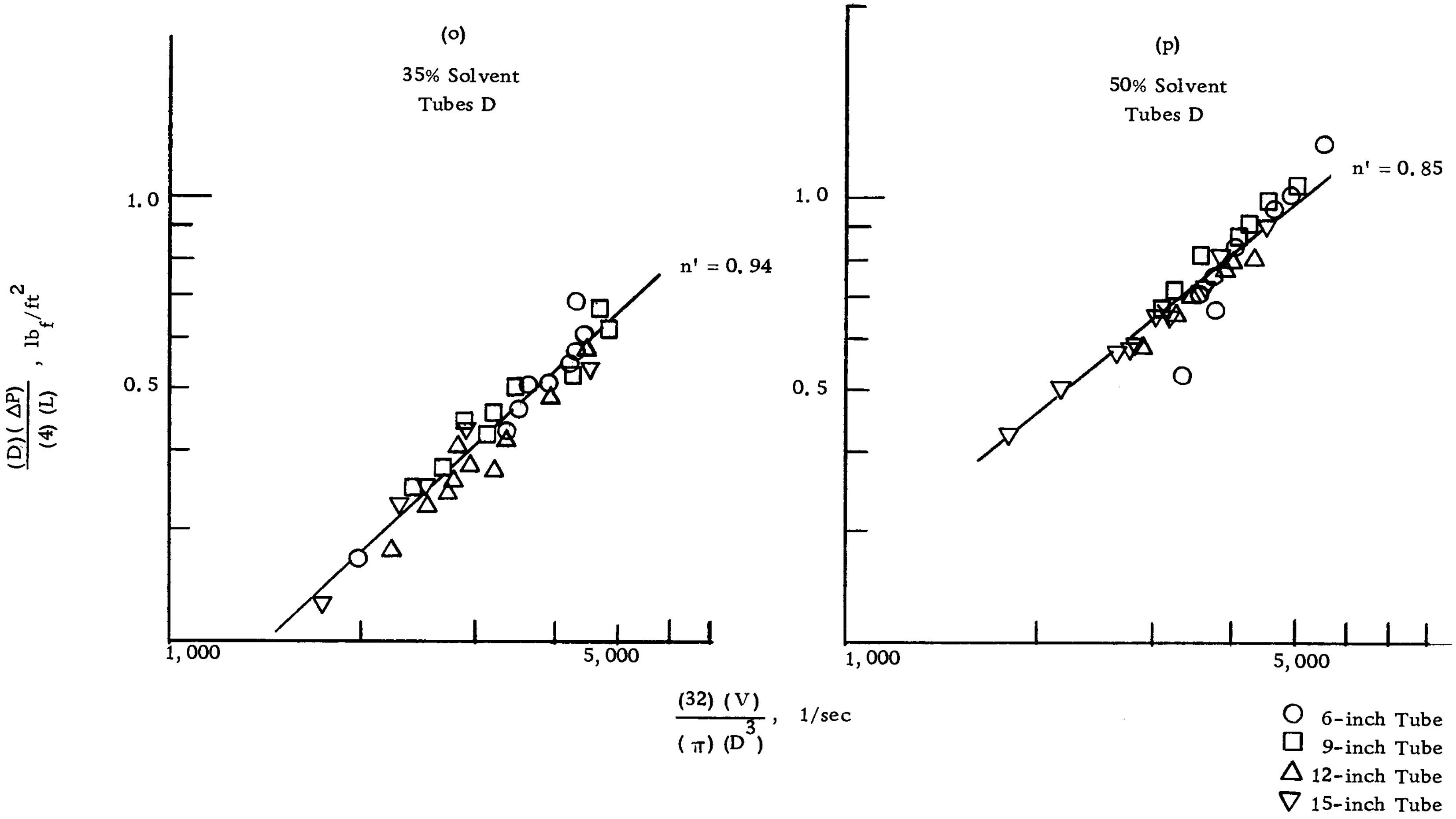

Figure 7 o, p. Shear Stress at Capillary Wall versus Reciprocal Second

For water and solvent, Figures 7a, and 7b, n' is 1.00 as it should be for Newtonian fluids. In most of the other cases n' is less than 1.00 indicating pseudoplastic behavior. For the 5% and 20% cases for tubes C, Figures 7j and 7k and the 20% case for tube D, Figure 7n, n' is greater than 1, indicating ditatant behavior. These results verify Figure 6.

Where values of n' are distinguishable for different tube lengths, these values generally decrease as the tube length increases. Also n' increases with tube diameter for a given length and concentration. This behavior is in agreement with Figure 3. Since the range of Reynolds numbers is well within the laminar region, there is either slip at the wall or some other anomalous behavior, or the fluid is time-dependent, i.e. thixotropic. If the fluid is time-independent, the values of n' can be explained according to the radial migration or phase separation effects previously presented.

Chinai and Schneider (8) determined the flow curves for a 10% copolymer solution obtained with capillary tubes of different lengths and same diameters. In agreement with Figure 3, they observed that the wall shear stress corresponding to a given shear rate decreased with an increase of tube length. Metzner and Brodkey (30) reported similar findings.

Figure 8 shows the effect of tube dimensions, in terms of the L/D ratio, on the flow-behavior indices for different dispersion

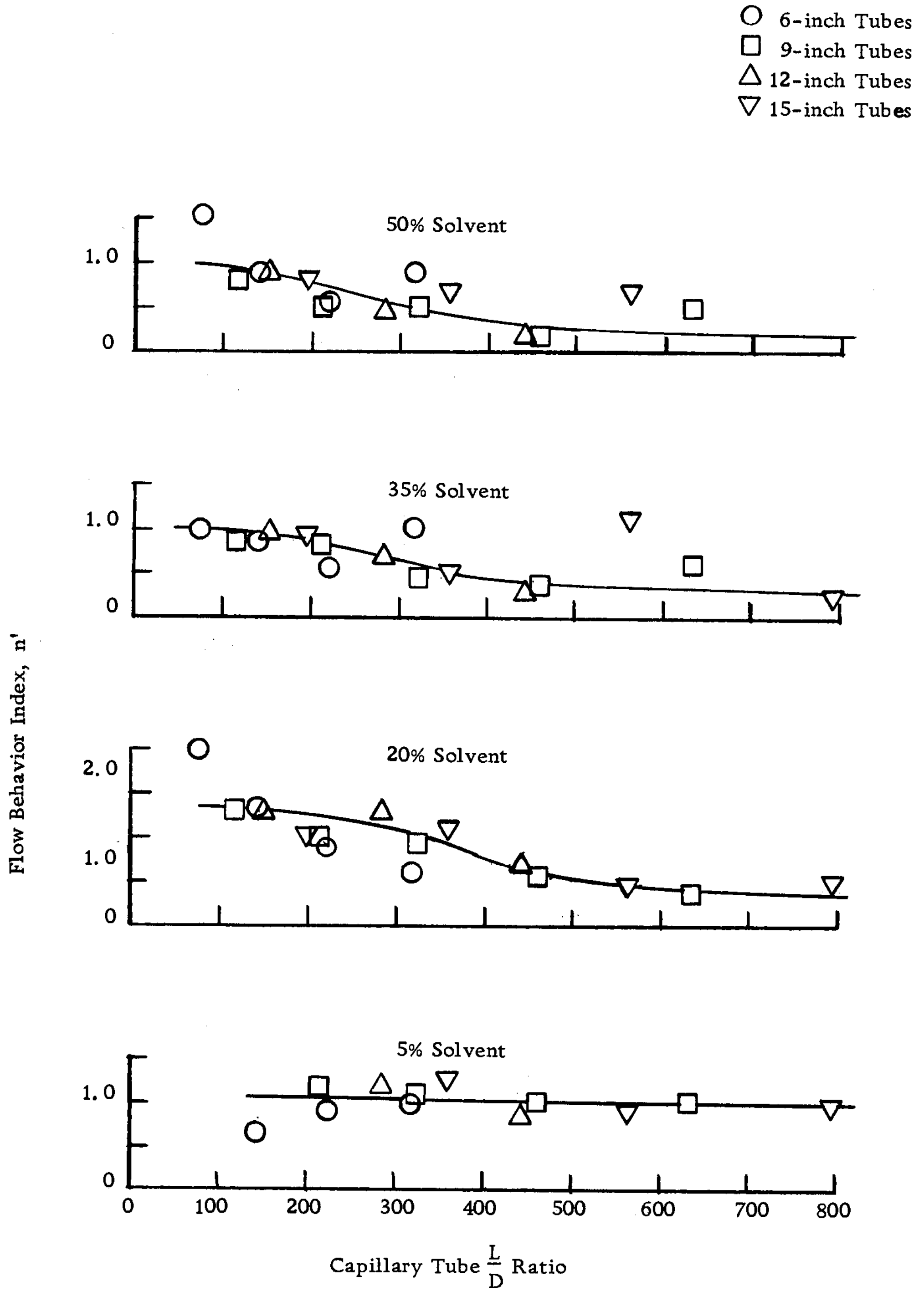

Figure 8. Flow-Behavior Index versus Capillary Tube $\frac{L}{D}$ Ratio

concentrations. The 5% dispersion demonstrates Newtonian behavior. Although the other dispersions are Newtonian at low values of L/D, they exhibit pseudoplasticity at higher L/D ratios. Again, this may be explained on the basis of radial migration or phase separation. At higher values of L/D, the probability is greater for the existence of the pure continuous phase adjacent to the wall.

In Figures 9a, 9b, 9c, and 9d the corrected pressure drop ΔP, is plotted versus tube length for the 5%, 20%, 35% and 50% dispersions respectively. Results are shown for different tube diameters at a mass flux of 720 $g/(sec)(in)^2$ or about 5 in/sec. Since there are only four data points for each curve, a detailed quantitative analysis is not justified. However various trends are indicated in these figures.

For a given tube diameter, the slope of $\Delta P/L$ increases with concentration, indicating that the apparent viscosity increases with concentration. For tubes of larger diameter i.e. tubes B and C in Figure 9a, and tube D in Figures 9b, 9c and 9d, $\Delta P/L$ is a straight line, indicating that the viscosity is constant throughout these tubes. However the other curves show a decrease in $\Delta P/L$ with increasing tube length. This is a strong indication of the presence of a lubricating film adjacent to the tube wall which becomes significant as the tube diameter decreases and the tube length increases. The decreasing slope of $\Delta P/L$ is especially evident for

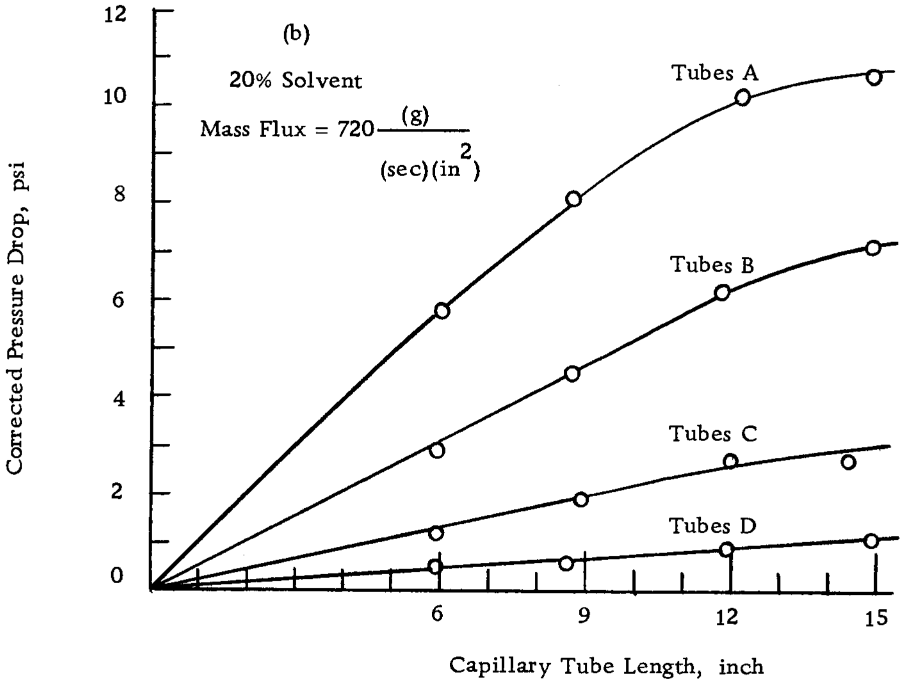

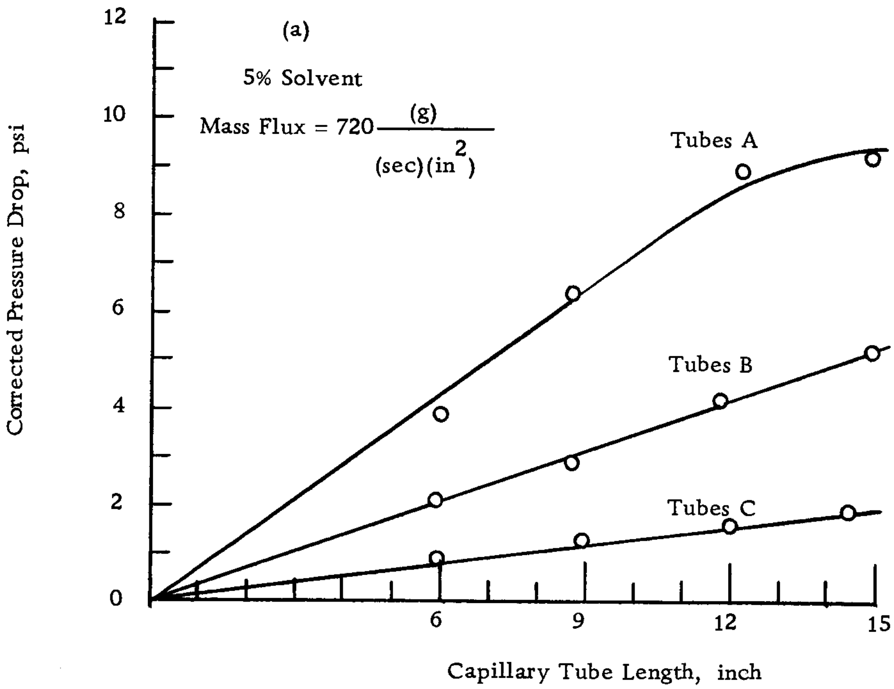

Figure 9 a, b. Corrected Pressure Drop versus Capillary Tube Length

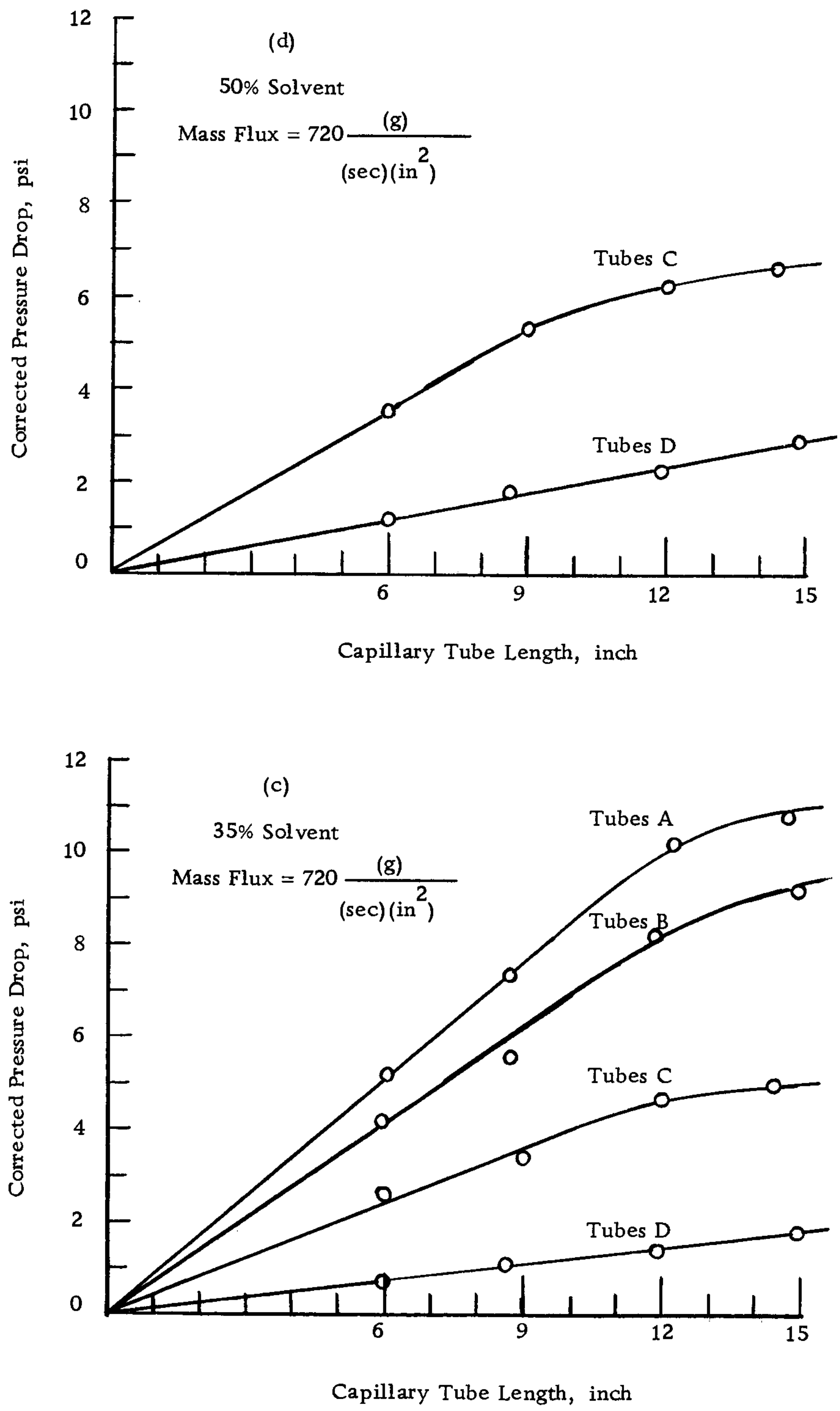

Figure 9 c, d. Corrected Pressure Drop versus Capillary Tube Length tubes A in Figure 9b and tubes C in Figure 9d.

These figures are especially informative since they indicate that the fluid behaves differently at different portions along the tube length. Where Figures 6, 7 and 8 showed that the dispersions acted as a pseudoplastic fluid, Figure 9 gives a better insight of why this is so, i.e. $\Delta P/L$ decreases with tube length. However, the cause of this can only be speculated as arising from either radial migration or phase separation.

In Figure 10, the relative fluidity, defined as the ratio of the viscosity of the continuous phase to the viscosity of the dispersion, is plotted as a function of the volume fraction of the dispersed phase for tubes A, B, C and D. The dispersion viscosities are those determined from the initial slopes of the curves in Figure 9. For comparison a previously determined curve (5) for liquid-liquid dispersions in turbulent flow is included, denoted by the dashed line. This curve fits the relationship $\mu_c/\mu_m = e^{-2.5\phi}$ which is applicable at room temperature and is restricted to dispersions with viscosity ratio range $1.0 < \frac{\mu_d}{\mu_c} < 15.0$ where μ_d is the viscosity of the dispersed phase.

The curves of tubes A, B, C and D indicate again that the dispersion viscosity increases with tube diameter at high concentrations. The good agreement with the curve for turbulent flow indicates that the dispersion viscosity in laminar flow is comparable to the viscosity in fully developed turbulent flow.

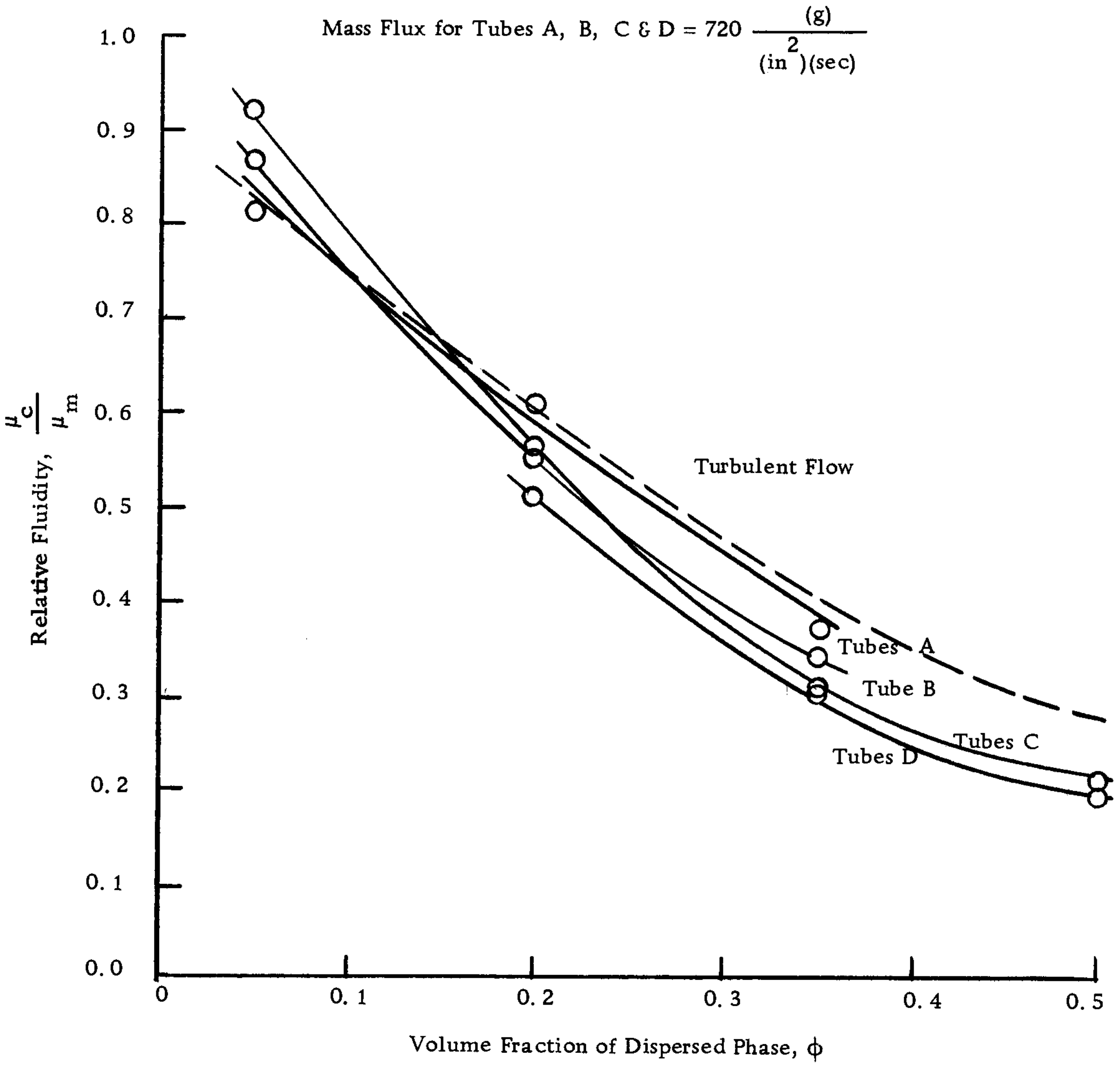

Figure 10. Relative Fluidity versus Volume Fraction of Dispersed Phase

CONCLUSIONS

A study has been made of the effect of tube dimensions on the laminar low viscosities of an unstable liquid-liquid dispersion. The dispersion was composed of a petroleum solvent in water.

Laminar flow viscosities, measured using a number of capillary tubes of varying lengths and diameters, increased with solvent concentration and tube diameter and decreased with tube length and flow rate. The diameter and length effects may be explained by the presence of a film of the continuous phase adjacent to the wall, due either to radial migration of the solvent particles or phase separation and coalescence, or both.

In laminar flow the dispersions generally appear to behave as a pseudoplastic fluid, the viscosity decreasing with flow rate through the capillary. However this may also be a result of radial migration or phase separation.

It was observed that a dispersion behaves differently as it flows through the capillary tube, the pressure drop over a given increment of tube decreasing along the tube length.

The relationship of relative fluidity versus volume fraction of the dispersed phase compared favorably with the result of a previous study.

RECOMMENDATIONS FOR FURTHER WORK

The following recommendations for further investigation of liquid-liquid dispersions are suggested:

1. Use a photographic technique to observe any wall effects or phase separation.
2. Devise an accurate method to measure the static pressure at regular intervals along the capillary. This may provide a clue to the type of flow (finely dispersed, bubble, slug, annular, stratified, etc.) occuring in each increment.
3. Determine the entrance effect.
4. Study the effect of tube dimensions on the viscosities of other liquid-liquid dispersions.
5. Extend the study to cover solvent concentrations up to and beyond the point of inversion.

BIBLIOGRAPHY

1. Bagley, E. B. End corrections in the capillary flow of polyethylene. Journal of Applied Physics 28: 624-627. 1959.

2. Berkowitz, N., C. Moreland and G. F. Round. The pipeline flow of coal-in-water suspensions. Canadian Journal of Chemical Engineering 41: 116-121. 1963.

3. Broughton, G. and L. Squires. The viscosity of oil-in-water emulsions. Journal of Physical Chemistry 42: 253-263. 1938.

4. Cengel, John Anthony. Viscosity of liquid-liquid dispersions in laminar and turbulent flow. Master's thesis. Corvallis, Oregon State University, 1959. 110 numb. leaves.

5. Cengel, J. A. et al. Laminar and turbulent flow of unstable liquid-liquid emulsions. Journal of the American Institute of Chemical Engineers 8: 335-339. 1962.

6. Chappelear, D. C. and K. R. Nickolls. High viscosity suspensions. Chemical Engineering Progress 60: 45-49. August, 1964.

7. Charles, M. E., C. W. Govier and G. W. Hodgson. Horizontal pipeline flow of equal density oil-water mixtures. Canadian Journal of Chemical Engineering 39: 27-36. 1961.

8. Chinai, Suresh N. and William C. Schneider. High-shear capillary viscosity studies on concentrated copolymer solutions. Journal of Applied Polymer Science 7: 909-922. 1963.

9. Claesson, Stig and Ulv Lohmander. Non-Newtonian flow of macromolecular solutions studied by capillary viscometry with a millionfold change in the velocity gradient. Makromolecular Chemie 44-46: 461-478. 1961.

10. Cross, Malcolm M. Rheology of non-Newtonian fluids: a new flow equation for pseudoplastic systems. Journal of Colloid Science 20: 417-437. 1965.

11. De Bruijn, J. B. Suspensions and sedimentation. Nature 164: 220-222. 1949.

12. Dodge, D. W. Fluid systems. Industrial and Engineering Chemistry 51: 839-840. 1959.

13. Drew, Thomas B. and John W. Hoopes Jr. (eds.) Advances in chemical engineering. vol. 1. New York, Academic Press, 1956. 448 p.

14. Drew, Thomas B., John W. Hoopes and Theodore Vermuellens (eds). Advances in chemical engineering. vol. 4. New York, Academic Press, 1963. 374 p.

15. Einstein, A. Eine neue Bestimmung der Moleküldimensionen. Annalen der Physik 19: 289-306. 1906.

16. Eveson, G. F., R. L. Whitmore and Stacey G. Ward. Use of coaxial-cylinder viscometers and capillary tube viscometers for suspensions. Nature 166: 1074. 1950.

17. Finnigan, Jerome Woodruff. Pressure losses and heat transfer for the flow of mixtures of immiscible liquids in circular tubes. Ph. D. thesis. Corvallis, Oregon State University, 1958. 154 numb. leaves.

18. Ford, T. F. Viscosity-concentration and fluidity-concentration relationships for suspensions of spherical particles in Newtonian liquids. Journal of Physical Chemistry 64: 1168-1174. 1960.

19. Goldsmith, H. L. and S. G. Mason. The flow of suspensions through tubes. I. Single spheres, rods and discs. Journal of Colloid Science 17: 448-476. 1962.

20. Govier, G. W., G. A. Sullivan and R. K. Wood. Upward vertical flow of oil-water mixtures. Canadian Journal of Chemical Engineering 39: 67-75. 1961.

21. Higgenbotham, G. H., D. R. Oliver and S. G. Ward. Viscosity and sedimentation of suspensions. IV. Capillary-tube viscometry applied to stable suspensions of spherical particles. British Journal of Applied Physics 9: 372-377. 1958.

22. Karnis, A., H. L. Goldsmith and S. G. Mason. Axial migration of particles in Poiseuille flow. Nature 200: 159-160. 1963.

23. Karnis, A., H. L. Goldsmith and S. G. Mason. The flow of suspensions through tubes. Canadian Journal of Chemical Engineering 44: 181-193. 1966.

24. Langhar, Henry L. Steady flow in the transition length of a straight tube. Transactions of the American Society of Mechanical Engineers 64: A55-A58. 1942.

25. Leviton, Abraham and Alan Leighton. Viscosity relationships in emulsions containing milk fat. Journal of Physical Chemistry 40: 71-80. 1936.

26. Lindgren, E. Rune. The transition process and other phenomenon in viscous flow. Arkiv for Fysik 12: 1-169. 1957.

27. Maron, S. H. and A. W. Sisko. Application of Ree-Eyring generalized flow theory to suspensions of spherical particles, II. Flow in low shear regions. Journal of Colloid Science 12: 99-107. 1957.

28. Maude, A. D. and R. L. Whitmore. The wall effect and the viscometry of suspensions. British Journal of Applied Physics 7: 98-102. 1956.

29. Merrill, Edward W. Basic problems in the viscometry of non-Newtonian fluids. ISA Journal 2: 462-465. 1955.

30. Metzger, Alfred P. and Robert S. Brodkey. Measurement of the flow of molten polymers through short capillaries. Journal of Applied Polymer Science 7: 399-410. 1963.

31. Metzner, A. B. and J. C. Reed. Flow of non-Newtonian fluids-correlation of the laminar, transition, and turbulent-flow regions. Journal of the American Institute of Chemical Engineers 1: 434-40. 1955.

32. Mooney, M. The viscosity of a concentrated suspension of spherical particles. Journal of Colloid Science 6: 162-170. 1951.

33. Nishimura, Norio. Viscosities of concentrated polymer solutions. Journal of Polymer Science, General Papers 3: 237-253. 1965.

34. Oldroyd, J. G. Elastic and viscous properties of emulsions and suspensions. Proceedings of the Royal Society of London, ser. A, 218: 122-132. 1958.

35. Oliver, D. R. Influence of particle rotation on radial migration in the Poiseuille flow of suspensions. Nature 194: 1269-1271. 1962.

36. Oliver, D. R. and Stacey G. Ward. Relationship between relative viscosity and volume concentration of stable suspensions of spherical particles. Nature 171: 396-397. 1953.

37. Ostwald, Wölfgang. Ueber die Geschwindigkeitsfunktion der Viskositat disperser systeme. I. Kolloid-Zeitschrift 36: 99-117. 1926.

38. Pepper, D. C. and P. P. Rutherford. The viscosity anomoly at low concentrations with polystyrenes of low molecular weight. Journal of Polymer Science 35: 299-301. 1959.

39. Perry, John H. (ed.). Chemical engineers' handbook. 3rd ed. New York, McGraw Hill, 1950. 1941 p.

40. Philippoff, W. and K. Hess. Zum viscositätsproblem bei organischen Kolloiden. Zeitschrift für Physikalische chemie, Abt. B., 32: 237-255. 1936.

41. Ram, Arie and Abraham Tamir. A capillary viscometer for non-Newtonian liquids. Industrial and Engineering Chemistry 56: 47-53. February, 1964.

42. Richardson, E. G. The flow of emulsions. II. Journal of Colloidal Science 8: 367-373. 1953.

43. Roller, Paul S. and C. Kerby Stoddard. Viscosity and rigidity of structural suspensions. Journal of Physical Chemistry 48: 410-425. 1944.

44. Roscoe, R. The viscosity of suspensions of rigid spheres. British Journal of Applied Physics 3: 267-269. 1952.

45. Rutgers, R. Relative viscosity and concentration. Rheologica Acta 2: 205-248. 1962. (Abstracted in Chemical Abstracts 59: 2199b. 1963)

46. Saunders, Frank L. Rheological properties of monodisperse latex systems. I. Concentration dependence of relative viscosity. Journal of Colloid Science 16: 13-22. 1961.

47. Segré, G. and A. Siberberg. Non-Newtonian behavior of dilute suspensions of macroscopic spheres in a capillary viscometer. Journal of Colloid Science 18: 312-317. 1963.

48. Segré, G. and A. Siberberg. Radial particle displacement in Poiseuille flow of suspensions. Nature 189: 209-210. 1961.

49. Shaver, Robert G. and Edward W. Merrill. Turbulent flow of pseudoplastic polymer solutions in straight cylindrical tubes. Journal of the American Institute of Chemical Engineers 5: 181-188. 1959.

50. Sherman, P. Studies in water-in-oil emulsions. I. The influence of dispersed phase concentration on emulsion viscosity. Journal of the Society of Chemical Industry 69(sup. 2): S71-S75. 1950.

51. Sherman, P. The viscosity of emulsions. Rheologica Acta 2: 74-82. 1962. (Abstracted in Chemical Abstracts 57: 7934f. 1962)

52. Siebert, E. E. Determination of intrinsic viscosity of polyacrolein. Journal of Polymer Science, Pt. C, 8: 87-95. 1965.

53. Simha, Robert. A treatment of the viscosity of concentrated suspensions. Journal of Applied Physics 23: 1020-1024. 1952.

54. Taylor, G. I. The viscosity of a fluid containing small drops of another fluid. Proceedings of the Royal Society of London, ser. A, 138: 41-48. 1932.

55. Thomas, David G. Transport characteristics of suspensions: VIII. A note on the viscosity of Newtonian suspensions of uniform spherical particles. Journal of Colloid Science 20: 267-277. 1965.

56. Van Wazer, J. R. et al. Viscosity and flow measurement. New York, John Wiley, 1963. 406 p.

57. Vand, Vladimir. Viscosity of solutions and suspensions. Journal of Physical Chemistry 52: 277-321. 1948.

58. Whitmore, R. L. Viscous flow of disperse suspensions in tubes. In: Rheology of Disperse Systems: Proceedings of a Conference held at the University College of Swansea, 1957 (Abstract) Chemical Abstracts 54: 2836f. 1960.

59. Wilkinson, W. L. Non-Newtonian fluids. New York, Permagon Press, 1960. 138 p.

60. Young, D. F. Coring phenomena in flow of suspensions in vertical tubes. ASME - Paper 60 - HYD - 12. 1960. ASME Gas Turbine Power and Hydraulic Conference paper. 8 p. (Abstract) Mechanical Engineering 82: 97. June, 1960.

APPENDICES

APPENDIX A

NOMENCLATURE

Latin Letter Symbols

Symbol	Explanation	Typical units
A	Area	ft^2
a	Constant in viscosity equations	
b	Constant in viscosity equations	
D	Diameter	ft
du/dy	Velocity gradient	1/sec
F	Force	lb_f
G	Mass flow rate	g/sec
g	Gravitational acceleration	ft/sec^2
g_c	Conversion factor, 32.17	$(lb_m)(ft)/(lb_f)(sec)^2$
gpm	Gallons per minute	
h	Height of manometer fluid	ft
K'	Consistency index	cp
k	Einstein constant, 2.5	
L	Length	ft
N	Volume fraction in mixture	
n'	Measure of the non-Newtonian behavior of a fluid	
P	Pressure	lb_f/ft^2

psi	Pounds per square inch	
Q	Volumetric flow rate	ft^3/sec
Re	Reynolds number	
r	Radius	ft
t	Temperature	^oF
u	Velocity	ft/sec
V	Volume	ft^3
W	Mass flow rate	lb_m/sec
wt	Sample weight	g

Greek Letter Symbols

Symbol	Explanation	Typical units
Δ	Finite difference	
θ	Time	sec
μ	Viscosity	cp
μ_a	Apparent viscosity	cp
μ_c	Continuous phase viscosity	cp
μ_d	Dispersed phase viscosity	cp
μ_m	Dispersion viscosity	cp
π	Constant , 3.1416	
ρ	Density	lb_m/ft^3
τ	Shear force per unit area	lb_f/ft^2
ϕ	Volume fraction of dispersed phase	

Subscripts

Symbol	Explanation
a	Apparent
c	Continuous phase
d	Dispersed phase
f	Force (as in lb_f)
h	Manometer fluid
m	Medium or mass (as in lb_m)
s	Solvent
w	Water

APPENDIX B

SAMPLE CALCULATIONS

Capillary Tube Radius Determination

Since the radius of a tube is used to the forth power in calculating viscosities, an accurate determination is important. Mercury at room temperature was drawn into the bore of a previously tared capillary tube. The weight and length of the mercury column was measured, and the tube radius calculated by the following equations:

$$V = \frac{wt}{\rho} = \pi r^2 L$$

and

$$r = \sqrt{\frac{wt}{(\pi)(L)(\rho)(2.53)^3}}$$

where V is the volume of mercury, cm^3; wt, weight of mercury, g; r, capillary tube radius, in; and ρ, density of mercury, g/cm^3.

For example, for capillary tube C-12, where wt=1.018 ± 0.003 g, $\rho = 13.53 \pm 0.01$ g/cm^3 and $L = 3.332 \pm 0.005$,

$$r = \sqrt{\frac{(1.018)}{(\pi)(3.332)(13.53)(2.53)^3}}$$

$$= 0.0209 \pm 0.0001 \text{ in.}$$

The probable error, $\pm$ 0.0001 in was calculated by the formula,

$$p_r = \pm \sqrt{\left(\frac{\partial r}{\partial wt}\right)^2 s_{wt}^{\ 2} + \left(\frac{\partial r}{\partial L}\right)^2 s_L^{\ 2} + \left(\frac{\partial r}{\partial \rho}\right)^2 s_\rho^{\ 2}}$$

where p_r is the probable error in r and s is the probable error in wt, L and ρ.

Four determinations of r gave the values, 0.0209 in, 0.0209 in, 0.0208 in and 0.0209 in. The standard deviation was $\pm$ 0.0001 in., as calculated by

$$\delta = \pm \sqrt{\frac{\Sigma (d)}{n-1}}$$

where δ is the standard deviation, d is the deviation of a single observation and n is the number of observations. The final value of r was 0.0209 $\pm$ 0.0001 in.

Laminar Flow Viscosity

The apparent viscosity of the dispersions in laminar flow was calculated from the equation,

$$\mu_a = \frac{(\pi)(\Delta P)(\theta)(r)^4(p)}{(8)(L)(wt)} - \frac{(0.149)(wt)}{(\pi)(L)(\theta)}$$

where μ_a is the apparent viscosity, cp; ΔP, pressure drop across the tube, lb_f/in^2; θ, elapsed time of measurement, sec; L, tube length, in; wt, weight of dispersion collected, g; and p, conversion factor, 1.043×10^8 $(g)(cp)/(lb_f)(sec)(in)$.

For run 35-27 with tube C-12, length 11.97 ± 0.05 in and radius 0.0209 ± 0.0001, weight of efflux = 201.7 ± 0.1 g, $\Delta P = 29.7$ mm Hg corresponding to 5.41 ± 0.05 psi, and $\theta = 180 \pm 2$ sec,

$$\mu_a = \frac{(\pi)(5.41)(180)(0.0209)^4(1.043)(10^8)}{(8)(11.97)(201.7)} - \frac{(0.149)(201.7)}{(\pi)(11.97)(180)}$$

$$= 3.00 \pm 0.05 \text{ cp.}$$

The probable error was calculated as shown previously.

The Reynolds number was calculated by

$$Re = \frac{(D)(u)(\rho)}{\mu_a} = \frac{(4)(G)(p)}{(\pi)(D)(\mu_a)}$$

where D is the tube diameter, in; u, velocity of fluid, ft/sec; ρ, density, lb_m/ft^3; μ_a, apparent viscosity; cp; G, mass flow rates, g/ sec; and p, conversion factor, 39.37 (in)(sec)/(cp)(g).

For run 35-27,

$$Re = \frac{(4)(201.7)(39.37)}{(\pi)(0.0418)(180)(3.00)} = 362 \pm 10$$

Shear Stress at Capillary Wall

The shear stress at the capillary wall was calculated by

$$\frac{(D)(\Delta P)}{(4)(L)} .$$

This quantity was plotted on a log-log scale against a quantity proportional to the rate of shear at the wall,

$$\frac{(32)(Q)}{(\pi)(D^3)} ,$$

from which the non-Newtonian behavior of the particular flow system was indicated. In the above equations, ΔP is the pressure drop, lb_f/ft^2, corrected for entrance and exit effects using Equation (19); D and L, the diameter and length of the capillary tube in ft; and Q, the volumetric flow rate, ft^3/sec.

For run 35-27,

$$\frac{(D)(\Delta P)}{(4)(L)} = \frac{(0.00348)(871)}{(4)(0.992)}$$

$$= 0.645 \pm 0.006 \ \frac{lb_f}{ft^2}$$

and

$$\frac{(32)(Q)}{(\pi)(D^3)} = \frac{(32)(4.64)(10^{-5})}{(\pi)(0.00348)^3}$$

$$= 1.03 \pm 0.02 \times 10^4 \ \frac{1}{sec}$$

APPENDIX C

PROPERTIES OF FLUIDS AND MANOMETER CALCULATIONS

Solvent and Water

The solvent used was a clear, colorless, commercial cleaning solvent, Shellsolv 360, manufactured by the Shell Oil Company.

The solvent densities as a function of temperature, measured by Finnigan (17, p. 133) are presented in Figure 11. The density of water at various temperatures, from Perry (39, p. 175) are included. Solvent viscosities at various temperatures, also determined by Finnigan, are reported in Figure 12 along with water viscosities reported by Perry (39, p. 374).

The density of immiscible liquid mixtures, such as the solvent-water system studied, is an additive quantity and may be calculated from the mixture law,

$$\rho_m = N_w \rho_w + N_s \rho_s$$

where N_w is the volume fraction of water and N_s is the volume fraction of solvent in the mixture.

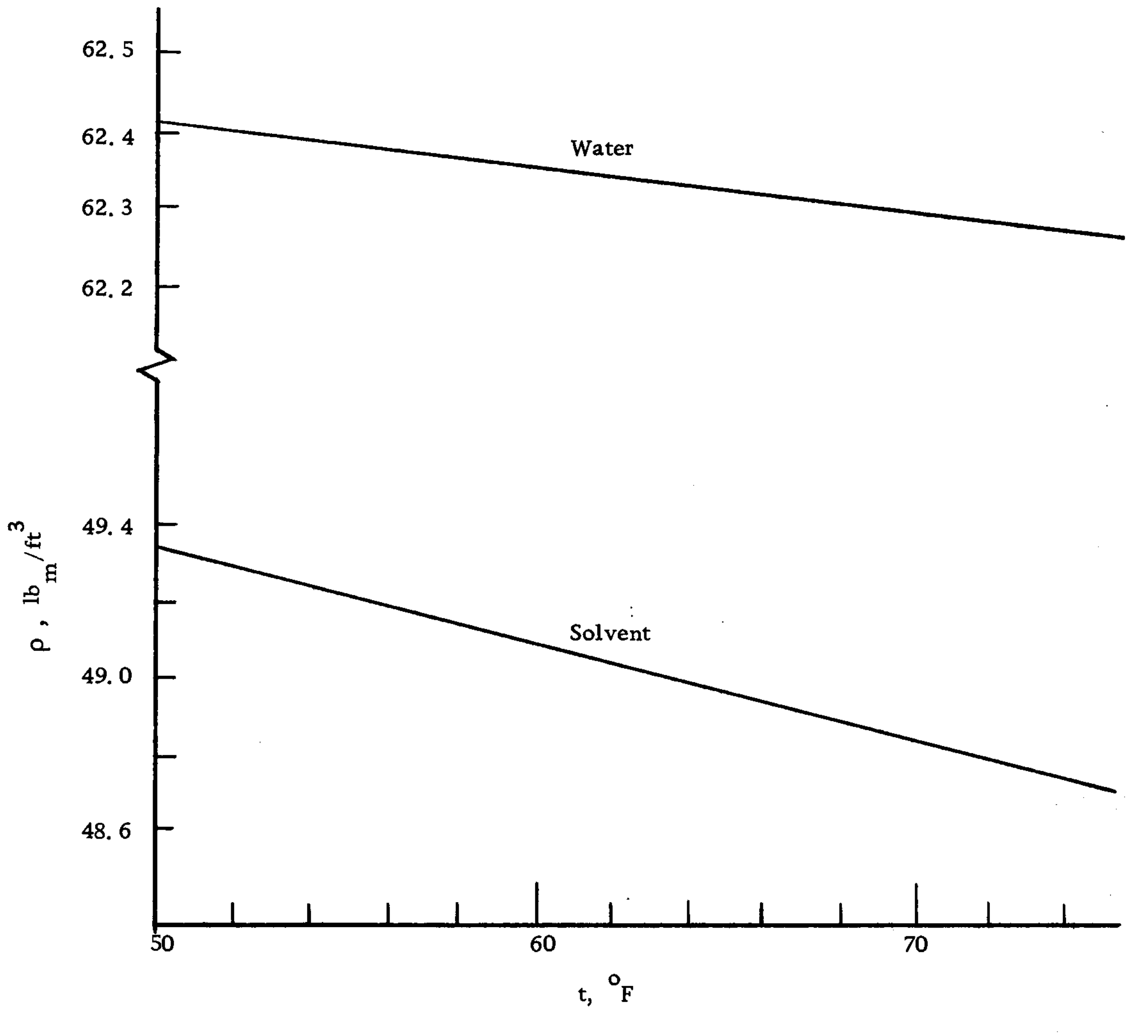

Figure 11. Density of Water and Solvent versus Temperature

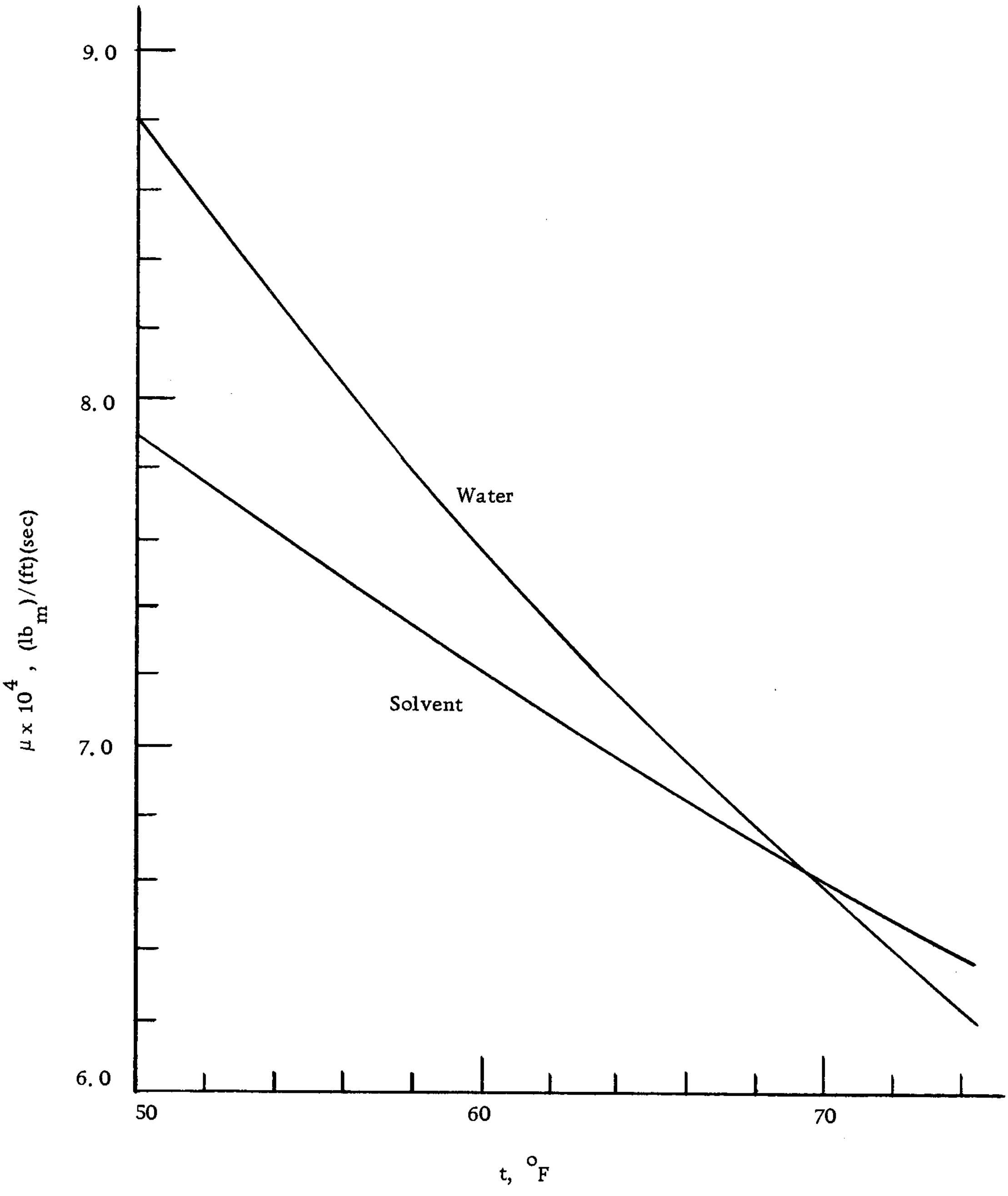

Figure 12. Viscosity of Water and Solvent versus Temperature

Manometer Calculations

The static pressure at the entrance to the capillary tube was calculated from open U-tube mercury and carbon tetrachloride manometer measurements. Referring to Figure 5, the static pressure is

$$P = (h\rho_h - l\rho_w)\frac{g}{g_c}$$

where P is the pressure, lb_f/ft^2; h the difference in levels of the manometer fluid, ft; l, the level difference between the point of interest and the manometer fluid in the left leg, ft; ρ_h, density of the manometer fluid, lb_m/ft^3; ρ_w, density of the fluid in the manometer line (water), lb_m/ft^3; g, acceleration due to gravity, ft/sec; and g_c, conversion factor, 32.17 $lb_m ft/lb_f sec^2$.

The point of measurement corresponded to a height of 48.3 cm on the mercury manometer scale and 66.8 cm on the carbon tetrachloride manometer scale (Figure 5). Using these values to find l for each case, charts were made to facilitate conversion of manometer liquid column measurements to static pressure in psi.

For example, for the mercury manometer, if the left leg reads 55.0cm and the right leg 45.0 cm, h = 10.0cm, l = 55.0 - 48.3 = 6.7cm. With ρ_h = 830 lb_m/ft^3 and ρ_w = 62.3 lb_m/ft^3,

$$P = [(10)(830) - (6.7)(62.3)](g)(p)/g_c$$
$$= 1.83 \text{ psi}$$

where p is the conversion factor, 2.28×10^{-4} $(ft^3)/(cm)(in)^2$.

Figure 13 is the conversion chart for the mercury manometer, and Figure 14 for the carbon tetrachloride manometer. The liquid densities are those at room temperature which was about $80^\circ F$ throughout the experiment.

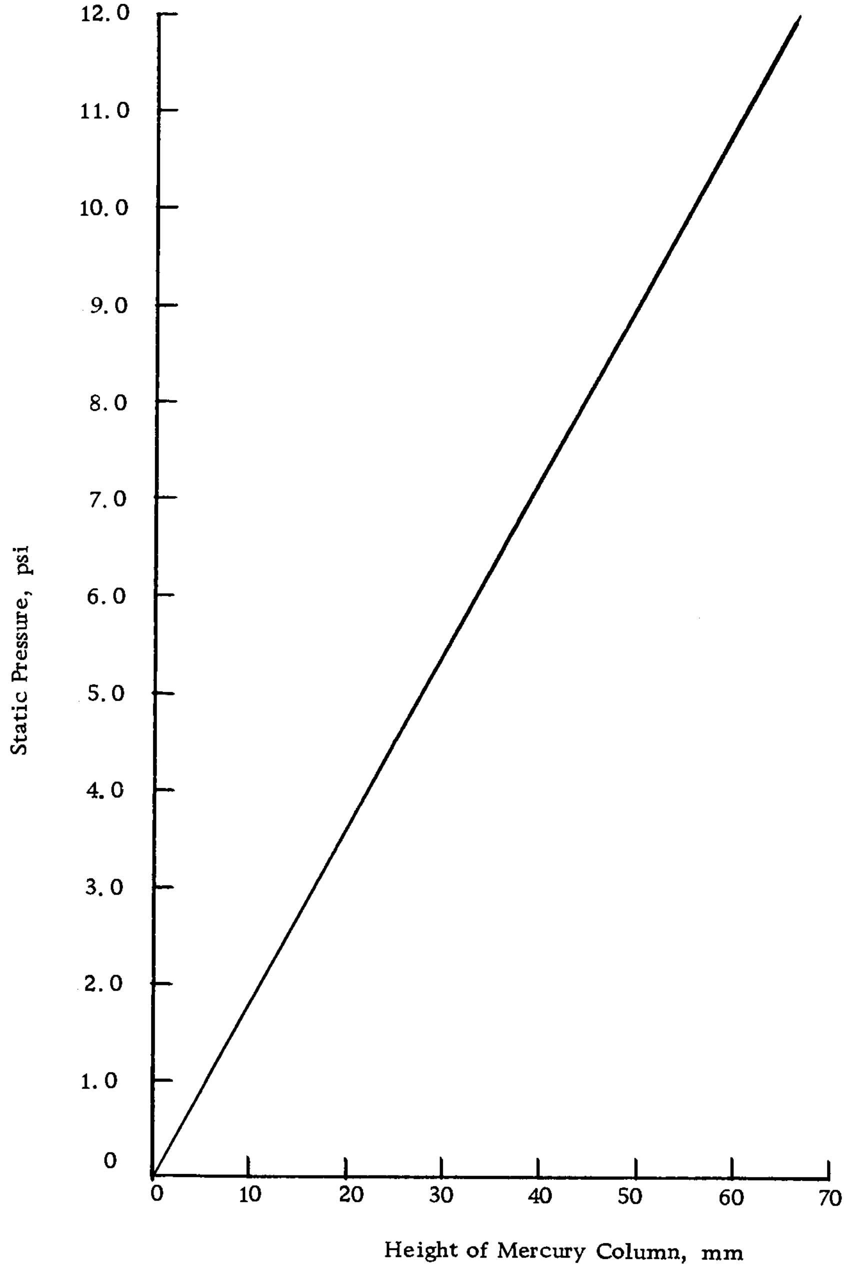

Figure 13. Static Pressure versus Height of Mercury Column

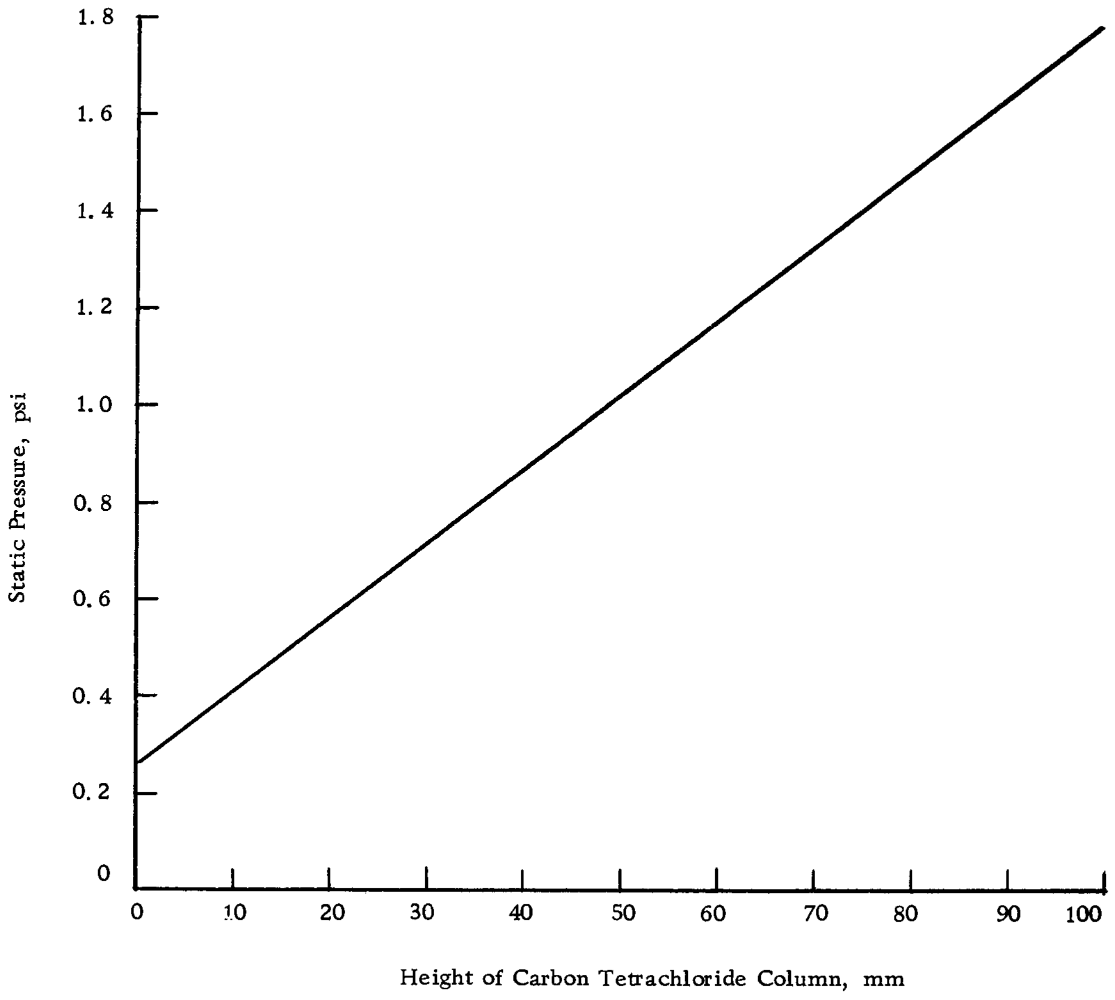

Figure 14. Static Pressure versus Height of Carbon Tetrachloride Column

APPENDIX D

TABULATED DATA

The run number code is as follows: the first number or symbol represents the nominal composition and the second number represents the run number within the series. Thus, 5-1 is the first run with 5% solvent in water, etc. Columns 2 to 6 are observed data and columns 7 to 10 are calculated data. In column 4, the manometer reading is in millimeters of mercury unless otherwise indicated.

(1)	(2)	(3)	(4)	(5)	(6)	(7)	(8)	(9)	(10)
Run no.	t, ^{o}F	Capillary tube no.	Manometer reading, mm	Weight Capillary tube efflux, g	Time of efflux, sec	μ_a, cp	Re	$(D)(\Delta P)/(4)(L)$, lb_f/ft^2	$(32)(V)/(\pi)(D^3)$, 10^{-4}/sec
5- 1	69.7	B- 9	39.0	256.5	300	1.10	2300	0.806	1.65
2	69.9	B- 9	35.8	237.2	300	1.05	2110	0.742	1.53
3	70.3	B- 9	29.4	200.5	300	1.04	1358	0.620	1.29
4	70.5	B- 9	24.2	167.1	300	1.04	1431	0.523	1.08
5	70.2	B- 9	17.9	127.1	300	1.05	1063	0.398	0.820
6	69.8	B- 9	13.3	96.8	300	1.04	795	0.300	0.624
7	69.9	B- 9	10.3	85.1	300	0.91	709	0.230	0.548
8	70.2	B-12	23.7	118.3	300	1.16	641	0.490	0.761
9	69.5	B-12	29.2	141.4	300	1.15	773	0.486	0.908

Appendix D -- Tabulated Data (Continued)

(1) Run no.	(2) t, °F	(3) Capillary tube no.	(4) Manometer reading, mm	(5) Weight Capillary tube efflux, g	(6) Time of efflux, sec	(7) μa, cp	(8) Re	(9) $(D)(\Delta P)/(4)(L)$, lb_f/ft^2	(10) $(32)(V)/(\pi)(D^3)$, 10^{-4}/sec
5 -10	70.2	B-12	33.6	162.0	300	1.15	874	0.551	1.04
11	70.4	B-12	37.7	182.0	300	1.15	996	0.619	1.17
12	70.2	B-12	37.7	178.6	300	1.17	955	0.616	1.15
13	69.5	B-12	42.4	198.7	300	1.17	1062	0.686	1.28
14	69.7	B-12	44.3	209.5	300	1.16	1130	0.718	1.35
15	70.2	B-12	46.1	214.6	300	1.19	1198	0.753	1.38
16	70.3	B-12	50.3	188.8	240	1.21	1339	0.850	1.52
17	70.3	B-15	53.6	215.8	300	1.08	1258	0.701	1.39
18	69.5	B-15	46.4	257.5	420	1.10	1053	0.602	1.18
19	70.0	B-15	40.6	114.3	210	1.14	911	0.554	1.05
20	69.9	B-15	37.6	151.5	300	1.12	851	0.506	0.976
21	70.1	B-15	33.9	88.4	195	1.14	748	0.460	0.876
22	70.1	B-15	30.2	124.4	300	1.09	717	0.404	0.800
23	69.7	B-15	25.0	103.0	300	1.08	544	0.340	0.604
24	70.4	B- 6	24.6	222.7	300	1.07	1310	0.721	1.41
25	69.7	B- 6	21.1	193.7	300	1.08	1126	0.632	1.25
26	70.0	B- 6	20.1	184.1	300	1.09	1068	0.608	1.19
27	70.2	B- 6	17.5	161.8	300	1.10	924	0.538	1.04
28	70.1	B- 6	14.0	134.1	300	1.10	765	0.447	0.864
29	70.7	B- 6	12.2	116.2	300	1.10	666	0.387	0.748
30	69.8	B- 6	8.6	81.3	300	1.13	451	0.292	0.524
31	69.8	A-12	41.2	103.5	630	1.15	243	0.413	1.54
32	69.6	A-12	44.4	78.2	450	1.17	397	0.444	1.54
33	70.1	A-12	47.9	108.7	600	1.22	397	0.456	1.63
34	69.6	A-12	52.0	117.8	600	1.21	434	0.518	1.70

Appendix D -- Tabulated Data(Continued)

(1) Run no.	(2) t, °F	(3) Capillary tube no.	(4) Manometer reading, mm	(5) Weight Capillary tube efflux, g	(6) Time of efflux, sec	(7) μ_a, cp	(8) Re	(9) $(D)(\Delta P)/(4)(L)$, lb_f/ft^2	(10) $(32)(V)/(\pi)(D^3)$, 10^{-4}/sec
5-35	70.3	A-12	56.4	129.7	600	1.20	481	0.568	1.84
36	70.5	A-12	59.0	134.9	600	1.21	486	0.593	2.11
37	70.4	A-12	61.3	118.9	510	1.20	518	0.608	2.18
38	69.7	A- 9	51.4	165.6	600	1.17	631	0.694	2.58
39	70.1	A- 9	54.1	139.7	480	1.16	671	0.726	2.72
40	69.7	A- 9	45.2	202.2	840	1.20	930	0.622	2.26
41	70.1	A- 9	39.3	124.8	600	1.20	464	0.537	1.95
42	70.2	A- 9	37.3	116.0	600	1.23	420	0.512	1.81
43	70.3	A- 9	31.7	95.1	600	1.29	316	0.441	1.48
44	70.1	A- 9	27.3	61.2	540	--	--	--	--
45	70.1	A- 9	30.0	85.3	540	1.24	337	0.423	1.48
46	69.9	A- 9	51.0	164.0	600	1.18	620	0.555	2.56
47	70.6	A- 6	44.6	239.8	660	1.06	916	0.845	3.40
48	69.6	A- 6	54.8	181.0	420	1.07	1077	1.012	4.04
49	69.7	A- 6	35.8	174.9	600	1.08	722	0.692	2.73
50	70.1	A- 6	29.6	116.4	480	1.08	594	0.576	2.28
51	70.3	A- 6	27.6	101.1	480	1.21	464	0.549	1.98
52	70.5	A- 6	24.7	73.3	360	1.07	508	0.490	1.91
53	70.3	A- 6	21.8	76.1	420	1.08	448	0.429	1.70
54	70.2	A- 6	54.9	133.9	300	1.03	1153	1.008	4.18
55	70.9	A- 6	40.6	185.6	340	1.01	910	0.761	3.22
56	70.0	A- 6	27.6	58.1	240	1.01	640	0.538	2.26
57	70.3	A-15	54.7	98.8	480	0.99	554	0.443	1.93
58	69.9	A-15	57.6	104.0	480	0.99	584	0.467	2.03
59	70.7	A-15	62.3	112.8	480	0.99	633	0.505	2.20
60	69.9	A-15	54.2	60.4	300	1.00	447	0.438	1.89

Appendix D -- Tabulated Data (Continued)

(1) Run no.	(2) t, °F	(3) Capillary tube no.	(4) Manometer reading, mm	(5) Weight Capillary tube efflux, g	(6) Time of efflux, sec	(7) μ a, cp	(8) Re	(9) $(D)(\Delta P)/(4)(L)$, lb_f/ft^2	(10) $(32)(V)/(\pi)(D^3)$, 10^{-4}/sec
5-61	70.3	A-15	59.8	67.2	300	1.00	599	0.487	2.10
62	69.7	A- 9	59.4	98.4	300	1.04	841	0.799	3.20
63	70.4	A- 9	50.3	99.0	360	1.15	639	0.679	2.71
64	70.2	A- 9	39.5	63.7	300	1.20	476	0.541	2.16
65	70.2	A- 9	45.6	158.5	300	1.20	534	0.615	2.46
66	69.8	C-12	28.2	560.5	300	1.56	1160	0.561	1.62
67	70.0	C-12	23.9	424.3	240	1.34	1273	0.456	1.52
68	70.0	C-12	12.9	291.8	240	1.08	1090	0.251	1.05
69	69.9	C-12	9.0	233.3	300	1.25	1128	0.189	0.672
70	70.0	C-12	17.2	357.7	240	1.09	1326	0.327	1.28
71	70.2	C-12	33.3	422.3	240	1.89	900	0.640	2.02
72	69.7	C- 6	30.8	416.5	150	1.81	1429	0.329	2.40
73	70.0	C- 6	22.7	347.9	150	1.62	1384	0.727	2.00
74	69.9	C- 6	7.0	250.3	180	1.21	1120	0.240	1.20
75	69.7	C- 6	6.3	183.7	180	1.14	765	0.230	0.880
76	69.6	C- 6	5.5	220.9	300	1.48	480	0.212	0.636
77	70.2	C-15	30.4	433.7	240	1.38	1269	0.482	1.56
78	70.2	C-15	23.3	293.0	180	1.14	1385	0.359	1.41
79	69.8	C-15	18.2	266.4	180	1.21	1179	0.293	1.28
80	69.5	C-15	12.5	192.2	180	1.00	1029	0.206	0.924
81	70.1	C-15	8.9	136.4	180	1.03	710	0.150	0.656
82	70.3	C- 9	19.9	325.4	180	1.38	1271	0.479	1.56
83	70.0	C- 9	15.6	289.4	180	1.26	1237	0.378	1.39
84	70.3	C- 9	12.1	260.2	180	1.03	1352	0.288	1.25

Appendix D -- Tabulated Data (Continued)

(1) Run no.	(2) t, °F	(3) Capillary tube no.	(4) Manometer reading, mm	(5) Weight Capillary tube efflux, g	(6) Time of efflux, sec	(7) μ_a, cp	(8) Re	(9) $(D)(\Delta P)/(4)(L)$, lb_f/ft^2	(10) $(32)(V)/(\pi)(D^3)$, 10^{-4}/sec
5-85	70.3	C- 9	7.8	176.7	180	1.08	875	0.204	0.848
86	70.7	C- 9	6.5	141.0	180	1.12	631	0.170	0.676
20- 1	70.1	B-12	53.9	160.9	240	1.48	623	0.889	5.98
2	70.1	B-12	47.0	168.7	300	1.57	500	0.791	5.01
3	70.0	B-12	41.5	140.8	300	1.68	526	0.707	4.18
4	69.8	B-12	35.3	113.8	300	1.80	397	0.611	3.38
5	70.0	B-12	31.7	107.1	300	1.80	374	0.548	3.18
6	69.9	B-12	28.5	90.4	300	1.88	302	0.507	2.68
7	70.5	B-12	34.5	111.3	300	1.80	389	0.598	3.31
8	70.0	B-12	38.0	124.4	300	1.74	444	0.655	3.70
9	70.0	B-12	43.6	144.2	300	1.71	529	0.737	3.73
10	70.0	B-12	48.9	172.7	300	1.69	641	0.823	5.14
11	70.3	B-12	55.5	207.2	300	1.59	820	0.916	6.15
12	69.6	B- 9	25.5	214.9	540	1.63	461	0.585	3.54
13	70.2	B- 9	33.0	153.1	300	1.61	597	0.737	4.55
14	70.1	B- 9	38.0	177.3	300	1.60	697	0.849	5.27
15	70.4	B- 9	42.1	196.6	300	1.58	780	0.927	5.84
16	70.0	B- 9	46.9	224.4	300	1.52	924	1.02	6.67
17	70.0	B- 9	50.7	245.1	300	1.48	1039	1.18	7.29
18	70.2	B-15	41.0	127.0	300	1.48	538	0.559	3.77
19	70.0	B-15	45.5	152.4	300	1.35	709	0.613	4.53
20	69.6	B-15	50.9	130.4	240	1.40	731	0.681	4.84
21	70.1	B-15	53.9	182.1	300	1.31	871	0.717	5.42
22	70.0	B-15	56.7	231.2	300	1.08	1343	0.743	6.87

Appendix D -- Tabulated Data (Continued)

(1) Run no.	(2) t, °F	(3) Capillary tube no.	(4) Manometer reading, mm	(5) Weight Capillary tube efflux, g	(6) Time of efflux, sec	(7) μa, cp	(8) Re	(9) $(D)(\Delta P)/(4)(L)$, lb_f/ft^2	(10) $(32)(V)/(\pi)(D^3)$, 10^{-4}/sec
20-23	70.1	B-15	58.3	198.1	240	1.01	1541	0.746	7.36
24	70.0	B-15	62.2	72.8	90	1.10	1385	0.795	7.23
25	70.2	B-15	57.0	191.1	300	1.33	905	0.757	5.68
26	70.1	B-15	60.0	215.3	300	1.23	1100	0.787	6.40
27	70.0	B- 6	30.3	209.0	300	1.53	858	0.951	6.22
28	70.2	B- 6	36.6	254.9	300	1.48	1081	1.13	7.53
29	69.6	B- 6	41.8	279.2	300	1.41	1244	1.22	8.30
30	69.8	B- 6	43.2	393.7	420	1.51	1167	1.28	8.36
31	69.7	B- 6	46.1	249.0	240	1.44	1358	1.34	9.24
32	70.3	B- 6	43.8	263.1	270	1.48	1113	1.29	8.68
33	69.9	C-12	20.4	228.0	180	1.72	720	0.421	1.13
34	69.7	C-12	27.3	278.7	180	1.87	801	0.560	1.39
35	69.8	C-12	32.9	376.6	210	1.91	795	0.660	1.60
36	69.3	C-12	34.6	332.1	180	1.95	915	0.695	1.64
37	69.6	C-12	37.4	354.3	180	1.95	977	0.754	1.76
38	70.0	C-12	40.7	374.1	180	2.00	1050	0.802	1.86
39	70.0	C-12	45.1	399.7	180	2.07	1038	0.885	1.98
40	69.9	C-15	24.9	251.5	180	1.53	705	0.412	1.25
41	69.9	C-15	30.2	297.2	180	1.53	833	0.488	1.47
42	69.6	C-15	34.9	338.7	180	1.59	915	0.579	1.68
43	70.0	C-15	38.1	363.2	180	1.55	1018	0.602	1.80
44	69.7	C-15	42.3	388.2	180	1.59	1047	0.661	1.93
45	69.5	C-15	45.1	406.7	180	1.63	1072	0.710	2.02
46	69.8	C- 6	9.5	201.0	180	1.67	646	0.356	0.996
47	70.0	C- 6	14.5	287.7	180	1.68	921	0.505	1.42

Appendix D -- Tabulated Data (Continued)

(1) Run no.	(2) t, °F	(3) Capillary tube no.	(4) Manometer reading, mm	(5) Weight Capillary tube efflux, g	(6) Time of efflux, sec	(7) μ_a, cp	(8) Re	(9) $(D)(\Delta P)/(4)(L)$, lb_f/ft^2	(10) $(32)(V)/(\pi)(D^3)$, 10^{-4}/sec
20-48	69.6	C- 6	19.4	345.6	180	1.93	960	0.689	1.72
49	69.8	C- 6	23.3	382.5	180	1.95	1054	0.806	1.90
50	70.0	C- 6	26.5	397.5	180	2.20	971	0.898	1.96
51	69.7	C- 9	9.5	104.6	120	1.54	244	0.257	0.776
52	69.7	C- 9	18.5	273.1	180	1.70	865	0.478	1.36
53	69.7	C- 9	22.7	305.2	180	1.77	970	0.577	1.51
54	70.3	C- 9	25.6	332.2	180	1.82	981	0.646	1.64
55	70.0	C- 9	28.0	346.8	180	1.92	971	0.713	1.72
56	70.0	C- 9	32.2	374.4	180	2.05	981	0.817	1.86
57	69.8	C- 9	34.7	394.1	180	2.07	1025	0.834	1.96
58	69.8	C- 9	30.8	366.7	180	1.99	990	0.745	1.90
59	70.3	D-12	27.5(CCl)	281.3	120	1.66	935	0.153	0.202
60	70.3	D-12	44.2(CCl)	368.1	120	1.66	1225	0.199	0.264
61	70.0	D-12	59.2(CCl)	230.4	90	1.95	1505	0.338	0.384
62	70.0	D-12	92.7(CCl)	399.2	90	1.85	1520	0.307	0.367
63	70.0	D-12	82.9(CCl)	382.4	90	1.75	1473	0.265	0.336
64	69.7	D-12	68.2(CCl)	350.3	90	1.58	1171	0.175	0.244
65	70.2	D- 9	5.5	324.5	90	1.94	1229	0.263	0.312
66	70.2	D- 9	64.2(CCl)	363.9	90	2.03	1318	0.308	0.349
67	70.0	D- 9	67.7(CCl)	397.8	90	1.99	1468	0.329	0.382
68	69.5	D- 9	9.8	310.7	60	2.25	1572	0.439	0.448
69	69.5	D- 9	64.6(CCl)	395.9	90	1.98	1471	0.330	0.380
70	69.6	D- 9	53.0(CCl)	347.6	90	1.89	1406	0.274	0.334
71	69.7	D- 9	38.9(CCl)	289.1	90	1.91	1128	0.230	0.277
72	69.5	D- 6	58.5(CCl)	294.5	60	1.75	1860	0.336	0.424

Appendix D -- Tabulated Data (Continued)

(1) Run no.	(2) t, °F	(3) Capillary tube no.	(4) Manometer reading, mm	(5) Weight Capillary tube efflux, g	(6) Time of efflux, sec	(7) μa, cp	(8) Re	(9) $(D)(\Delta P)/(4)(L)$, lb_f/ft^2	(10) $(32)(V)/(\pi)(D^3)$, 10^{-4}/sec
20-73	69.5	D- 6	49.2(CCl)	278.5	60	1.66	1850	0.303	0.401
74	69.5	D- 6	41.2(CCl)	246.9	60	1.72	1586	0.275	0.356
75	69.8	D- 6	60.6(CCl)	293.5	60	1.88	1721	0.358	0.424
76	69.8	D- 6	47.1(CCl)	265.1	60	1.85	1579	0.308	0.382
77	69.5	D- 6	75.5(CCl)	313.4	60	2.18	1586	0.446	0.451
78	69.7	D-15	63.7(CCl)	204.4	60	1.58	1434	0.179	0.295
79	69.7	D-15	46.5(CCl)	240.9	90	1.66	1068	0.175	0.232
80	70.0	D-15	53.0(CCl)	262.5	90	1.67	1156	0.191	0.252
81	69.7	D-15	78.0(CCl)	235.2	60	1.59	1635	0.241	0.339
82	69.7	D-15	8.55	255.1	60	1.52	1854	0.252	0.367
83	69.7	D-15	11.1	269.3	60	1.95	1521	0.342	0.388
84	69.7	D-15	12.2	282.2	60	2.05	1520	0.377	0.406
85	69.7	A-12	56.5	132.6	720	1.41	347	0.567	1.77
86	69.5	A-12	53.8	97.8	600	1.56	279	0.544	1.57
87	69.5	A-12	58.8	214.4	1020	1.29	452	0.593	1.98
88	69.3	A-12	57.4	188.7	960	1.34	392	0.575	1.89
89	69.5	A-12	61.3	204.6	960	1.23	492	0.610	2.19
90	69.8	A- 9	44.7	123.9	600	1.39	396	0.616	1.98
91	69.9	A- 9	51.9	154.6	660	1.41	442	0.711	2.26
92	69.9	A- 9	55.3	174.3	660	1.32	534	0.751	2.54
93	70.0	A- 9	60.0	191.1	600	1.17	727	0.804	3.08
94	69.6	A- 9	61.3	258.1	780	1.16	761	0.826	3.20
95	70.0	A- 9	61.3	196.8	660	1.21	659	0.776	2.87
96	70.0	A- 9	53.7	167.5	600	1.21	618	0.727	2.69
97	70.3	A- 6	34.9	136.8	600	1.45	420	0.724	2.20

Appendix D -- Tabulated Data (Continued)

(1) Run no.	(2) t, °F	(3) Capillary tube no.	(4) Manometer reading, mm	(5) Weight Capillary tube efflux, g	(6) Time of efflux, sec	(7) μa, cp	(8) Re	(9) $(D)(\Delta P)/(4)(L)$, lb_f/ft^2	(10) $(32)(V)/(\pi)(D^3)$, 10^{-4}/sec
20-98	70.0	A- 6	38.8	148.5	600	1.42	466	0.770	2.39
99	68.9	A- 6	41.6	161.7	600	1.38	519	0.815	2.60
100	70.0	A- 6	44.1	186.2	600	1.25	663	0.853	2.99
101	70.3	A- 6	46.9	191.8	600	1.30	657	0.912	3.08
102	70.2	A- 6	49.0	267.1	780	1.26	745	0.945	3.30
103	70.2	A- 6	51.9	227.8	600	1.18	870	0.984	3.66
104	70.1	A-15	53.3	97.2	600	1.24	353	0.439	1.56
105	70.0	A-15	54.4	102.3	600	1.21	376	0.450	1.64
106	70.1	A-15	57.4	106.8	600	1.22	389	0.472	1.72
107	70.1	A-15	59.2	112.7	600	1.20	415	0.485	1.81
108	70.0	A-15	61.5	127.3	600	1.08	524	0.501	2.04
35- 1	69.6	C- 9	14.7	134.9	180	2.97	244	0.427	0.690
2	70.0	C- 9	21.1	193.0	180	2.93	354	0.604	0.988
3	70.0	C- 9	26.6	220.0	180	3.21	368	0.755	1.12
4	70.0	C- 9	32.7	279.2	180	3.17	474	0.911	1.43
5	70.0	C- 9	38.3	339.6	180	2.85	628	1.03	1.73
6	70.0	C- 9	43.1	387.2	180	2.74	760	1.13	1.98
7	70.3	C- 9	39.9	345.8	180	3.04	508	0.930	1.77
8	70.3	C- 9	34.4	287.1	180	3.35	375	0.834	1.47
9	70.0	C- 9	29.6	233.1	180	3.04	611	1.12	1.19
10	70.0	C- 9	23.7	182.6	180	3.53	278	0.689	0.932
11	70.0	C- 6	24.2	264.3	180	3.50	318	0.990	1.35
12	70.0	C- 6	18.6	189.2	180	3.92	260	0.798	0.968
13	70.4	C- 6	14.4	158.1	180	3.62	235	0.617	0.808

Appendix D -- Tabulated Data (Continued)

(1) Run no.	(2) t, °F	(3) Capillary tube no.	(4) Manometer reading, mm	(5) Weight Capillary tube effect, g	(6) Time of efflux, sec	(7) μ a, cp	(8) Re	(9) $(D)(\Delta P)/(4)(L)$, lb_f/ft^2	(10) $(32)(V)/(\pi)(D^3)$, 10^{-4}/sec
35-14	70.3	C- 6	20.7	169.2	120	3.09	436	0.844	1.30
15	70.1	C- 6	25.2	284.6	180	3.34	458	1.02	1.46
16	70.0	C- 6	27.5	301.1	180	3.42	474	1.11	1.54
17	70.0	C- 6	31.8	348.2	180	3.34	562	1.25	1.78
18	70.0	C- 6	38.1	284.1	120	3.13	731	1.43	2.18
19	69.8	C- 6	35.0	250.0	120	3.39	596	1.37	1.91
20	69.8	C- 6	29.2	304.1	180	3.62	451	1.19	1.56
21	69.5	C-12	26.9	171.5	180	3.22	286	0.590	0.876
22	69.7	C-12	33.2	232.6	180	2.88	435	0.716	1.19
23	70.3	C-12	38.6	286.0	180	2.65	580	0.812	1.46
24	70.3	C-12	42.1	352.4	180	2.25	840	1.10	1.80
25	70.2	C-12	39.6	290.4	180	2.68	584	0.831	1.48
26	70.0	C-12	36.0	258.3	180	2.77	482	0.764	1.32
27	69.5	C-12	29.7	201.7	180	3.00	362	0.645	1.03
28	70.3	C-12	29.8	209.0	180	2.88	391	0.645	1.47
29	70.1	C-12	37.2	282.1	180	2.59	586	0.779	1.44
30	70.0	C-15	31.7	208.1	180	2.47	453	0.551	1.06
31	69.8	C-15	36.8	243.8	180	2.23	588	0.630	1.24
32	69.6	C-15	38.1	265.7	180	2.25	664	0.649	1.36
33	70.0	C-15	43.7	445.0	240	2.01	894	0.719	1.69
34	70.0	C-15	47.3	374.0	180	1.90	1059	0.761	1.90
35	69.8	C-15	48.3	377.3	180	1.88	1079	0.782	1.93
36	70.2	C-15	51.8	416.0	180	1.95	1150	0.870	2.12
37	70.4	C-15	54.1	473.0	180	1.63	1568	0.826	2.42

Appendix D -- Tabulated Data (Continued

(1) Run no.	(2) t, °F	(3) Capillary tube no.	(4) Manometer reading, mm	(5) Weight Capillary tube efflux, g	(6) Time of efflux, sec	(7) μa, cp	(8) Re	(9) (D)(Δ P)/(4)(L), lb_f/ft^2	(10) (32)(V)/(π)(D^3), 10^{-4}/sec
35-38	69.6	B-12	49.3	132.5	300	2.14	388	0.846	0.911
39	69.9	B-12	51.4	152.9	300	1.92	500	0.876	1.04
40	69.7	B-12	53.5	149.9	300	2.04	461	0.913	1.03
41	69.8	B-12	56.4	166.5	300	1.92	544	0.954	1.14
42	70.3	B-12	59.5	241.0	300	1.34	1127	0.972	1.65
43	70.7	B-12	46.8	128.7	300	2.09	386	0.804	0.881
44	69.7	B-12	46.2	108.4	300	2.47	275	0.801	0.750
45	70.1	B- 6	39.7	167.9	300	2.74	384	1.32	1.16
46	70.0	B- 6	43.7	201.9	300	2.45	518	1.43	1.38
47	70.0	B- 6	46.6	213.0	300	2.46	543	1.51	1.46
48	69.7	B- 6	49.0	226.8	300	2.42	642	1.58	1.56
49	70.0	B- 6	5.17	248.2	300	2.30	678	1.64	1.70
50	70.0	B- 6	54.1	329.3	300	1.67	1239	1.58	1.56
51	70.1	B- 6	50.3	248.3	300	2.33	668	1.60	1.70
52	70.0	B-15	54.6	127.2	300	1.96	408	0.743	0.870
53	70.0	B-15	51.1	116.5	300	2.01	361	0.699	0.796
54	70.0	B-15	49.6	117.8	300	1.93	383	0.676	0.807
55	69.7	B-15	46.4	110.2	300	1.92	361	0.632	0.754
56	69.8	B-15	42.2	101.5	300	1.91	333	0.578	0.694
57	70.8	B- 9	37.8	168.5	420	2.45	308	0.881	0.824
58	70.4	B- 9	40.4	133.5	300	2.33	360	0.930	0.915
59	70.1	B- 9	44.0	162.4	300	2.06	495	0.999	1.11
60	69.3	B- 9	45.0	171.3	300	1.99	541	1.02	1.17
61	70.0	B- 9	48.9	176.3	300	2.10	529	1.10	1.21
62	70.0	B- 9	52.4	196.9	300	2.00	618	1.17	1.35
63	70.3	B- 9	58.9	278.8	300	1.49	1174	1.24	1.91

(1) Run no.	(2) t, °F	(3) Capillary tube no.	(4) Manometer reading, mm	(5) Weight Capillary tube efflux, g	(6) Time of efflux, sec	(7) μa, cp	(8) Re	(9) $(D \times \Delta P)/(4 \times L)$, lb_f/ft^2	(10) $(32 \times V)/(\pi \times D^3)$, 10^{-4}/sec
35-64	70.0	B- 9	57.8	268.4	330	1.71	896	1.25	1.69
65	69.6	B- 9	55.3	360.6	480	1.81	782	1.22	1.54
66	69.7	D- 6	22.6(CCl)	133.0	60	3.11	473	0.270	0.199
67	70.3	D- 6	54.8(CCl)	223.6	60	2.77	931	0.427	0.334
68	70.3	D- 6	72.7(CCl)	264.6	60	2.98	1033	0.514	0.396
69	70.3	D- 6	91.8(CCl)	299.6	60	3.09	1071	0.605	0.448
70	70.3	D- 6	67.9(CCl)	246.2	60	3.16	860	0.507	0.368
71	70.3	D- 6	60.7(CCl)	234.1	60	3.03	854	0.463	0.350
72	70.3	D- 6	84.7(CCl)	289.9	60	3.00	918	0.566	0.432
73	70.3	D- 6	81.7(CCl)	284.8	60	2.96	1064	0.548	0.425
74	70.3	D- 6	90.2(CCl)	289.0	60	3.09	1033	0.584	0.432
75	70.3	D- 9	83.6(CCl)	222.1	60	3.27	750	0.454	0.332
76	69.7	D- 9	92.8(CCl)	230.5	60	3.39	750	0.491	0.344
77	69.7	D- 9	81.8(CCl)	213.3	60	3.38	697	0.452	0.319
78	69.7	D- 9	77.1(CCl)	205.3	60	3.32	683	0.426	0.306
79	70.0	D- 9	71.2(CCl)	192.7	60	3.42	621	0.414	0.288
80	70.0	D- 9	56.0(CCl)	162.2	60	3.41	526	0.348	0.242
81	70.0	D- 9	63.0(CCl)	177.5	60	3.40	577	0.378	0.266
82	69.7	D- 9	10.9	276.9	60	3.04	1008	0.524	0.413
83	69.7	D- 9	13.2	315.0	60	3.36	1033	0.663	0.470
84	69.7	D- 9	12.6	323.1	60	3.02	1182	0.611	0.484
85	70.3	D-12	14.8	300.1	60	2.99	1110	0.586	0.448
86	69.8	D-12	12.4	262.2	60	2.88	1004	0.479	0.392
87	69.7	D-12	10.9	230.7	60	2.96	862	0.435	0.336

Appendix D -- Tabulated Data (Continued)

(1) Run no.	(2) t, °F	(3) Capillary tube no.	(4) Manometer reading, mm	(5) Weight Capillary tube efflux, g	(6) Time of efflux, sec	(7) μ a, cp	(8) Re	(9) (D)(ΔP)/(4)(L), lb_f/ft^2	(10) (32)(V)/(π)(D³), 10^{-4}/sec
35-88	69.7	D-12	97.7(CCl)	190.0	60	3.31	908	0.410	0.284
89	69.7	D-12	91.0(CCl)	217.4	60	2.63	913	0.372	0.324
90	69.7	D-12	89.5(CCl)	197.3	60	2.89	738	0.374	0.295
91	69.7	D-12	84.0(CCl)	185.9	60	3.00	684	0.360	0.278
92	69.8	D-12	77.9(CCl)	182.9	60	2.86	706	0.341	0.274
93	69.8	D-12	58.7(CCl)	150.1	60	2.86	580	0.280	0.224
94	69.8	D-12	72.3(CCl)	170.0	60	2.92	643	0.324	0.254
95	70.3	D-15	17.6	304.0	60	2.91	1155	0.578	0.454
96	70.0	D-15	15.6	270.3	60	2.99	997	0.525	0.404
97	70.0	D-15	13.3	233.0	60	3.00	858	0.455	0.348
98	69.8	D-15	11.9	213.5	60	2.98	790	0.416	0.290
99	69.7	D-15	9.8	168.5	60	3.20	582	0.350	0.252
100	69.7	D-15	86.8(CCl)	153.0	60	3.15	536	0.313	0.228
101	69.7	D-15	56.8(CCl)	116.5	60	3.02	426	0.230	0.174
102	70.0	A-15	64.0	81.9	600	1.81	201	0.536	1.36
103	69.5	A-15	50.1	33.6	600	3.41	44	0.420	0.560
104	70.1	A-15	51.3	36.5	600	3.25	50	0.431	0.608
105	69.8	A-15	52.2	46.7	1020	4.20	29	0.437	0.458
106	70.3	A-15	53.4	40.6	600	3.04	60	0.447	0.677
107	70.0	A-15	55.5	51.9	600	2.58	90	0.466	0.864
108	70.3	A-12	57.4	60.8	600	2.66	102	0.590	1.01
109	70.4	A-12	55.5	69.9	720	2.69	96	0.570	0.972
110	69.6	A-12	53.5	55.4	600	2.73	90	0.551	0.924
111	69.7	A-12	51.5	49.7	600	2.93	76	0.531	0.828

Appendix D -- Tabulated Data (Continued)

(1) Run no.	(2) t, °F	(3) Capillary tube no.	(4) Manometer reading, mm	(5) Weight Capillary tube efflux, g	(6) Time of efflux, sec	(7) μa, cp	(8) Re	(9) $(D)(\Delta P)/(4)(L)$, lb_f/ft^2	(10) $(32)(V)/(\pi)(D^3)$, 10^{-4}/sec
35-112	70.6	A-12	49.0	58.7	720	2.84	77	0.506	0.816
113	70.1	A-12	45.6	41.7	600	3.10	60	0.471	0.695
114	69.9	A- 9	45.2	64.3	600	2.79	106	0.642	1.07
115	69.0	A- 9	42.0	45.9	600	3.62	57	0.596	0.765
116	69.5	A- 9	51.0	91.3	720	2.65	128	0.725	1.27
117	70.1	A- 9	55.3	84.1	600	2.59	144	0.783	1.40
118	70.0	A- 9	59.3	127.6	600	1.84	309	0.840	2.13
119	69.9	A- 6	32.7	167.7	780	1.46	394	0.686	2.15
120	70.1	A- 6	40.9	162.6	720	1.72	349	0.854	2.08
121	69.9	A- 6	55.3	180.5	600	1.75	460	1.16	3.01
122	69.9	A- 6	47.9	151.1	600	1.81	371	1.00	2.52
123	69.6	A- 6	42.2	133.2	600	1.81	328	0.882	2.22
50- 1	70.2	A- 6	47.3	97.2	600	2.79	155	0.991	1.68
2	69.8	A- 6	52.6	122.0	660	2.63	188	1.08	1.91
3	70.1	A- 6	55.5	139.9	600	2.27	274	1.61	2.42
4	69.7	A- 6	39.8	72.9	600	3.12	104	0.832	1.26
5	70.0	A- 6	35.7	64.4	600	3.19	90	0.750	1.11
6	70.2	A- 6	30.9	58.8	600	3.02	87	0.651	1.01
7	70.0	A- 9	41.4	26.0	600	6.27	18	0.586	0.448
8	70.1	A- 9	49.9	34.1	600	5.79	26	0.709	0.588
9	69.6	A- 9	57.1	57.9	660	4.28	55	0.809	0.908
10	69.8	A- 9	53.3	35.8	600	5.88	27	0.756	0.617
11	69.9	A- 9	45.3	28.9	600	6.22	21	0.646	0.498
12	70.3	A-12	45.7	19.4	600	6.68	13	0.472	0.334
13	69.9	A-12	49.1	22.9	600	6.60	15	0.507	0.395

Appendix D -- Tabulated Data (Continued)

(1) Run no.	(2) t, °F	(3) Capillary tube no.	(4) Manometer reading, mm	(5) Weight Capillary tube efflux, g	(6) Time of efflux, sec	(7) μa, cp	(8) Re	(9) $(D)(\Delta P)/(4)(L)$, lb_f/ft^2	(10) $(32)(V)/(\pi)(D^3)$, 10^{-4}/sec
50- 14	69.8	A-12	53.5	26.3	600	5.75	20	0.551	0.454
15	70.1	A-12	52.0	24.7	600	5.96	19	0.536	0.425
16	69.9	A-12	47.0	20.6	600	6.45	14	0.486	0.355
17	70.1	B-15	38.9	47.3	300	3.85	77	0.543	0.336
18	70.5	B-15	43.0	54.8	300	3.67	94	0.600	0.310
19	69.7	B-15	48.9	62.5	300	3.64	108	0.679	0.445
20	70.0	B-15	51.6	66.7	300	3.61	116	0.718	0.474
21	69.5	B-15	53.7	77.2	300	3.23	150	0.743	0.549
22	70.6	B-12	43.2	53.3	300	4.71	71	0.766	0.371
23	70.1	B-12	47.0	62.9	300	4.41	90	0.840	0.439
24	70.0	B-12	50.9	73.7	300	4.41	90	0.840	0.514
25	70.6	B-12	53.7	113.9	300	2.74	261	0.932	0.794
26	70.3	B-12	50.4	106.6	300	2.75	243	0.877	0.744
27	69.6	B-12	45.7	84.6	300	3.18	244	0.814	0.588
28	70.4	B-12	51.6	95.9	300	3.15	191	0.904	0.669
29	70.2	B-12	47.0	85.5	300	3.24	166	0.827	0.594
30	69.8	B-12	53.1	191.2	300	3.07	207	0.928	0.704
31	70.2	B- 9	41.0	90.5	300	3.57	160	0.966	0.631
32	70.1	B- 9	45.9	110.9	300	3.25	214	1.08	0.669
33	70.2	B- 9	43.6	104.3	300	3.28	200	1.16	0.726
34	69.8	B- 9	48.3	116.6	300	3.26	224	1.15	0.811
35	70.4	B- 9	55.7	164.3	300	2.60	397	1.28	0.990
36	70.8	B- 6	36.8	104.6	300	4.21	156	1.27	0.728
37	69.8	B- 6	41.2	103.4	300	4.78	136	1.42	0.720

Appendix D -- Tabulated Data (Continued)

(1) Run no.	(2) t, °F	(3) Capillary tube no.	(4) Manometer reading, mm	(5) Weight Capillary tube efflux, g	(6) Time of efflux, sec	(7) μa, cp	(8) Re	(9) $(D)(\Delta P)/(4)(L)$, lb_f/ft^2	(10) $(32)(V)/(\pi)(D^3)$, 10^{-4}/sec
50- 38	69.8	B- 6	43.4	123.4	300	4.19	185	1.49	0.857
39	69.9	B- 6	46.9	133.7	300	4.16	202	1.60	0.930
40	69.6	B- 6	50.6	151.0	300	3.95	240	1.72	1.05
41	69.8	B- 6	53.8	188.0	300	3.31	357	1.79	1.32
42	69.7	B- 6	37.1	100.3	300	4.45	141	1.29	0.697
43	69.9	B- 6	31.5	79.2	300	4.82	103	1.10	0.550
44	70.0	C-15	24.8	147.6	240	3.76	158	0.444	0.586
45	69.8	C-15	30.9	194.1	240	3.55	223	0.552	0.770
46	70.0	C-15	34.4	221.2	240	3.44	259	0.612	0.876
47	70.0	C-15	39.0	263.0	240	3.25	326	0.687	1.04
48	69.5	C-15	43.3	295.2	240	3.20	373	0.758	1.17
49	70.5	C-15	48.5	252.9	180	3.10	439	0.840	1.34
50	70.0	C-15	52.3	297.5	180	2.80	571	0.892	1.57
51	69.6	C-15	52.9	312.1	180	2.68	626	0.893	1.65
52	69.5	C-12	29.6	135.4	180	4.59	158	0.664	0.716
53	69.7	C-12	32.1	152.8	180	4.35	189	0.710	0.808
54	69.3	C-12	35.3	180.8	180	4.01	242	0.775	0.956
55	69.4	C-12	37.6	198.4	180	3.82	272	0.832	1.52
56	70.1	C-12	41.3	237.0	180	3.52	362	0.916	1.25
57	70.5	C-12	43.9	273.8	180	3.19	461	0.925	1.45
58	70.3	C-12	45.3	266.9	180	3.42	408	0.978	1.41
59	69.5	C-12	48.9	299.1	180	3.26	494	1.04	1.58
60	70.2	C- 9	29.1	152.3	180	5.29	155	0.861	0.804
61	70.5	C- 9	31.4	171.4	180	4.77	204	0.932	0.960
62	70.3	C- 9	35.5	227.5	180	4.22	290	1.03	1.20

Appendix D — Tabulated Data (Continued)

(1) Run no.	(2) t, °F	(3) Capillary tube no.	(4) Manometer reading, mm	(5) Weight Capillary tube efflux, g	(6) Time of efflux, sec	(7) μa, cp	(8) Re	(9) $(D)(\Delta P)/(4)(L)$, lb_f/ft^2	(10) $(32)(V)/(\pi)(D^3)$, 10^{-4}/sec
50- 63	70.3	C- 9	38.5	251.5	180	4.08	332	1.10	1.33
64	70.3	C- 9	41.1	264.5	180	4.13	345	1.17	1.40
65	69.5	C- 9	43.8	302.2	180	3.80	425	1.23	1.60
66	69.6	C- 9	46.0	324.1	180	3.68	474	1.28	1.71
67	70.0	C- 9	48.9	375.6	180	3.29	615	1.32	1.99
68	70.0	C- 6	16.4	140.3	180	4.83	157	0.729	0.742
69	69.7	C- 6	18.8	163.3	180	4.72	186	0.829	0.864
70	70.0	C- 6	20.8	182.7	180	4.55	266	1.10	0.968
71	70.3	C- 6	25.0	261.6	180	4.55	295	1.22	1.19
72	70.1	C- 6	28.4	250.0	180	4.43	340	1.34	1.32
73	69.7	C- 6	33.6	280.9	180	4.75	318	1.43	1.49
74	69.7	C- 6	38.4	341.6	180	4.31	425	1.59	1.81
75	69.7	D-15	25.6	291.3	60	4.78	675	0.905	0.450
76	69.7	D-15	22.1	246.6	60	4.97	548	0.802	0.382
77	70.7	D-15	20.0	234.0	60	4.75	545	0.725	0.362
78	70.0	D-15	17.6	197.4	60	5.05	431	0.650	0.305
79	70.0	D-15	15.4	170.0	60	5.20	361	0.576	0.263
80	69.8	D-15	13.4	140.3	60	5.47	283	0.502	0.217
81	69.7	D-15	11.1	116.9	60	5.54	235	0.423	0.181
82	69.7	D-15	15.4	178.1	60	4.99	394	0.580	0.276
83	69.7	D-15	17.8	207.2	60	4.86	470	0.657	0.320
84	69.7	D-15	17.8	207.4	60	4.86	470	0.657	0.328
85	70.0	D-12	18.0	258.9	60	4.67	613	0.792	0.401
86	70.0	D-12	15.7	225.7	60	4.78	523	0.701	0.349
87	70.0	D-12	14.3	207.6	60	4.75	483	0.646	0.321

Appendix D -- Tabulated Data (Continued)

(1) Run no.	(2) t, ^{o}F	(3) Capillary tube no.	(4) Manometer reading, mm	(5) Weight Capillary tube efflux, g	(6) Time of efflux, sec	(7) μ a, cp	(8) Re	(9) $(D)(\Delta P)/(4)(L)$, lb_f/ft^2	(10) $(32)(V)/(\pi)(D^3)$, 10^{-4}/sec
50- 88	70.0	D-12	12.0	170.3	60	4.78	394	0.706	0.356
89	70.0	D-12	17.3	251.9	60	4.63	603	0.762	0.390
90	70.3	D-12	18.3	268.7	60	4.69	635	0.825	0.416
91	70.3	D-12	13.0	187.1	60	4.84	428	0.591	0.290
92	70.3	D- 9	19.2	327.6	60	5.10	709	1.05	0.507
93	70.3	D- 9	17.5	292.0	60	5.35	603	0.981	0.452
94	70.3	D- 9	15.9	267.5	60	5.41	545	0.907	0.414
95	70.0	D- 9	15.5	265.8	60	5.28	555	0.878	0.411
96	69.8	D- 9	13.8	227.3	60	5.68	442	0.809	0.352
97	69.7	D- 9	12.2	201.3	60	5.70	390	0.717	0.312
98	70.3	D- 9	11.5	198.0	60	5.44	402	0.675	0.306
99	70.3	D- 6	14.4	357.1	60	4.93	800	1.21	0.552
100	70.0	D- 6	12.4	319.3	60	4.82	731	1.01	0.494
101	69.5	D- 6	11.7	299.2	60	4.93	670	0.960	0.463
102	69.7	D- 6	9.9	260.9	60	4.89	496	0.842	0.404
103	70.0	D- 6	91.1(CCl)	242.9	60	4.87	469	0.748	0.376
104	70.0	D- 6	80.8(CCl)	244.1	60	4.31	625	0.666	0.378
105	70.0	D- 6	62.9(CCl)	214.7	60	3.83	619	0.528	0.332
S- 1	70.0	A-12	25.5	32.3	300	1.10	261	0.256	1.28
2	69.8	A-12	29.8	73.0	600	1.12	290	0.297	1.52
3	70.1	A-12	32.5	81.6	600	1.10	330	0.330	1.61
4	70.0	A-12	37.4	84.2	600	1.11	338	0.349	1.66
5	70.5	A-12	44.1	115.0	600	0.94	544	0.439	2.28
6	70.0	A-12	49.3	75.5	360	0.96	583	0.491	2.49
7	69.0	A-12	52.0	80.6	360	0.94	639	0.514	2.77

Appendix D -- Tabulated Data (Continued)

(1) Run no.	(2) t, ^{o}F	(3) Capillary tube no.	(4) Manometer reading, mm	(5) Weight Capillary tube efflux, g	(6) Time of efflux, sec	(7) μa, cp	(8) Re	(9) $(D \times \Delta P)/(4 \times L)$, lb_f/ft^2	(10) $(32 \times V)/(\pi \times D^3)$, 10^{-4}/sec
S- 8	69.8	A-12	20.9	51.3	600	1.03	222	0.215	1.01
9	70.2	A-12	23.7	59.5	600	0.98	269	0.231	1.18
10	69.9	A-12	20.4	29.9	360	1.01	223	0.207	0.984
11	70.4	A-12	22.8	34.4	360	1.11	233	0.233	1.13
12	69.3	A-12	22.7	33.4	360	1.14	220	0.231	1.10
13	70.3	A-15	22.5	27.3	360	1.13	179	0.188	0.898
14	70.5	A-15	29.6	38.1	360	1.06	267	0.246	1.25
15	69.9	A-15	37.0	47.1	360	1.06	330	0.304	1.55
16	70.7	A-15	45.1	95.8	600	1.06	402	0.370	1.89
17	70.1	A-15	51.2	43.5	240	1.06	456	0.420	2.15
18	69.1	A-15	41.9	42.7	300	1.10	345	0.343	1.69
19	70.1	A- 6	31.2	59.6	240	1.12	592	0.610	2.94
20	69.6	A- 6	25.7	46.2	240	1.19	432	0.536	2.28
21	69.2	A- 6	18.9	35.5	240	1.17	338	0.380	1.75
22	69.6	A- 9	18.6	21.9	240	1.32	184	0.259	1.08
23	69.6	A- 9	28.0	41.9	300	1.30	286	0.391	1.66
24	69.7	A- 9	34.9	58.0	300	1.14	452	0.473	2.29
25	70.6	A- 9	42.4	69.6	300	1.14	543	0.574	2.75
26	69.6	A- 9	45.5	71.3	300	1.20	528	0.622	2.82
27	70.6	A- 9	32.4	53.8	300	1.13	423	0.455	2.12
W- 1	70.0	A-12	29.0	87.2	600	0.97	793	0.304	1.35
2	69.9	A-12	33.5	101.3	600	0.98	921	0.350	1.56
3	70.2	A-12	39.4	118.2	600	0.97	1076	0.413	1.83
4	70.1	A-12	42.6	128.3	600	0.97	1168	0.446	1.98

Appendix D -- Tabulated Data (Continued

(1) Run no.	(2) t, ^{o}F	(3) Capillary tube no.	(4) Manometer reading, mm	(5) Weight Capillary tube efflux, g	(6) Time of efflux, sec	(7) μa, cp	(8) Re	(9) $(D \times \Delta P)/(4 \times L)$, lb_f/ft^2	(10) $(32 \times V)/(\pi \times D^3)$, 10^{-4}/sec
W- 5	69.9	A-12	53.5	158.7	600	0.98	1441	0.560	2.56
6	70.0	A-12	59.2	177.9	600	0.97	1618	0.619	2.77
7	69.6	A-12	62.2	183.4	600	0.99	1669	0.652	2.84
8	70.0	A-12	32.2	95.8	600	0.98	870	0.338	1.48
9	70.1	A-12	37.8	124.9	660	0.98	1135	0.396	1.76
10	70.7	A-12	50.2	148.3	600	0.98	1349	0.526	2.30